Lappeenranta University of Technology
School of Engineering Science
Chemical Engineering
Chemical and Process Engineering

Saara Laamanen

Defining Surface Chemical and Rheological Properties of Resins for Curtain Coating

Master's Thesis

Examiners: Prof. Satu-Pia Reinikainen
D.Sc. Eeva Jernström

TIIVISTELMÄ

Lappeenrannan teknillinen yliopisto
School of Engineering Science
Kemiantekniikka
Chemical and Process Engineering

Saara Laamanen

Verhopäällystyksessä käytettävien hartsien pintakemiallisten ja reologisten ominaisuuksien määrittäminen

Diplomityö, 2018

143 (+ 29) sivua, 48 (+ 14) kuvaa, 21 (+ 15) taulukkoa ja 5 liitettä

Tarkastajat: Prof. Satu-Pia Reinikainen, TkT Eeva Jernström
Ohjaajat: FT Suvi Pietarinen, FM Sanna Valkonen, FM Mauno Miettinen

Hakusanat: fenoli-formaldehydi hartsit, ligniini, vaneri, verhopäällystys, pintajännitys, venymäviskositeetti

Fenoli-formaldehydi hartseja käytetään vaneriliimojen raaka-aineena. Biopohjaisella ligniinillä voidaan korvata osa hartsin myrkyllisestä ja öljypohjaisesta fenolista. Vaneriliimaus voidaan suorittaa esimerkiksi verhopäällystyksellä. Verhopäällystyksen haasteena on vakaan ja ehjän verhon muodostuminen, johon voidaan vaikuttaa päällystysmateriaalin pintakemiallisilla ja reologisilla ominaisuuksilla. Matala pintajännitys ja korkea venymäviskositeetti edesauttavat verhon muodostumista.

Tässä työssä selvitettiin verhopäällystyksessä käytettävän kaupallisen fenoli-formaldehydi- ja ligniini-fenoli-formaldehydihartsin pintakemiallisten ja reologisten ominaisuuksien erot, valittiin hartseille sopivat analyysimenetelmät, joilla ominaisuudet voidaan onnistuneesti määrittää, sekä tutkittiin eri lisäaineiden vaikutuksia ligniinihartsin ominaisuuksiin. Lopputuloksena määritettiin toimintakuvaajat lisäaineiden annostusmäärälle, kun tavoitellaan hartsin korkeaa venymäviskositeettia.

ABSTRACT

Lappeenranta University of Technology
School of Engineering Science
Chemical Engineering
Chemical and Process Engineering

Saara Laamanen

Defining Surface Chemical and Rheological Properties of Resins for Curtain Coating

Master's Thesis, 2018

143 (+ 29) pages, 48 (+ 14) figures, 21 (+ 15) tables and 5 appendices

Examiners: Prof. Satu-Pia Reinikainen, D.Sc. Eeva Jernström
Supervisors: PhD Suvi Pietarinen, M.Sc. Sanna Valkonen, M.Sc. Mauno Miettinen

Keywords: phenol-formaldehyde resins, lignin, plywood, curtain coating, surface tension, extensional viscosity

Phenol-formaldehyde resins are used as a raw material for plywood adhesives. Bio-based lignin can be used as a partial replacement to toxic and petroleum-based phenol. Plywood gluing can be performed for example by curtain coating. The challenge of curtain coating is formation of a stable and uniform curtain, which can be affected by surface chemical and rheological properties of the coating material. Low surface tension and high extensional viscosity assist successful curtain formation.

In this thesis, the differences in surface chemical and rheological properties of commercial phenol-formaldehyde resin for curtain coating and lignin-phenol-formaldehyde resin were determined, suitable analytical methods to successfully measure these properties were selected, and effects of commercial additives on properties of lignin-phenol-formaldehyde resin were studied. As final results, operational windows for dosage of additives were determined, when high extensional viscosity of the resin is pursued.

ACKNOWLEDGEMENTS

This work was carried out in UPM Northern Europe Research Center (NERC), Lappeenranta, between June and November in 2018. The research center has been a supportive, open-minded and friendly working environment for the past few years. I'm grateful for being part of this innovative team of professionals. Special thanks to Lignin team, which has needed my input, offered interesting tasks and helped to learn and develop myself during the years. It is a pleasure to work with you daily. Thank you for Suvi Pietarinen, Sanna Valkonen and Mauno Miettinen for supervising this work. Thank you for your trust and helpful guides.

I’m also thankful for Satu-Pia Reinikainen and Eeva Jernström from Lappeenranta University of Technology for supervising this work. Thank you for your important feedback, support and commitment. I’m grateful for the department of chemical engineering for offering challenges and successes during the years of studies. LUT, thank you for devoting to students, building a forerunner state of mind and offering excellent keys for the future.

Five years ago, when moving to Lappeenranta, I was excited and nervous about the new city, new university and new life. Thank you for KeTeK ry and LTKY that I got to be part of creating and developing the student life over the years. Thank you for the girls of business-reinforced Kemistiperhe: Annina, Heini, Anna, Satu, Tuuli and Riikka, without you Lappeenranta would not have felt like home already from the first days. Thank you also for my other friends for making the student life unforgettable, and thank you for my friends from Kauniainen that I'm always able to come back to you.

Thanks to my family, especially to my parents, for always supporting me and trusting the choices I've made. Thank you for providing a loving environment to grow and even though you haven't helped with math homework lately, I've learned a lot from you. Last but definitely not least, thank you Jere. You've always helped me whenever needed and made me feel better, listened my stories patiently and laughed at my jokes. Thank you.

Saara Laamanen
Lappeenranta, 23.11.2018

TABLE OF CONTENTS

LIST OF SYMBOLS

A	area	[m^2]
A_{dry}	dry coverage	[g/m^2]
b	regression coefficients	-
Bo	Bond number	-
c	concentration	-
d	diameter	[m]
E’	storage modulus of complex viscoelastic modulus	[mN/m]
E’’	loss modulus of complex viscoelastic modulus	[mN/m]
E*	complex viscoelastic modulus	[mN/m]
F	force	[N]
F_d	correction coefficient	-
f	correction coefficient	-
ΔG	free energy change	[J]
G	shear modulus	[Pa]
G_e	equilibrium modulus	[Pa]
G’	storage modulus of complex shear modulus	[Pa]
G’’	loss modulus of complex shear modulus	[Pa]
G*	complex shear modulus	[Pa]
g	gravitational acceleration	[m/s^2]
h	height	[m]
h_c	curtain thickness	[m]
l	length	[m]
M	torque	[J]
m	mass	[kg]
n	number of replicates	-
P	pressure	[Pa], [bar]
Q	volumetric flow rate per unit width	[m^2/s]
S	spreading coefficient	[J/m^2]
s	distance	[m]
r	radius of a circle	[m]
Re	Reynolds number	-

t	time	[s]
U	velocity	[m/s]
u	conveyor velocity	[m/s], [m/min]
V	volume	[m^3]
v_c	curtain velocity	[m/s]
v_d	damage propagation velocity	[m/s]
v_0	nozzle exit velocity of the curtain	[m/s]
W_a	work of adhesion	[J/m^2]
W_i	work of immersion	[J/m^2]
We	Weber number	-
x	curtain height	[m]
x_1, x_2	explanatory variables in regression	-
y	response variable to be modelled	-
β	correction coefficient	-
γ	shear strain	-, [%]
γ_L	linearity limit	[%]
$\dot{\gamma}$	shear rate	[1/s]
δ	phase shift	[°]
ε	Hencky strain	-
$\dot{\varepsilon}$	Hencky strain rate	[1/s]
η	(shear) viscosity	[mPas], [cP]
η_E	extensional viscosity	[mPas], [cP]
η_0	zero-shear viscosity	[mPas], [cP]
η^*	complex viscosity	[mPas], [cP]
λ	relaxation time	[s]
λ_E	elongational relaxation time	[s]
θ	contact angle	[°]
ν	kinematic viscosity	[m^2/s]
ρ	density	[kg/m^3]
$\Delta\sigma$	correction coefficient	[mN/m]
σ	surface tension	[mN/m]
σ_c	critical surface tension	[mN/m]

σ_{LG}	surface tension at the interface of liquid/gas	[mN/m]
σ_{SG}	surface tension at the interface of solid/gas	[mN/m]
σ_{SL}	surface tension at the interface of solid/liquid	[mN/m]
σ^+	acid (electron acceptor) parameter of surface tension	[mN/m]
σ^-	base (electron donor) parameter of surface tension	[mN/m]
τ	shear stress	[Pa]
ω	angular velocity/frequency	[rad/s]

LIST OF ABBREVIATIONS

CMC	Critical micelle concentration
Df	Defoamer
DMC	Dry matter content
EXP	Experiment
F	Formaldehyde
HMW	High-molecular-weight
LMW	Low-molecular-weight
LPF	Lignin-phenol-formaldehyde
M_N	Number average molecular weight
M_W	Weight average molecular weight
MLR	Multiple linear regression
NaOH	Sodium hydroxide
P	Phenol
PF	Phenol-formaldehyde
R&D	Research and development
S/D	Surfactant/Defoamer
ST	Surface tension
Surf	Surfactant

1 GRAPHICAL ABSTRACT

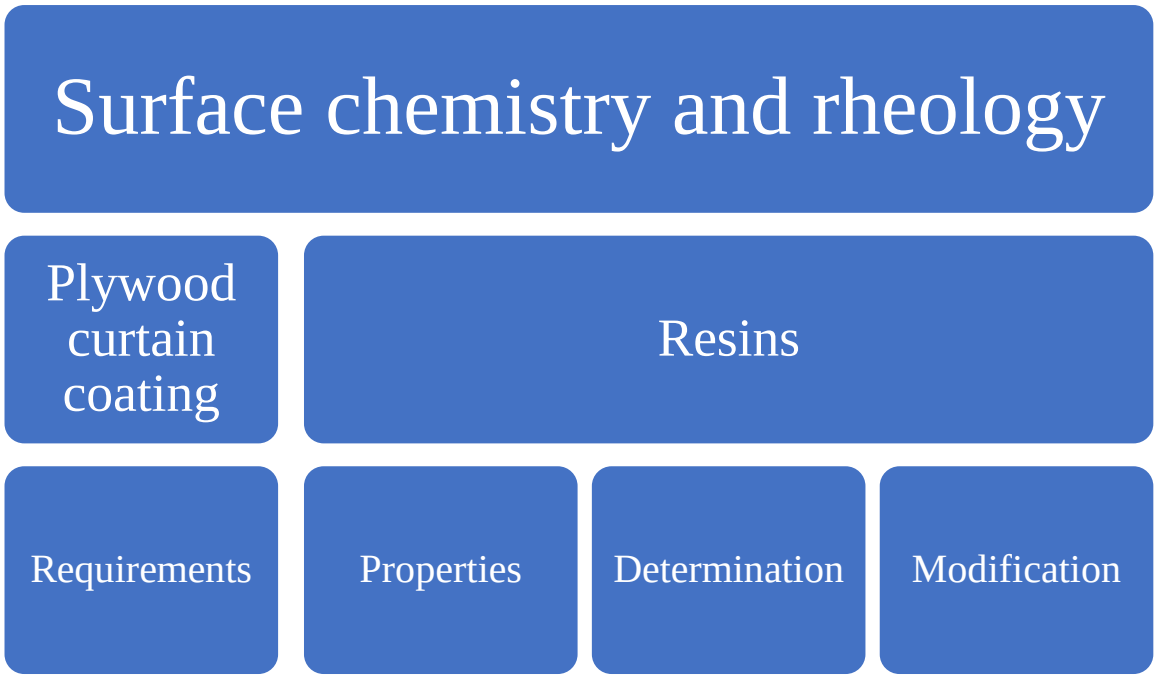

Figure 1 In this thesis, characteristics for LPF resin additive composition for curtain coating of plywood were defined.

2 INTRODUCTION

Major principle in sustainable development is comprehensive use of raw materials in an energy efficient way. This is important because the global use of available raw material resources has been excessive and irresponsible, and the fossil resources are at risk of ending completely (oil and natural gas in approximately 50 years). Demand is to find new bio-based alternatives for coal- and petroleum-based chemicals (Alén, 2011). Thus, for example forest industrial companies are converting the conventional paper and pulp mills into biorefineries. In biorefineries sustainable principles are applied, when wide variety of biomass feedstock is used for production of biochemicals and other novel bioproducts (Alén, 2011).

One of the new biorefinery products is lignin, a wood component which binds cellulose and hemicellulose together in wood. Conventionally in kraft pulping, lignin is dissolved into the cooking liquor. This black liquor is concentrated into higher solids content and burned. (Alén, 2011) Over the years there has been some end-use applications for black liquor and lignin, but during the last decades the true potential of lignin has been noticed. The amount

of potentially available lignin from wood and side streams from pulp industry is 70 million tons (Dunky, 2003), thus making it also a relatively cheap raw material. Lignin is renewable and biodegradable, and its complex structure offers multiple end-use possibilities.

Research and development (R&D) in lignin business focuses on separation of lignin from black liquor and development of new high-value, industrial scale lignin applications. Lignin can be used for example in wood adhesives. Wood adhesives compose of resins, water, fillers and required additives. Phenol-formaldehyde (PF) resins are one of the most used resins but have remarkable disadvantages in toxicity and price. Because of its phenolic nature, lignin can be applied into resins as a partial replacement to fossil-based phenol, thus forming the concept of lignin-phenol-formaldehyde (LPF) resins.

Commercial example of use of lignin in PF resins is WISA® BioBond plywood products, which have been glued with adhesive containing LPF resin technology developed by UPM Biochemicals. It was launched in the fall of 2017 as a sustainable alternative for production of plywood and it is an innovative example of circular economy (WISA BioBond, 2018). In the adhesive of WISA® BioBond products, 50 % of the used phenol is replaced by lignin and the adhesive retains the same high-quality properties as conventional PF resin-based adhesives (UPM Biofore, 2018).

The goal of UPM is to adopt WISA® BioBond gluing technology to all of its plywood mills. In plywood production, multiple adhesive spreading methods are used, most remarkably roller and curtain coating. Curtain coating of veneer with LPF resin-based adhesive requires more R&D. For curtain coating in general, low surface tension and high extensional viscosity of the coating material are required (Beneventi & Guerin, 2005; Birkert et al., 2006). Thus, successful curtain formation and uniform spreading of the coating material onto the base material can be achieved. However, the emerging adhesive material for this kind of application is unique. There is no research available about the resin properties, which are characteristic for achieving a stable curtain. It is required to find out the suitable analytical methods for measurement of these properties and the right methods to affect these properties.

2.1 Objectives of thesis

This thesis determines the essential surface chemical and rheological properties of resins for successful application in curtain coating of veneer. One of the objectives of the thesis is to choose suitable analytical methods for measurement of the surface chemical and rheological properties for permanent laboratory use. The effect of commercial additives and their dosage on these essential properties are determined.

The final objective of this thesis is to develop LPF resin composition for adhesive to be used in curtain coating of veneer in plywood production.

2.2 Scope and outcome of thesis

Scope of this thesis is presented in Figure 2.

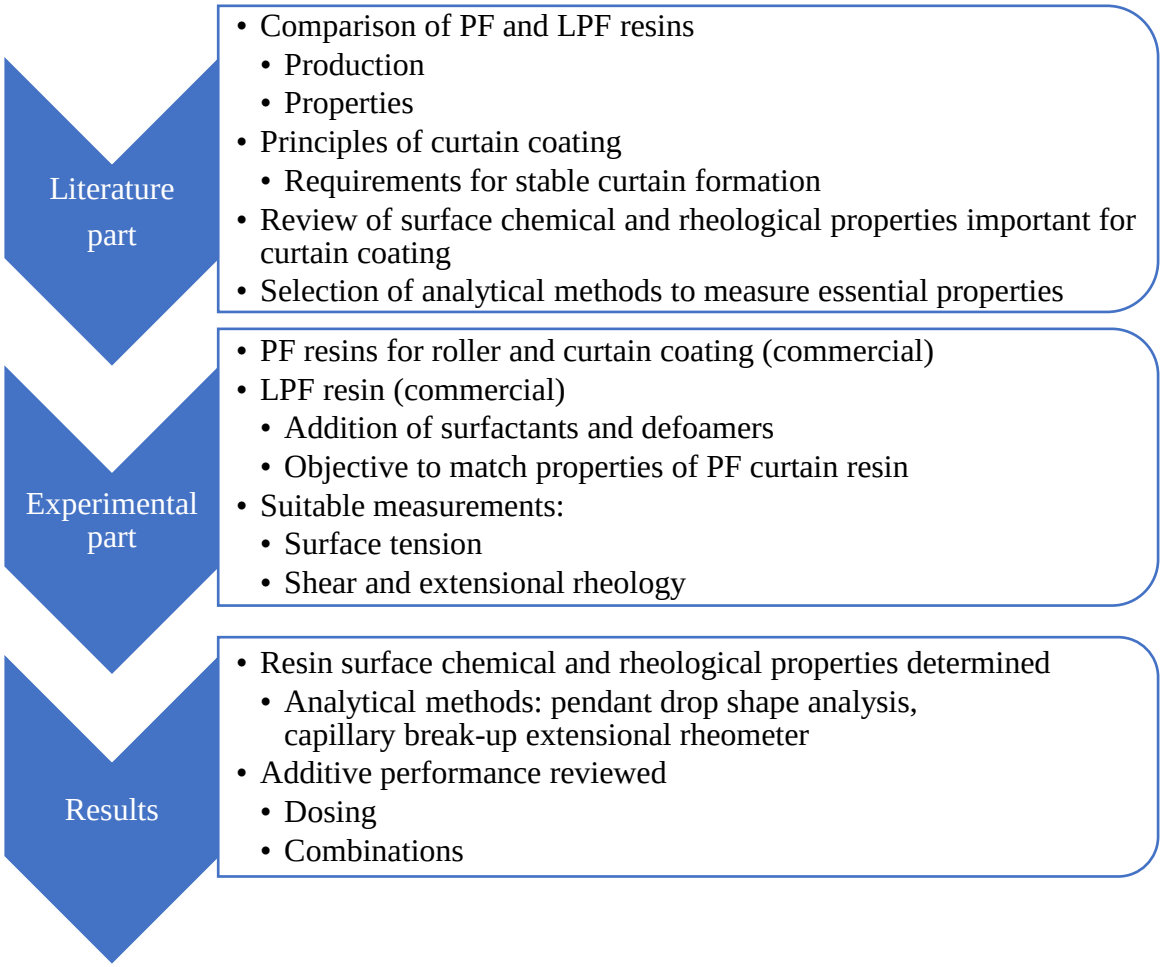

Figure 2 Scope of this thesis.

2.3 Introduction of company

UPM-Kymmene Oyj (UPM) is a forest-based bioindustrial company with six business areas, sales over 10 billion euros and over 19 000 employees in 46 countries. Business areas include biorefining in terms of pulp, timber and biofuels, electricity production, self-adhesive labels, paper and specialty papers and plywood. UPM is a Biofore Company referring to its business concept of using wood as a raw material in an innovative and efficient way. UPM's aim is to develop new high-quality alternatives to non-renewable materials profitably and responsibly. (UPM-Kymmene Oyj, 2018)

Along with UPM's business areas, other operations include wood sourcing and forestry, and UPM Biocomposites and UPM Biochemicals business units. This thesis is done for UPM Biochemicals, precisely for Lignin business. Related to Lignin business, UPM offers sustainable solutions such as UPM BioPiva^{TM} softwood kraft lignin powders for lignin-phenol-formaldehyde resin compositions, to replace their fossil-based raw materials. It is utilized in WISA® BioBond gluing technology (UPM Biochemicals, 2018).

UPM Northern Europe Research Center (NERC) is located in Lappeenranta, next to Kaukas mill site. The practical research of this thesis was carried out in NERC. R&D work in NERC focuses mostly on development of production processes of biochemicals and biofuels, fiber, paper and pulp (UPM Kaukas, 2018).

LITERATURE PART

Next, phenol-formaldehyde resins are reviewed in detail. Application of lignin in resins is studied, and resins are compared. Principles of curtain coating, partly based on paper technology, are studied. Factors affecting formation of stable curtain, surface chemical and rheological properties, are determined theoretically. Known, available analytical methods for determination of surface chemical and rheological properties are reviewed. Methods to affect these properties are determined.

3 PHENOL-FORMALDEHYDE RESIN

Resins are viscous liquids occurring in nature and produced synthetically, and used for adhesive production. Synthetic resins may be for example phenol-, urea- or melamine-formaldehyde resins (or mixtures of these), epoxy resins or isocyanate resins. Phenol-formaldehyde (PF) resins were the first synthetically produced polymers to be developed commercially (Pizzi, 2003b). Since their emergence, their use in the plywood industry grew rapidly as the most widely used adhesive (Sellers, 1985). Next, production and properties of PF resins are studied.

3.1 Production of PF resins

Phenolic resins are polycondensation products of the reaction of phenol (C_6H_5OH, Figure 3A) and formaldehyde (CH_2O, Figure 3B). In a condensation reaction, two or more molecules are combined and water or another simple substance is released. Chemical structure of phenol-formaldehyde (PF) resins is complex, because phenol as a polyfunctional molecule may react with formaldehyde in both *ortho* (two substituents next to each other in the aromatic ring) and *para* (two substituents on the opposite ends of the aromatic ring) positions (Pizzi, 2003b). Phenolic resin chemistry, structure, characteristic reactions and kinetic behavior has been widely studied in order to achieve specific physical properties for use in adhesive technology.

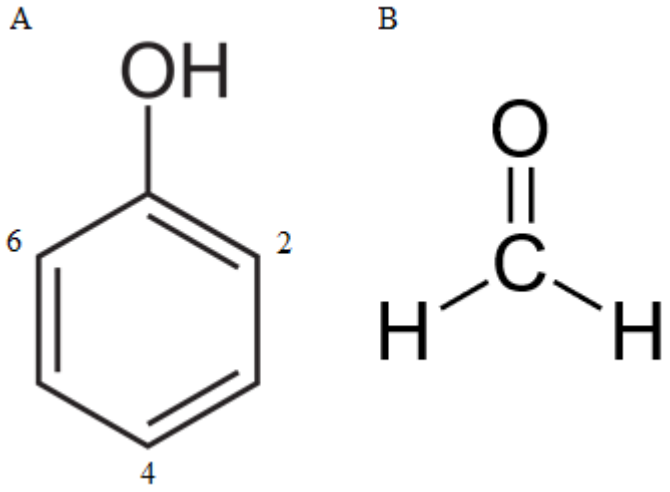

Figure 3 Chemical structure of A) phenol (C_6H_5OH) and B) formaldehyde (CH_2O).

Condensation reaction of phenol and formaldehyde happens in two phases. Phenol can react with formaldehyde at three possible *ortho* or *para* positions (sites 2, 4 and 6, Figure 3A), which allows 1-3 formaldehyde units to attach to the aromatic ring. Thus, phenol and formaldehyde form hydroxymethylolphenol (phenolic alcohol, Figure 4), di- and tri-alcohols. Formaldehyde can react with two phenols. (Pizzi, 2003b; Morrel, 2014)

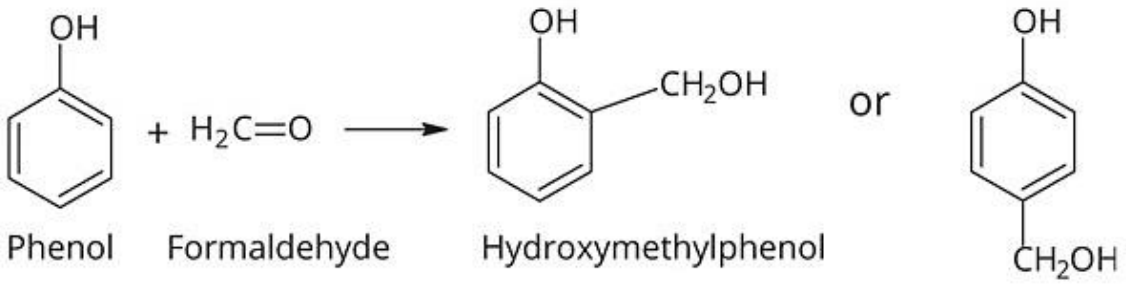

Figure 4 Reaction of phenol and formaldehyde to form hydroxymethylphenol in *ortho* and *para* positions, respectively from left to right (Morrel, 2014).

In the second stage of the reaction, upon heating, first linear polymers and then highly-branched structures are formed (modelled by Halász et al. (2001)). Phenolic alcohols, which contain reactive hydroxymethylol groups, commonly condense with available reactive positions in the phenolic ring (*ortho* or *para* to the hydroxyl group) to form methylene bridges. Phenolic alcohols may also condense with other hydroxymethylol groups to form ether links. In both cases water is released. (Pizzi, 2003b; Morrel, 2014) In Figure 5, methylene bridge and ether bridge are performed.

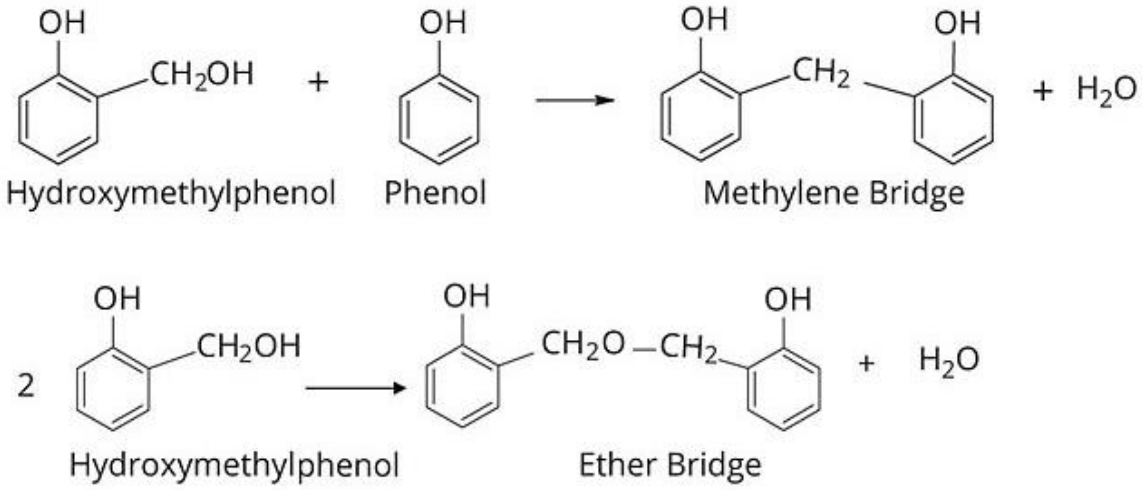

Figure 5 Hydroxymethylphenol reacts with available phenol to form methylene bridge or with each other to form ether bridge (Morrel, 2014).

Phenols condense with formaldehyde in the presence of acid or alkaline catalyst in high temperature. Thus, there are two types of PF resins, novolak and resol resins. Novolak resins are produced with acid (pH < 7) catalyst, and formaldehyde to phenol ratio < 1 (excess of phenol) (Sellers, 1985). Novolaks are by nature thermoplastic phenolic resins, which melt and flow during heating. Melting happens because novolaks are primarily linear and have no reactive hydroxymethylol groups (hardening agents) in its molecule and therefore cannot condense with other novolak molecules as the temperature rises but need additional formaldehyde to act as a hardener (Sellers, 1985; Pizzi, 2003b). Resol resins are produced with alkaline (pH > 7) catalyst, and formaldehyde to phenol ratio > 1 (excess of formaldehyde) (Sellers, 1985). Resols are thermosetting resins, which are irreversible hardened in high temperatures. Resol molecules contain reactive hydroxymethylol groups which condense forming large molecules, without addition of a crosslinker/hardener (Pizzi, 2003b). With resol resins, the glue joint is in principle one big adhesive molecule. Resols can be produced in wide variety of viscosities and molecular weights, and thus have more end-use possibilities than novolaks. Resins used in plywood production are commonly resol resins.

In the production of resol resins using alkaline catalyst, the first substitution reaction is faster than the subsequent condensation reaction. Thus, phenolic alcohols are initially the predominant intermediate compounds for the production. The differences between acid- or alkaline- catalyzed process are in the rate of aldehyde attack on the phenol, the subsequent

condensation of the phenolic alcohols and the nature of the condensation reaction. (Pizzi, 2003b)

Resol resins have three stages describing their curing and solubility. A-stage resol is initial resol, the product of resin cooking. Initial resols are flowing, having low molecular weight, and they are soluble in water and organic solvents like alcohols. Initial resols withstand extensive environmental factors (Sellers, 1985). When A-stage resol is heated, it turns into more viscous and swollen form as the molecular crosslinking initiates, and it is insoluble. This B-stage resol is called resitol and it is an intermediate stage. C-stage resol, resite, is achieved by further heating. Resites are greatly polymerized, having high molecular weight, totally insoluble and thermoset, they do not swell or melt anymore (Sellers, 1985).

Mildly condensed liquid resols have on average less than two phenolic nuclei in the molecule, whereas solid resols have on average 3-4, but with wider distribution of molecular sizes. In resols, small amounts of phenol, phenolic alcohols, formaldehyde and water are also present. Heating causes crosslinking through uncondensed phenolic alcohol groups, and possibly through reaction of formaldehyde liberated by the breakdown of the ether links. (Pizzi, 2003b)

Resol condensation (polymerization) reactions depend on resin cooking conditions: molar ratio of formaldehyde to phenol (F:P), temperature, reaction time, pH, the catalyst (Sellers, 1985) and dry matter content (DMC) of the resin. The higher the F:P ratio, the more branched/crosslinked structure of the adhesive, and thus better strength and moisture resistance properties (Sellers, 1985). As an alkaline catalyst for resols for plywood production, sodium hydroxide (NaOH) is preferred, since it has better water solubility than for example ammonia-, ammine- and amide-catalyzed phenolic resins. So, sodium hydroxide maintains the solubility (Pizzi, 2003b) and reduces viscosity (Sellers, 1985) of the PF resin. The amount of sodium hydroxide also affects the chemical reactivity, speed of cure and dry-out resistance. The dosage of catalyst can be done in 1-3 phases, so also the polymerization happens in 1-3 phases. Temperature is the second catalyst for the polymerization reaction, thus determining the polymer structure of the resin and the curing speed. The reaction temperature is 80-100 °C (Pizzi, 1994). The DMC affects also the

polymerization rate and viscosity of the resin. The reaction time is 1-8 h depending on pH, F:P ratio, temperature and possible presence of reaction retarders (Pizzi, 1994).

Viscosity of the resin is in relation to polymerization rate. As the polymerization proceeds, viscosity increases (Morrel, 2014), but the polymerization time has to be sufficient for molecules to react. The polymerization time and number of polymerization phases affect the free formaldehyde content of the finished resin and the strength of the polymer structure. Also stable and efficient mixing of the resin during cooking is critical to ensure controlled and uniform cross-linking. By lowering the temperature, polymerization can be slowed down, and higher temperature accelerates the reaction. When the desired viscosity of the resin has been reached, the temperature is lowered, which stops the polymerization reaction at the point where the resin is still water-soluble and reactive (Pizzi, 1994). The desired viscosity is determined based on end-use application of the resin. In the plywood hot-press, high temperatures are again applied, which allows resin to cure to final C-stage (Sellers, 1985).

Depending on the end-use application, the resin composition varies. Demands for resins may vary between plywood mills or between countries and continents depending on the final product (characteristics and requirements based on standards), known technologies for adhesive application (rollers, curtain, spray or extruder coater) and used raw materials (costs and availability, for example typically used wood species). Typical resol resin composition for application in plywood production is presented in Table I (Sellers, 1985).

Table I Typical resol resin chemical ratios and composition for application in plywood production (modified from Sellers (1985)).

Chemical ratios	**mol ratio range**
F:P	1,9-2,2
NaOH:P	0,4-0,6
Composition	**DMC % range**
PF (excluding NaOH)	25-35
NaOH	2,5-9,5
Starch	0,1-1,0

Urea	0-5,0
Methanol	0-4,0
Tackifier	0,01-0,05
Anti-foam agent	0,005-0,1
Plasticizer	0,05-0,5
Wetting agent	0,005-0,1
Curtain additives	0-1,0
Total	40-45

For softwood (conifer) plywood, higher resin alkali content and higher molecular weight are required when compared to hardwood (broadleaved tree) plywood resin. Thus, softwood plywood cure at faster rate and hardwood plywood requires longer pressing time. On the other hand, the cold-press tack (preliminary adhesion) is not as good with hardwood than with softwood. (Pizzi, 2003b)

3.2 Properties of PF resins

The most remarkable resin properties are viscosity, dry matter content (DMC), pH and gel time (Sellers, 1985). These properties have an effect on resin end-use possibilities, as already reviewed in resin cooking conditions. Typically, resins for plywood have DMC of 40-45 % and viscosity of 150-600 cP at 25 °C (Pizzi, 2003b). Other properties are alkalinity, free formaldehyde content, phenol and methanol content, molar mass and conductivity. Properties of PF resins are modified in order to achieve mill specific regulations by varying the resin composition and cooking conditions.

Special additives may also be added to resin composition to meet performance requirements. Some commercially utilized chemical additives and their effect on PF resin properties are summarized in Table II. Additives are a raw material cost, which are desired to be avoided or minimized to reduce production costs. For example, plasticizers and tackifiers are usually avoided unless absolutely needed (Sellers, 1985). However, additives are a simple way to obtain specific properties, and usually the required amount of additive is not high (Table I). Too high amount of additive causes adverse effects on PF resin performance. Curtain coating adhesives require special additives and relatively high amount of them, because stable curtain formation is a challenge hard to overcome with only resin composition adjustments

(Sellers, 1985). Additives must be compatible in the resol PF resin environment, for example high alkalinity (Seller, 1985).

Table II Additives and their effect on resins to meet performance requirements (collected from Sellers (1985) and Pizzi (2003)).

Additive	**Effect**
Starch	Improved dry-out resistance, improved cold-press tack
Urea	Reduced amount of free formaldehyde, phenol substitute, viscosity reduction, shortened hot-press time
Methanol	Solvent, improved adhesive penetration into wood
Tackifier	Improved cold-press tack
Anti-foam agent	Reduced foam generation upon mixing the adhesive, accelerated foam collapse
Plasticizer	Improved resin flow for highly polymerized resins
Wetting agent	Optimized resin flow, improved adhesive penetration into wood
Curtain coating additives	Improved curtain formation and stability (surfactants such as wetting agents, film-forming celluloses such as thickeners)

In addition, fillers, extenders and hardeners are generally added to the plywood adhesive mix. They are applied to accelerate curing of the glue joint in the hot-press by increasing the solids content of the resin. Shorter hot-press saves energy consumption of the process. For example, flours and calcium carbonates can be used as fillers and formaldehyde as hardener.

The requirements for plywood PF resin/mixed adhesive include:

- sufficient cold-press tack
- sufficient dry-out resistance for open-time in production (time before pressing)
- fast cure rate in hot pressing to save pressing time

- high wood failure results (over 90 %), low glue joint failure
- free formaldehyde in resin (relates to process handling)
- storability of resin.

The optimal composition of PF resin must be carefully designed in order to achieve minimum requirements. As stated, the higher F:P molar ratio, the better strength properties, but meanwhile also free formaldehyde content increases. High free formaldehyde content results fumes in production and is toxic for humans. Good strength properties of the cured resin are essential to ensure high quality products. The glue joint must be stronger than wood (Koponen, 2002). This is observed when piece of plywood is teared apart and glue joint becomes visible. If the glue joint is highly covered with wood splinters, the glue joint is strong (high wood failure).

Resin/adhesive should not dry-out before pressing, since otherwise the veneers will not stick together. Dry-out is affected by wettability of the resin, but too wet resin penetrates too much into the wood. The higher polymerized resin, the faster curing in the plywood production (Sellers, 1985), but here the resin is also more viscous which complicates the spreading of resin/adhesive. Also, the amount of sodium hydroxide affects the curing and dry-out resistance, but excess of sodium hydroxide results slower gel time and higher penetration of resin into wood (Pizzi, 1994).

All resol solutions are thermosetting resins, which continue polymerization even in low temperatures (5-15 °C). The storage time of resins is limited, since the viscosity increases slowly by itself. The lower the temperature, the slower polymerization. The viscosity of the resin is temperature-dependent, the viscosity is higher in low temperatures, and vice versa. (Sellers, 1985) Only resin is stored for longer times, since the viscosity of finished adhesive with fillers increases even faster. The disposal of liquid resins and adhesives must be carried out at specific waste treatment plants. Cured resin can be disposed as non-hazardous waste.

The biggest advantages of PF resol resins are in moisture and heat resistance when compared to other resins, which allows their exterior use (Koponen, 2002; Pizzi, 2003b). Highly crosslinked nature of phenolics gives them their hardness and thermal stability, and that makes them impervious to most chemical attacks and solvation (Morrel, 2014). High

modulus of elasticity, tensile strength, dimensional stability and low flammability are typical for PF resins.

PF resins used in Finnish plywood production are not toxic. High alkalinity may cause skin reactions, eye damage and it may be corrosive to metals. However, the main raw materials, phenol and formaldehyde, are both acutely toxic chemicals (Merck KGaA, 2017a; Merck KGaA, 2017b). The exposure to phenol and formaldehyde (via skin, mouth or breathing) causes death, cancer and mutagenic effect, and is a major risk in resin production. Other disadvantages are non-renewability of raw materials and their relatively high cost. Phenol is synthetically produced from crude oil and formaldehyde from natural gas, which both are fossil-based raw materials (Sellers, 1985). Phenol price is related to oil price and fluctuates. When compared to urea-formaldehyde resins, PF resins require longer pressing times and the glue joint is dark by color, which makes it visually less attractive (Pizzi, 1994; Dunky, 2003). However, superior durability properties of PF resin enable multiple end-use possibilities and maintains the PF resin demand.

3.3 Plywood adhesives

Plywood adhesive composes of resin, water, fillers and possible additives. Resin production is stopped at the point where it is still liquid, reactive and soluble in water (Koponen, 2002). A typical plywood adhesive composition is presented in Table III (Pizzi and Ibeh, 2014).

Table III Typical plywood adhesive composition (Pizzi and Ibeh, 2014).

Component	Parts per hundred resin
Phenolic resin	100
Water	0-20
Filler	5-10
Extender	0-10
Hardener (formaldehyde)	0-5
Solubilizer (NaOH)	0-10

Fillers, extenders and hardeners are used to accelerate the curing of adhesive in hot-press and to achieve desired viscosity of the adhesive. Fillers increase the solids content of the resin and addition of formaldehyde (hardener) accelerates the polymerization reaction of the PF resin. Powder fillers thicken the adhesive. The thickening phenomenon lasts for a few hours, which must be taken into account in adhesive preparation. Water is added as a solvent

to the adhesive composition to adjust the solids content and viscosity to desired values. Water evaporates in the hot-press, and thus, the solids of the adhesive finally form the glue joint. Generally, adhesives are mixed daily in the plywood mills, since storing of resins is more stable. Proper mixing of the adhesive is important, since homogenous composition of the resin is critical, but generation of foam is undesired. Special additives may be added to the resin or adhesive composition and are reviewed more precisely earlier in properties of PF resins. Resins and additives must be compatible to be applied together (for example high pH must be considered).

Adhesive is spread onto the veneers, where easy application and uniform and sufficient layer of adhesive is important. Viscosity of the resin is one of the main parameters in adhesive spreading. Piled up veneers may not be directly pressed, and adhesive must endure the production open-time without drying. After the cold-press, preliminary adhesion, tack, must keep the veneer assembly together. In the hot-press, resin polymerization reaction, curing, is finished. Hardening characteristics of the resin, reactivity and crosslinking, affect the pressing temperature and time. If the glue joint is wet after pressing, the pressing temperature is too low and pressing time too short. Adhesive must not be absorbed too much into the wood. Here, too moist veneer, too low viscosity of the adhesive and too low pressing temperature affect the glue joint quality. After the press, glue joint must be stronger than wood. (Koponen, 2002; Dunky, 2003) Typical values of PF resins and plywood production are presented in Table IV.

Table IV Properties of PF resins and plywood production (Pizzi, 1994; Koponen, 2002).

Property	**Typical values**
Resin pH	11,0-12,5
Resin solids content	41-52 %
Resin storage time (25 ºC)	3 months
Veneer moisture content	max 6 %
Open time in production (time between adhesive application and cold-press)	max 30 min
Cold-press pressure	0,5-1 MPa
Cold-press time	5-10 min
Closed time in production (time between cold- and hot-press)	1-12 h

Hot-press pressure	Birch: 1,7-1,8 MPa Softwood: 1,1-1,3 MPa Mixed: 1,3-1,5 MPa
Hot-press temperature	125-130 ºC

To summarize, general requirements for plywood adhesive and requirements to intensify plywood production process are presented in Table V (Dunky, 2003).

Table V General requirements of plywood adhesive and requirements to intensify plywood production process (Dunky, 2003).

General requirements of plywood adhesive	**Requirements to intensify plywood production process**
Composition, solids content, viscosity, purity, color and smell, compatibility for additives	Cheaper raw materials and alternative products
Easy application, low risks	Modification of the wood surface
Gluing quality, climate resistance	Better hygroscopic behavior of boards (e.g. lower thickness swell, better outdoor performance (moisture resistance))
Cold tack behavior, hardening characteristics (reactivity, hardening, crosslinking)	Shorter press time, shorter cycle times → increased production rates
Emission of monomers, VOC and formaldehyde	Reduction of emissions during production and the use of wood-based panel
Ecological behavior: life cycle analysis, waste water, disposal etc.	Utilization of life cycle assessment, energy and raw material balances, recycling and reuse
Storage stability, low transportation risks	

3.4 Applications

PF resins are used for wood binders, especially for plywood and particleboard. Other possibilities are for example, another wood composites, such as oriented strand board (OSB) and laminated veneer lumber (LVL), laminate binding, such as high pressure laminates (HPL) and insulation glass fibers (Pizzi and Ibeh, 2014).

In particleboards, wood chips are generally sprayed with resin, a chip mat is formed and pressed (Pizzi, 2003b). Particle board resins should thus have relatively low viscosity and strongly pseudoplastic behavior is preferred (BASF, 2016). Also for OSB resin, lower viscosity is preferred and for example urea may be added to resin composition to reduce viscosity (Winterowd et al., 2010). Laminate resins differ remarkably from wood binding resins. Laminate is composed of stacked, resin impregnated papers. In resin production, it is not desired to form large polymer chains, the molecular weight and viscosity are kept low. This is achieved by one polymerization step, cooking in low temperature and long cooking time, in addition to calm mixing. This way efficient impregnation is achieved.

Phenolic resins can also be applied for example in binding of foundry molds (resol and novolak resins) and together with other resins (urea-formaldehyde and/or melamine-formaldehyde) (Pizzi, 2003b). PF resins can be for example applied into the core layers of multi-layer wood composites and laminates, and other resins can be used for binding the surface layers. Thus, finished product has good strength and moisture resistance properties, but the dark color of PF resin can be avoided in the surface.

4 LIGNIN-PHENOL-FORMALDEHYDE RESIN

Lignin is the second most abundant biopolymer after cellulose, located in the cell walls of plants. However, lignin is largely ignored as a raw material. Purified lignin contains high number of functional hydroxyl groups, which makes it an attractive target for research and development (R&D) of new bio-based alternatives for fossil-based chemicals, transportation fuels, carbon fibers etc. (Alén, 2011; Valmet, 2018). The principles of sustainable development promote utilizing renewable raw materials energy and cost efficiently. Application of lignin perfectly fits for this purpose and offers multiple end-use possibilities. Next, lignin and its application in resins are studied.

4.1 Lignin

Lignin is a wood cell structural component in addition to carbohydrates (cellulose and hemicellulose). Non-structural components (extractives, some water-soluble organics and inorganics) represent a minor fraction of wood cells and are mostly composed of low-

molecular weight compounds, largely situated outside the cell wall. In the wood cell wall, also some small amounts of pectins, starch and proteins are present. (Alén, 2011)

The distribution of structural components varies between the different parts of the tree and wood species. Stem wood is the biggest part of the wood generally utilized for pulping. Stem wood cellulose, hemicellulose and lignin contents of the wood dry matter content are approximately 40-45 %, 25-35 % and 20-30 %, respectively. Softwood usually contain less hemicellulose and more lignin than hardwood. A typical chemical composition of dry stem wood is presented for both softwood and hardwood in Table VI. It can be concluded that high molecular mass substances compose 95 % of the wood dry matter and low molecular mass substances 5 %. Tropical species usually contain more extractives and tropical hardwood contain more lignin.

When compared to bark of the wood, the amount of extractives, organics and inorganics is multiple and the amount of structural components is 40-70 %. Forest residue is more similar to stem wood. With bark and forest residue, the variation between different species is stronger. Lignin is also available from other plants, referred as non-wood lignocellulosic materials. These are classified into agricultural residues (for example sugar cane bagasse and rice straw), natural-growing plants (for example bamboo and reeds) and non-wood crops grown primarily for their fiber content (for example bast fibers such as jute and hemp). An average chemical composition of bark, forest residue and non-wood feedstock are presented in Table VI.

Table VI Chemical composition of dry stem wood for softwood and hardwood, bark (inner and outer bark), forest residue and non-wood feedstock as percentages of the feedstock dry matter content (collected from Alén (2011)).

Component	**Softwood (pine)**	**Hardwood (birch)**	**Bark**	**Forest residue**	**Non-wood feedstock**
Cellulose	40-45 %	40-45 %	20-30 %	35-40 %	30-45 %
Hemicellulose	25-30 %	30-35 %	10-15 %	25-30 %	20-35 %
Lignin	25-30 %	20-25 %	10-25 %	20-25 %	10-25 %
Extractives	3,5 %	3,5 %	5-20 %	~ 5 %	5-15 %
Other organics	~ 1 %	~ 1 %	5-20 %	~ 3 %	-
Inorganics	0,5 %	0,5 %	2-5 %	~ 1 %	0,5-10 %
Proteins	-	-	-	-	5-10 %

A plant cell (wood cell is called fiber) is hollow. The cell wall composes of two layers. Lumen, central cavity, is surrounded by relatively thick secondary wall layer, which further composes of three sublayers, S_3, S_2 and S_1, respectively from inside outwards. Sublayers are separated based on the orientation of their structural elements (microfibrils) and, to some extent, the chemical composition. Secondary wall layer is surrounded by thin primary wall. Between adjacent cell primary walls, middle lamella is located. (Alén, 2011)

The middle lamella between the cells and primary wall of the cell composes mostly of lignin (65 % of the total dry matter content of the layers, softwood) and secondary wall of polysaccharides (75 % of the total dry matter content of the sublayers, softwood). However, since the S_2 sublayer is the thickest sublayer, most of lignin is actually located in there. (Alén, 2011) From this it can be concluded, that the function of lignin in wood is to bind fibers together by filling the space between the cells, and to bind cellulose and hemicellulose together in secondary cell wall. Lignin has complex, three-dimensional structure which contributes to this function. Highly cross-linked structure offers durability, mechanical strength and resistance to moisture, UV-radiation and bacterial and fungal attack (Mattinen, 2016).

Lignin is by nature amorphous, heterogenous, hydrophobic, complex polymer. Lignin aromatic structural elements, phenylpropane units, are cross-linked randomly. (Mattinen, 2016) There are two major classes of lignins: native lignins and technical lignins. Native lignins can by further divided based on their natural origin and lignin type:

- softwood lignin, referred as guaiacyl lignin
- hardwood lignin, referred as guaiacyl-syringyl lignin
- grass lignin, referred also as guaiacyl-syringyl lignin, but includes also *p*-hydroxyphenyl derivatives.

Terms guaiacyl and guaiacyl-syringyl lignins originate from the three basic *p*-hydroxycinnamyl alcohols, from which the structural elements are derived for each lignin type (Alén, 2011; Mattinen, 2016). Majority of lignin structural building blocks are bonded by either ether linkages (C-O-C) or carbon-carbon linkages (C-C). In addition to these, numerous miscellaneous linkages and minor structures are known.

Technical lignins are industrial by-products, mainly from chemical pulping. Technical lignins are generally the raw materials for the new generation lignin-based products. The whole tree is desired to convert into attractive end-products. Thus, lignin separation technologies have been developed to be integrated with pulp mills, where conventionally only cellulose and hemicellulose are utilized as pulp. Lignin supply scale-up is thus relatively simple. Technical lignins are (Alén, 2011):

- kraft lignin (sulphate lignin), derived from kraft (sulphate) pulping of wood
- alkali lignin (soda lignin), derived from soda-AQ pulping of wood
- lignosulphonates, derived from sulphite pulping of wood
- organosolv lignin, derived from organic solvent pulping of wood
- acid hydrolysis lignin, derived from acid hydrolysis processes of wood.

Kraft lignin is the most essential technical lignin to be used as raw material since its availability from kraft pulping, which is the most widely used pulping technology worldwide.

One known, commercial example of lignin separation technologies is LignoBoost process offered by Valmet. LignoBoost is developed to produce kraft lignin from black liquor. In conventional kraft pulping, lignin is dissolved into the cooking liquor, white liquor, containing mainly sodium hydroxide and sodium sulphite. Thus, cellulose and hemicellulose fibers are cleaved. The cooking liquor turns into black liquor, of which dry matter content approximately 25-31 % is lignin (Alén, 2011). Black liquor is concentrated into higher solids content and burned, since the calorific value is high. With LignoBoost process, the black liquor is taken from the evaporation plant, and lignin precipitated with carbon dioxide (CO_2). Lignin is then dewatered, conditioned with acidified wash water and again dewatered, resulting practically pure lignin cakes. Lignin is usually dried to desired solids content (for example 65-95 %). LignoBoost increases the capacity of the black liquor evaporation recovery boiler. Produced lignin is suitable for production of biochemicals, for sulphonation and removing odorous compounds is possible. LignoBoost plants currently operate at Domtar (USA) and StoraEnso (Finland). (Valmet, 2018)

Lignin functional groups are methoxyl, phenolic and aliphatic hydroxyl groups and some terminal aldehyde groups in the side chain. Relatively few phenolic hydroxyl groups are free, because they tend to bond with adjacent phenylpropane units. (Alén, 2011) Lignin has

antioxidant property from the radical scavenging capacity of phenolic groups, and lignin can act as thermoplastic or thermosetting material due to its aromatic structure (Mattinen, 2016).

Detailed chemical structure of lignin remains unsolved, since the isolation of lignin always causes partial degradation of lignin. Lignin has complex, irregular structure. Multiple different schemas of lignin chemical structure have been proposed (Figure 6). Lignin has variable molecular size due to random cross-linking of the polymer originating from radical-coupling reactions between phenolic radicals (Calvo-Flores and Dobado, 2010).

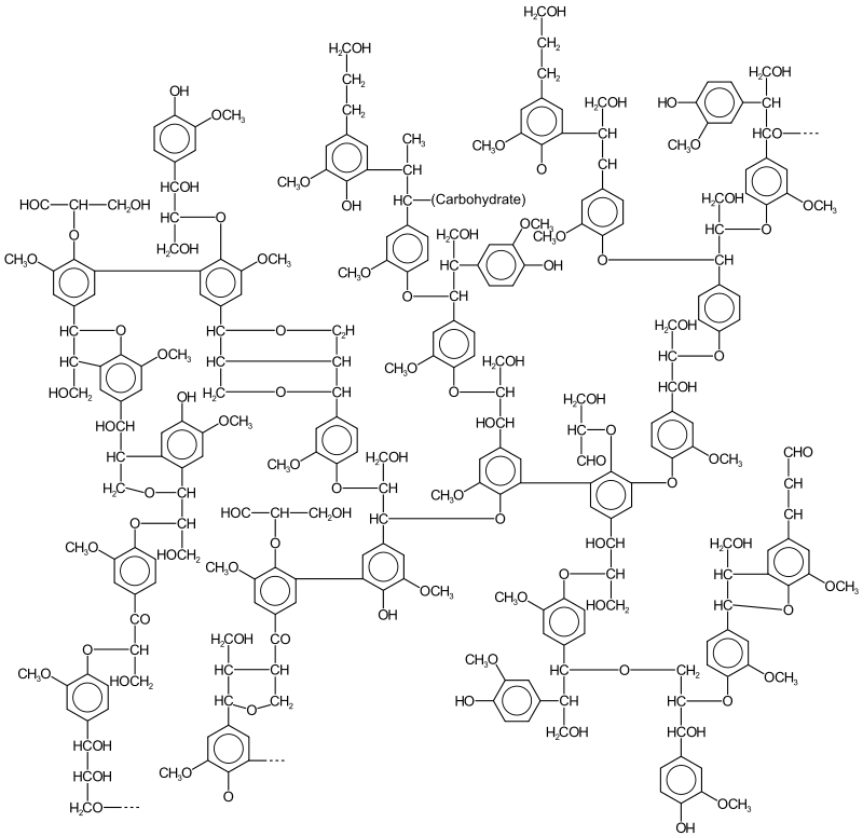

Figure 6 Chemical structure of lignin (Glazer and Nikaido, 1995).

Since technical lignins are abundantly available from pulping processes, the price of lignin is profitable. Lignin as a bio-based, renewable and sustainably sourced raw material is an attractive alternative for fossil-based chemicals. It is also non-toxic, which is a remarkable advantage for process safety. Complex structure of lignin is both a possibility and a disadvantage. Research and development of lignin-based products is challenging, because the precise chemical structure is not known and thus the compatibility to replace conventional chemicals or other raw materials is not known. Also, the lignin raw material

feedstock is not as constant as with synthetic chemicals. This may result variation also in the end-product quality. On the other hand, wide variety of functional groups enable multiple end-use possibilities. Complex structure also is the basis for durability and mechanical strength.

4.2 Applications

The most essential source of lignin is black liquor from pulping process, since this way the wood components are completely utilized, and an effective separation technology for lignin exists (LignoBoost). Apart from burning the black liquor as bioenergy, black liquor has been used only for a few applications. However, since the economic and environmental potential of lignin has been noticed, new end-use possibilities have been widely screened and developed.

Earlier, lignin application has focused on using lignosulfonates. Lignosulphonates can be used as binders, dispersant agents for pesticides, emulsifiers and heavy-metal sequestrants. They can for example stabilize emulsions of unmixed liquids (asphalt emulsions, pesticide formulations, wax emulsions, pigments and dyes) making them highly resistant to break-down and low toxicity allows their use as binders in animal feed and soil stabilizers in agriculture. (Calvo-Flores and Dobado, 2010) Synthetic vanillin and dimethylsulfoxide are also well-known products derived from lignin, but they have only relatively low market volume (Holladay et al., 2007).

Opportunities of lignin utilization has been categorized by Holladay et al. (2007) and are presented in Table VII. The focus is nowadays more in high-value products (macromolecules and aromatics), such as low-molecular-weight (LMW) compounds as an alternative for petrochemical industry and active carbon and carbon fibers (Calvo-Flores and Dobado, 2010).

Table VII End-use opportunities of lignin (collected from Holladay et al. (2007)).

Product type	**Characteristics**	**Examples**
Power, fuel and syngas	Lignin used as a carbon source	Heat, power, methanol/dimethyl ether, green gasoline via Fischer-Tropsch technology, mixed alcohols
Macromolecules	Lignin isolated as natural, high-molecular weight molecule	Vanillin, dimethylsulfoxide, carbon fiber, composites, copolymers, resins, adhesives
Aromatics and miscellaneous monomers	Lignin macromolecular structure degraded but aromatic nature maintained	Benzene, toluene, xylene, phenol, lignin monomer molecules, oxidized lignin monomers, diacids, polyols

Lignin as a copolymer can be utilized either directly or chemically modify lignin beforehand. Due to its aromatic nature, lignin can be incorporated into a wide range of reactions, such as alkylation, methylolation, sulfonation, oxidation and reduction. Without modification lignin can be used in phenol-formaldehyde (PF) resins as a filler, in polyolefin (polyethylene or polypropylene) or polyester polymers, as a source for polyurethanes (polyethylene or polypropylene glycols) and bio-plastics (Calvo-Flores and Dobado, 2010). Chemical modification contributes to determination of lignin functional groups. Chemically modified lignin can be used in PF resins as a substitution to phenol. Chemical modification activates lignin by introducing more reaction sites towards formaldehyde.

Incorporation of lignin into biopolymer adhesives as a reinforcement for biocomposites has gained maybe most of the R&D interest. Complex structure and reactivity of lignin usually challenge the blending of lignin with other polymers. Thus, focus is also in improvement of mixing properties, and in thermal and mechanical strength enhancements. (Mattinen, 2016)

Nonetheless, there are only a few commercial examples of utilization of lignin in modern day applications. UPM's WISA® BioBond plywood products have been glued with adhesive containing LPF resin and it is in industrial scale use. In the adhesive, 50 % of the used phenol is replaced by kraft lignin and the adhesive retains the same high-quality

properties as conventional PF resin-based adhesives. The proportion could be further increased with BioPiva^{TM} lignin. (UPM Biochemicals, 2018; WISA BioBond, 2018)

Lignin as a raw material has been studied over a century and amount of research required demonstrates the complexity of lignin utilization. New technologies to convert lignin economically into high-quality end-products are required. When the commercial applications expand, supply of lignin can be easily multiplied, since lignin separation plant is relatively simply to integrate next to a conventional pulp mill. There are approximately 70 million tons of lignin annually available only from the pulp mills, of which only a couple of percentages are used commercially (Dunky, 2003).

4.3 Production of LPF resin

Due to large consumption and rising prices of fossil resources, increasing concern and awareness of environmental issues, lignin utilization as phenol substitution in phenol-formaldehyde (PF) resins has been widely considered. This is due to its amorphous and aromatic nature, structural phenylpropane units somehow comparable to phenol. During pulping and isolation of lignin from black liquor, lignin structure degrades but also lignin water solubility is enabled (Pizzi, 1994). Other possible bio-based alternatives for wood adhesives are for example tannins, proteins, carbohydrates or unsaturated oils.

Direct reaction of raw lignin with phenol and formaldehyde has performed lignin acting more like a filler in adhesive composition rather than as a substitute for phenol. This is due to low reactivity of lignin (macromolecule) when compared to small molecule phenols, which contain more reactive sites for polymerization reactions (Mattinen, 2016). Practically, the reactive sites of lignin are already filled. Lignin has only approximately 0,3 reactive sites in phenylpropane unit, whereas phenol has three reactive sites (Hu et al., 2011; Mankar et al., 2012), and in addition, those reactive sites may be filled with functional groups.

Rather low-molecular-weight (LMW) lignin should be used in production of lignin-phenol-formaldehyde (LPF) resins. It can be assumed to be less cross-linked, having naturally more reactive sites free towards formaldehyde. This has been recognized for example by McVay et al. (1993), who concluded that LMW lignin has higher reactivity and lower viscosity than high-molecular-weight (HMW) lignin. Low viscosity of the lignin contributes less to

viscosity development of the phenolic resin. LMW lignin was obtained by two-step ultrafiltration process. However, technical lignins available generally have high-molecular-weight. Softwood lignins are easier to utilize into PF resins due to open ortho positions in the chemical structure (Mankar et al., 2012). Lignin can be added at the beginning or during the cooking procedure, or at the end of the condensation reaction (with a following reaction step between the lignin and the phenolic resin) (Pizzi and Ibeh, 2014).

As a solution for low reactivity of lignin, methods to chemically modify lignin prior the application into the resin have been developed. Modification increases the chemical reactivity of lignin hydroxyl groups, number of reactive sites in lignin towards formaldehyde or depolymerizes lignin. Modification fastens the polymerization reaction of lignin and formaldehyde and improves strength properties of the finished adhesive. Most studied lignin modification methods are methylolation (also known as hydroxymethylation and hydroxyalkylation), demethylation (also known as dealkylation) and phenolation (Hu et al., 2011: Laurichesse and Avérous, 2014).

Methylolation introduces hydroxymethyl (-CH_2OH) groups to lignin molecule. Methylolation is performed in alkaline medium, where lignin reacts with formaldehyde. Major advantage of this method is direct incorporation into PF resol resin preparation. In phenolation of lignin, phenol condensates with lignin aromatic rings and side chains. As a result, lignin molecular weight is reduced, and reactive sites are emerged. Phenolation is performed on acidic medium and used especially for lignosulfonates. After phenolation of lignin, it is possible to produce both resol and novolak PF resins. Demethylation treatment removes methyl groups from blocking the reactive aromatic hydroxyl groups in lignin structure. Demethylation is sulfur-mediated in alkaline medium, and it is possible to remove one or both methyl groups ortho to phenolic hydroxyl group. (Hu et al., 2011: Laurichesse and Avérous, 2014)

Another method for increasing the reactivity of lignin is alkalation of lignin (Pietarinen et al., 2014). In alkalation, lignin is first treated with hydroxide of an alkali metal (for example NaOH), and heated. It is possible to combine phenolation prior to alkalation or hydroxymethylation after the alkalation. Alkalation as a method for increasing the reactivity of lignin has been used especially for plywood adhesive production (Pietarinen et al., 2014).

So, in the production of LPF resins, modification of lignin beforehand has been proved profitable. It would be advantageous, if lignin modification could be integrated into the resin production process as a first processing step, which is possible at least with methylolation, phenolation and alkalation methods (McVay,1993; Raskin et al., 2001; Pietarinen et al., 2014). McVay (1993) used hydroxymethylation for softwood kraft lignin to increase reactivity prior to PF resin preparation. For hardwood kraft lignin, phenolation was used for lignin prior to PF resin preparation. Resin production should result a resin with same properties than conventional PF resin, which would enable functionable adhesive mixing, spreading and curing in plywood production.

Still, partial substitution of phenol with lignin has been challenging. For example, modification of organosolv lignin with methylolation, use of lignin separated from eucalyptus (by acetosolv delignification), oil palm (by kraft and soda pulping), jute sticks and grass (by soda pulping), use of unmodified or modified kraft lignin (Mankar et al., 2012), lignosulphonates or pulping liquors (Pizzi, 1994) are widely studied methods to replace phenol in PF resins. However, during modification, undesirable side reactions may occur (Laurichesse and Avérous, 2014), highly acidic conditions (especially required for lignosulphonates modification) may be corrosive to steel reactors (Pizzi, 2003a) and due to varying lignin feedstock, constant properties for resins are not achieved (Dunky, 2003). Addition of lignin into resins may affect the resin preparation methods, weaken the adhesive strength properties, decrease resistance to moisture, slow down the pressing time etc. Also, lignin function in PF resins has been questioned, whether it actually participates in resin polymerization reactions, or does it act like a filler despite the addition point and possible modification (Pizzi and Ibeh, 2014).

In laboratory or pilot scale researches during the past 20 years, approximately 40-70 % of the weight of the phenol may have been replaced by lignin without remarkable changes in resin cooking procedures, plywood process conditions or finished resin, adhesive or plywood quality (Danielson and Simonson, 1998; Pizzi, 2003a; Mankar et al. 2012; Laurichesse and Avérous, 2014). In patents, approximately 15-30 % of the weight of the phenol replaced by lignin has been proved successful (Doering, 1992; Raskin et al., 2001; Winterowd et al., 2010). However, commercialization has not been done extensively.

4.4 Properties of LPF resin

The objective of production of lignin-phenol-formaldehyde (LPF) resins is to achieve the same properties for LPF resin than to conventional phenol-formaldehyde (PF) resins without lignin. It is desired, that the LPF resin production process does not differ remarkably from PF resin production process to ensure efficiency. The major differences of LPF resin production process and properties to PF resins reported are higher viscosity and slower curing (McVay, 1993).

Generally available high-molecular-weight (HMW) lignin has relatively high viscosity, which results rapid viscosity development of the resin during cooking. Thus, polymerization of the resin may not be as developed as with PF resins, even though the same viscosity is achieved. Viscosity development must be hindered by lower temperature and calm mixing to control and ensure uniform crosslinking of the substances in resin mixture. Polymerization degree affects the curing time of the resin, since more polymerized resin cures faster. Complete substitution of phenol with lignin in PF resins has been hindered due to these challenges, but research and development is continuing to achieve higher substitution portions.

These phenomena have been reported for example by Peng and Riedl (1994), Danielson and Simonson (1998) and Pizzi (1994; 2003a). Peng and Riedl (1994) studied chemical kinetics (reaction rate and reaction rate constant) of curing reaction of PF resins mixed with ammonium salt lignin or methylolated ammonium salt lignin fillers. The chemical kinetics are related to increase of number average molecular weight (M_n). It was discovered, that viscosity is closely related to weight average molecular weight (M_w). Cure rate of the resin decreased by the increasing the amount of lignin fillers.

Danielson and Simonson (1998) noticed more rapid viscosity development of LPF resin when compared to PF resin when producing resin with 50 % phenol substitution with unmodified kraft lignin. LPF resin polymerization was controlled by lowering the resin cooking temperature and prolonging the cooking time. LPF resin also required 1 minute longer hot-pressing time of plywood (or higher temperature), but resulted similar or better end-product properties than with conventional PF resin.

Pizzi (1994; 2003a) reported successful 30 % substitution of phenol with methylolated lignin, when producing plywood resin, without any performance changes. It was stated, that there is a possibility to increase the amount of substitution by prolonging the pressing time and increasing pressing temperature. It can be concluded, that curing of LPF resin differs to conventional PF resins, and longer pressing times and higher pressing temperatures are generally required.

5 CURTAIN COATING

Plywood is wood product used for furniture and building material. Plywood composes of thin (for example 1,5 mm thick) wood sheets, veneers, onto which adhesive is spread. Adhesive spreading methods can be categorized to contact and non-contact methods. Curtain coating is one of the non-contact adhesive application methods. Other used coating methods are for example rollers (requires mechanical contact) and spraying (non-contact). Next, plywood production is shortly described, curtain coating as an adhesive spreading method and properties of suitable curtain coating materials are studied more detailed.

5.1 Principles of curtain coating

In plywood production, adhesive is spread onto one or both sides of the veneers and veneers are cross-piled to enhance mechanical strength of the finished plywood. The number of veneers for the plywood assembly depends on the desired thickness of the final product. Veneer piles are first cold-pressed in room temperature and high pressure and later hot-pressed in high temperature and differencing pressure zones. The high temperature in the hot press hardens the adhesive finally. Cold press is usually required because after the cold press it is possible to store the plywood for 1-12 hours and thus effectively use the capacity of the hot press. After the cold press the veneers already stick together and are easily movable. (Koponen, 2002)

Curtain coating is one of the methods to spread the adhesive in plywood production. There are two main types of curtain coaters, slot and slide applicators, of which the slot applicator (also known as pressure head curtain coater) is more widely used (Sellers, 1985). In Figure 7, a basic slot curtain coater is presented. The adhesive is pumped up to the applicator head, and the gap at the bottom of the head is closed. When the adjustable gap opens, the adhesive

curtain falls freely down as a thin film. The adhesive curtain settles onto one side of the veneer, when the veneer moves through the curtain on high speed production line. Excess adhesive is collected into trough straight under the coating head for re-pumping.

Figure 7 Basic slot curtain coater.

In the assembly phase, the required number of similar, coated veneers are cross-piled and blank surface veneer is placed on top of the plywood. Then the plywood is pressed. Curtain coating is recommended especially for thick or varying sizes of veneers, which are impractical to input through the rollers or would often require roller adjustment (Koponen, 2002).

Range of operational parameters for veneer curtain coating are presented in Table VIII, collected from Sellers (1985).

Table VIII Range of operational parameters for curtain coating of veneer (Sellers, 1985).

Parameter	**Range**	**Unit**
Width of the applicator (width of the curtain)	660-2440	mm
Positive displacement pump, operating pressures	1725-3450	kPa

Applicator head, operating pressures	12-35	kPa
Conveyor speed (production line)	60-120	m/min
Width of the gap (curtain thickness)	1,5-2,5	mm
Height of the curtain	50-350	mm
Operating temperature	24-35	°C

A few notes about the operating parameters (Sellers, 1985):

- Applied coating layer thickness is varied by the speed of pumping and the speed of conveyor. Layer thickness is directly proportional to pump speed and indirectly proportional to conveyor speed. Furthermore, the speed of the conveyor is usually fixed in production. Thus, only pump speed is varied to control the applied spread of adhesive.
- So, the gap width practically affects the curtain thickness, but only in terms of curtain quality. Smaller gap promotes faster fall of the curtain and wider gap promotes more stable curtain. Gap width has no effect on total adhesive curtain applied. More viscous adhesive requires wider gap.
- Height of the curtain influences the falling velocity of the curtain. The higher the curtain, the faster velocity.

Advantages of curtain coating include achieving evenly thick spread layer of adhesive and fast speed of the production (Sellers, 1985; Triantafillopoulos et al., 2004). In addition, less adhesive is wasted in the production. Despite the surface of the veneer, evenly thick and well covering layer of adhesive is spread since no mechanical contact is applied. With rollers, the surface of the adhesive is even, but the thickness of the layer may vary depending on the surface uniformity of the veneer. If there is thicker layer of adhesive in the notches of the veneer, hardening of the adhesive is not uniform in the hot-press, since distribution of moisture is not uniform. Mechanical contact may harm the veneers as they move through the rollers, which affects the productivity of the process. The production of plywood is faster

and simpler when compared to rollers. Speed of the adhesive application is slower with rollers, because rotation of big rollers is a restricting factor. With rollers, adhesive is spread onto both sides of the veneer, so in the assembly phase there is more workload when blank veneer is placed between the adhesive containing veneers. Simpler production prevents problems and losses in production, is easy to automatize and reduces maintenance, thus lowering the production costs (Sellers, 1985; Koponen, 2002).

A major challenge in curtain coating is formation of a stable curtain. This requires special composition of the coating material and optimized process parameters. Formation of the curtain is studied next.

5.2 Formation of curtain

When studying the curtain itself, there are three interesting phases to be examined: formation of the curtain, free fall of the curtain (curtain flow) and collision of the curtain with the base material (Triantafillopoulos et al., 2004; Beneventi & Guerin, 2005). The curtain must be stable and uniform to ensure homogenous application of the coating material onto the base material. The major requirement is that curtain is not supposed to tear at any stage. Rupture of the curtain results uncovered areas in the base material, which affects the quality of the finished product.

In curtain coating of paper, an operational window has been presented by applying Reynolds number (Re) and a speed ratio of the curtain velocity (v_c) at the moment of collision to the base material and the conveyor velocity (u). Reynolds number describes the flow behavior of the falling curtain, defined for this case (Triantafillopoulos et al., 2004; Birkert et al., 2006):

$$Re = \frac{\rho Q}{\eta}, \tag{1}$$

where ρ density of the coating material
Q volumetric flow rate per unit width
η viscosity.

Flow rate is defined:

$$Q = h_c v_c, \tag{2}$$

where h_c curtain thickness.

The curtain velocity at the moment of collision with base material can be approximated (Schweizer, 2004; Birkert et al., 2006):

$$v_c = \sqrt{v_0^2 + 2gx}, \tag{3}$$

where v_0 nozzle exit velocity of the curtain
g gravitational acceleration
x curtain height, accelerating distance.

For typical industrial curtain heights, v_0 is much smaller than the square root term in equation (3). Thus, v_0 can usually be neglected. (Schweizer, 2004)

Operational window for curtain coating (Figure 8) describes the optimal relationship of process parameters and the challenges related to curtain coating. Outside the operational window, heel formation, bead pulling and air entrainment take place causing uneven spreading of the coating material and curtain rupture (Triantafillopoulos et al., 2004). Operational window can be achieved by modifying the Reynolds number (density and viscosity of the coating material, flow rate by controlling the pumping) and speed ratio (height of the curtain, conveyor speed). Weight of the application material and machine speed has to be suitable, since in paper coating only the required amount of application material is pumped onto the base paper, and there is no excess material. With low coating weights, too high and too low machine speeds cause rupture of the curtain. High coating weights cause overloading of the material at high machine speeds and heel formation at the collision zone at low machine speeds. (Birkert et al., 2006)

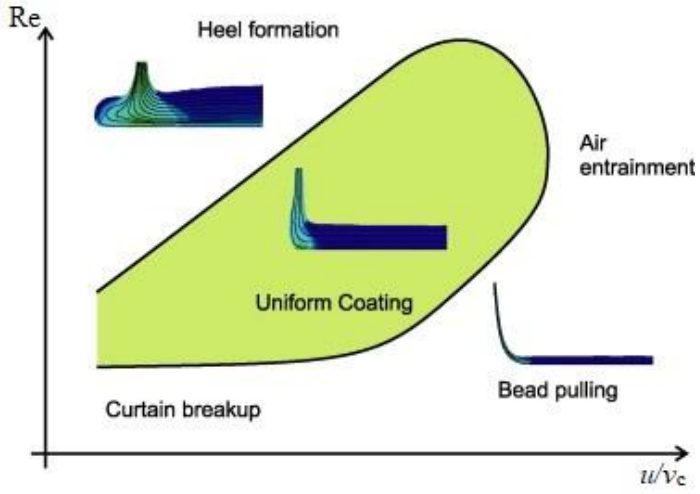

Figure 8 Sketch of an operational window for paper curtain coating, Reynolds number (Re) as a function of ratio of conveyor speed to curtain speed at the moment of collision (u/v_c) (modified from Becerra and Carvalho (2011)).

Thin curtain is vulnerable for surrounding air flows in the production. Slice gap of the curtain coater is approximately equal to thickness of the curtain. During the curtain fall and elongation, the curtain becomes thinner. The higher the curtain the more air flow can affect the curtain. Air bubbles in the curtain material may cause curtain rupture which results uncovered areas in the base material (Triantafillopoulos et al., 2004). Because of air entrainment, small air bubbles can remain between the coating and base material, which affects the quality of finished product. Here, the curtain thickness (slice gap) and height can be adjusted, and production surroundings can be covered from air flows.

Theoretically there are a few mathematical models to define curtain stability. First, it has been stated that curtain velocity must be higher than the propagation velocity of the free edge of the curtain (Triantafillopoulos et al., 2004). Propagation velocity of the free edge (v_d) relates to a hole in the curtain (caused by a disturbance) and its movement. If the hole moves upstream ($v_c < v_d$), the hole will cause curtain rupture. If the hole moves downstream ($v_c > v_d$), the hole will be carried away. Free edge propagation velocity is defined (Schweizer, 2004):

$$v_d = \sqrt{\frac{2\sigma}{\rho h_c}}, \tag{4}$$

where σ surface tension.

Secondly, inertia forces of the curtain must be stronger than surface tension of the curtain (Schweizer, 2004):

$$\rho h_c v_c^2 > 2\sigma, \tag{5}$$

The relationship of inertia forces and surface tension is also described by the Weber number (We). Stability criteria related to Weber number is that the curtain is stable if We > 2 (Schweizer, 2004; Triantafillopoulos et al., 2004; Beneventi & Guerin, 2005). Weber number is defined:

$$We = \frac{\rho Q v_c}{\sigma} = \frac{\rho h_c v_c^2}{\sigma}, \tag{6}$$

As seen from the equations (4) and (6), surface tension has a strong influence on curtain stability. The lower the surface tension, the higher the Weber number, and thus better stability of the curtain. High surface tension of the coating material causes contraction of the curtain, which narrows the curtain. Also spreading of the adhesive is not spontaneous (Hse, 1972). Low surface tension allows air to escape from the coating material (Sellers, 1985). Based on equation (6), also thick curtain, fast moving curtain and high volumetric flow rate per unit width promote stable curtain.

Schweizer (2004) has presented practical guidelines for stable curtains; flow rates above minimum (aqueous fluids: 1,0 cm^2/s per centimeter width) and surface tension below maximum (aqueous fluids: 40 mN/m). Minimum conveyor speed u_{min} can be approximated:

$$u_{min} > \frac{1000 \rho c Q_{min}}{A_{dry}}, \tag{7}$$

where c solids concentration

Q_{min} minimum volumetric flow per unit width

A_{dry} dry coverage.

The available mathematical models for behavior of free falling films to predict curtain formation and stability apply properties such as density, viscosity and surface tension of the coating material and operational parameters. The composition of the coating material undeniably affects these properties, but the relationship is not well defined (Beneventi & Guerin, 2005). Thus, the development of optimal curtain composition relies on experimental tests. In addition, the equation of Weber number (6) does not include viscosity, which however has been recognized as an important factor for curtain stability. The validity of simple stability criteria is widely discussed in the literature (Becerra and Carvalho, 2011).

Extensional viscosity of the coating material is very important in curtain coating in addition to surface tension (Beneventi & Guerin, 2005). Gravity, inertia and viscous and capillary forces control the spread of the coating material when it freely falls towards the base material (Triantafillopoulos et al., 2004). Firstly, when the curtain falls, the curtain elongates slightly by the gravity. Curtain height affects the elongation, the higher curtain the longer falling time and greater elongation. Secondly, the curtain collides with the base material, which causes elongation of the curtain to the direction of the base material movement. The elongation is the more significant the higher the speed difference is between the curtain falling speed and the speed of the base material. The collision is very rapid in paper curtain coating. High strain rate is a challenge, because the coating film should not rupture at this sudden elongation. (Birkert et al., 2006) Also Becerra and Carvalho (2011) conclude high extensional viscosity liquids creating more stable curtains. The collision is not as rapid with adhesive as a coating material and veneer as a substrate, since conveyer speeds are not as high in plywood production.

Within a short length of the curtain when the curtain has just started to freely fall (transition zone), viscous forces inhibit the curtain velocity, and thus affects the Weber number. This length is the longer the higher the viscosity of the coating material. Highly viscous curtains have been recognized to form a stable curtain even when $We < 2$, if the height of the curtain is shorter than transition zone (Schweizer, 2004; Triantafillopoulos et al., 2004). Practically this has not been significant, because the length of transition zone is very short, about 1 mm (Schweizer, 2004).

5.3 Curtain coating resin/adhesive

Curtain coating phenol-formaldehyde (PF) resins and adhesive compositions have been patented by Clausen et al. (1965), Järvi (1969), Robitschek et al. (1974) and Bond and Moehl (1975). In the production of resins, formaldehyde:phenol (F:P) molar ratio varies from 1,6 to 2,5 (Clausen et al., 1965; Järvi, 1969; Bond and Moehl, 1975). Example of an PF curtain coating adhesive composition is performed in Table IX (Robitschek et al., 1974).

Table IX Example of PF adhesive for curtain coating (Robitschek et al., 1974)

Substrate	**Parts per weight**
PF resin	75,86
Water	11,49
Corn cob filler	5,75
Wheat flour thickener	4,6
50 % caustic soda	2,3

All patents concluded requirement of additives to improve curtain-forming qualities of the adhesive, curtain stability and uniform spreading of the adhesive (Table X).

Table X Curtain improving additives used in patents, collected from Clausen et al. (1965), Järvi (1969), Robitschek et al. (1974) and Bond and Moehl (1975).

Thickening agent		**Surface active agent**		**Reference**
Substrate	Amount, % of the PF resin weight	Substrate	Amount, % of the PF resin weight	
Cellulose derivatives, preferred: hydroxyethylcellulose, carboxymethylcellulose and methylcellulose	0,1-2	Anionic/non-ionic, preferred: dodecyldiphenol ether disulphonic acid, sodium salt	2-4	Clausen et al. (1965)
Cellulose derivatives, preferred: hydroxyethylcellulose	0,1-0,2	Anionic, preferred: sodium-2-ethylexyl sulfate	1-2	Järvi (1969)

Curtain improving additives		
Substrate	Amount, % of the PF resin weight	**Reference**
2,4,7,9-tetrametyl-5-decyne-4,7-diol or ethylene, propylene- or butylene glycol ether thereof (with 1-10 mols of glycol per mol of diol)	Preferred: 0,025-0,3, commercially relevant: 0,05-0,2	Robitschek et al. (1974)
Sodium lignosulfonate	3-6	Bond and Moehl (1975)
Tributyl phosphate	0,25-0,75	Bond and Moehl (1975)

Specific viscosity properties of PF adhesives for curtain coating were met by addition of thickening agent. Clausen et al. (1965) reported absence of a thickening agent requiring a thinner curtain which causes greater possibility to curtain breaks. Both Clausen et al. (1965) and Järvi (1969) reported use of mixture of high- and low-molecular-weight PF resins. High-molecular-weight (HMW) resin is highly advanced, but low-molecular-weight (LMW) resin provides improved flowing, lower spreading weight and longer open-time durability of the resin. Järvi (1969) reported viscosity much over 800 cP causing problematic air entrainment. Viscosity affects spreading of the adhesive and formation of the glue joint. Viscosities of the patented curtain coating PF resins and adhesives are presented in Table XI. Optimal adhesive viscosity is regulated by operational parameters of the plywood production. Curtain coating of softwood requires more adhesive applied than for hardwood due to its porous structure. Thus, thicker curtain is required. Thicker curtain is obtained by higher viscosity of the adhesive.

Table XI Viscosity of PF resins and adhesives for curtain coating of veneer (collected from Clausen et al. (1965), Järvi (1969) and Robitschek et al. (1974)).

Viscosity of the PF resin	**Viscosity of the adhesive**	**Reference**
220-540 cP, preferred: 300 cP (21 ºC)	300-350 cP (21 ºC)	Clausen et al. (1965)
600-800 cP (21 ºC)	220-800 cP, preferred 500 cP (21-24 ºC)	Järvi (1969)
Not available	Example 1600 cP (25 ºC)	Robitschek et al. (1974)

Lowered surface tension was found to correlate with better curtain formation. Surface tension was lowered with surface active agents. Robitschek et al. (1974) reported addition of 0,01 % of 2,4,7,9-tetrametyl-5-decyne-4,7-diol additive already showing improvement of curtain stability. Diol additive used was Surfynol 104 produced by AirProducts.

Bond and Moehl (1975) studied especially the importance of surface tension of the PF adhesive to obtain successful curtain coating. Surface tension values of examples in the patent are presented in Table XII.

Table XII Surface tension of PF adhesive without and with additives (Bond and Moehl, 1975).

Patent example	**Surface tension, mN/m**
PF adhesive without additives	69,7
PF adhesive with 0,5 % tributyl phosphate	68,4
PF adhesive with 5,4 % lignosulfonate	66,8
PF adhesive with 5,4% lignosulfonate and	
0,1 % tributyl phosphate	60,4
0,2 % tributyl phosphate	58,1
0,5 % tributyl phosphate	50,2

It was reported, that PF adhesive without additives and PF adhesive with only tributyl phosphate did not form sufficient curtain stability. Patent claimed PF adhesive with lignosulphonate and tributyl phosphate in amounts of 3-6 % and 0,25-0,75 % of the PF resin weight, respectively. From here it can be concluded, that 0,25 % of tributyl phosphate with lignosulphonate is sufficient to obtain a good curtain, which would indicate surface tension of approximately 55 mN/m. By Järvi (1969) it was also concluded, that surface tension of 30-55 mN/m is required to obtain a good curtain.

Dry matter content of the adhesive relates to the viscosity and formation of the glue joint. PF resin solids content is typically 40-50 %, and adhesive solids content typically 20-40 % (Clausen et al., 1965; Järvi, 1969; Robitschek et al., 1974). Gel time gives insight about the curing of the resin. Higher pH glue joint has better durability, typical pH of the PF adhesive is 9-13,5 (Robitschek et al., 1974). Adhesive was applied 118-135 g/m^2 for 2 cm thick veneer, and 11-16 g/m^2 less for 0,25 cm thick veneer. Pressing of plywood composing of 5 veneers, in total 2 cm thick, was performed in approximately 150 ºC for 7-8 minutes. (Clausen et al., 1965)

There are no major differences in PF resins preparation process despite the subsequent adhesive application method such as roller or curtain coating. The desired general properties of finished resin and adhesive are met in same ways than described previously in PF resin chapter 3. Specific viscosity and surface chemical properties (for example surface tension) of adhesives required by curtain coating method are adjusted with special additives which are not required in other coating methods. Surface chemical and rheological properties of resins are studied more carefully next.

6 SURFACE CHEMISTRY OF RESINS

As stated in previous chapter, surface tension of the coating material has an essential role in successful formation and stability of the free falling curtain. In addition, other surface chemical phenomena may give useful information about the curtain behavior or adhesive properties on the veneer surface. Physical chemistry of plywood resin surfaces must be studied in order to achieve effective application in curtain coating. Methods to affect these surface chemical properties and analytical methods to measure these properties are determined. Among the surface chemical analyses, the most potential are selected for the experimental part of this work.

6.1 Surface chemical properties

Interactions on the surfaces of liquid/liquid, liquid/solid, liquid/gas, gas/solid and solid/solid phase systems are studied. Surface chemical phenomena are based on free energy at the interface of two phases. Capillarity concerns interfaces that are sufficiently mobile to assume an equilibrium state. It deals with macroscopic and statistical behavior of interfaces and it can be measured as a free energy per unit area or as a force per unit length (Adamson, 1976). Basic equation describing capillarity has been given by Young and Laplace, which allows equilibrium surfaces to be treated mathematically (Adamson, 1976):

$$\Delta P = \frac{2\sigma}{r}, \tag{8}$$

where ΔP pressure difference across the film

σ surface tension

r bubble radius.

Young-Laplace equation (8) conclude, that the smaller the bubble, the greater the pressure of air inside the bubble when compared to surrounding air pressure. This is due to decrease of surface energy as the bubble increases, which is balanced by pressure difference across the film.

Interesting phenomena at the interfaces include contact angle, surface free energy and surface tension. Static contact angle (θ) is the angle of which liquid forms on the surface of liquid, gas and solid matter, between two liquids or two liquids and a solid. Generally contact angle is used for measuring the wetting of a solid by a liquid. Here, if $\theta > 90°$, the liquid does not wet the solid and the surface is hydrophobic. If $\theta < 90°$, the liquid wets partly the solid and if $\theta < 10°$, the liquid practically wets the solid completely (Figure 9). (Shaw, 1980)

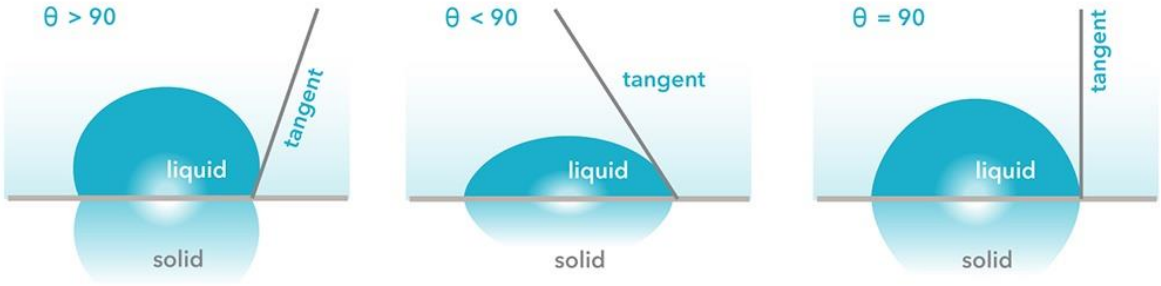

Figure 9 Contact angle, wetting of a surface (Biolin Scientific, 2018a).

Dynamic contact angle is measured when the phase boundary is in actual motion. Advanced/advancing (for static/dynamic) contact angle is acquired when the drop has recently expanded, and it approaches the maximum contact angle value. Receded/receding (for static/dynamic) contact angle is acquired when the drop has recently contracted, and it approaches the minimum contact angle value. For water, advancing and receding angles are sensitive to the hydrophobic and hydrophilic domains, respectively. The difference between the maximum and minimum contact angle values is referred as hysteresis. Hysteresis can be described, when studying a sessile drop on a tilting surface. When the surface is completely smooth, the drop will immediately start to move, and there is no difference between advancing, receding and equilibrium contact angle. However, in practice, the surface is never completely smooth. When the surface is tilted, drop will stay still, but the advancing contact angle may be observed on the lowering side of the surface and receding contact angle on the lifting side of the surface. Hysteresis is caused by contamination of the solid surface or liquid, surface roughness or surface immobility on macromolecular scale (Adamson, 1976). When as small contact angle as possible is required, determination of receding angle via hysteresis is important.

Surface free energy and surface tension both describe the free energy of the surface and are mathematically equivalent (Adamson, 1976). Surface free energy is used for solid surfaces and surface tension for liquid surfaces. Surface energy composes of polar and dispersive component. Polar component gives information about the hydrophobicity or hydrophilicity of the surface. High polar component results small contact angle, and small polar component results high contact angle, thus surfaces are hydrophobic and hydrophilic, respectively. Dispersive component gives information about how non-polar substances behave on the surface. However, also critical surface tension is a useful value to describe wettability of a solid surface, especially when characterizing low energy surface that are being wetted by non-polar liquids (Biolin Scientific, 2018b). Both are determined by contact angle measurements, described more precisely later.

There are three types of wetting that can be studied via components of surface free energy:

1) spreading wetting
2) adhesional wetting
3) immersional wetting.

In spreading wetting, liquid is spreading on the surface of the solid so that the solid/liquid and liquid/gas interfacial areas increase and the solid/gas interfacial area decreases (Shaw, 1980). The liquid spreads spontaneously over the solid surface when spreading coefficient *S* is positive or zero. The spreading coefficient can be determined:

$$S = -\frac{\Delta G_s}{A} = \sigma_{SG} - (\sigma_{SL} + \sigma_{LG}), \quad (9)$$

where ΔG_s free energy change due to spreading
A interfacial area
σ_{SG} surface tension at the interface of solid/gas
σ_{SL} surface tension at the interface of solid/liquid
σ_{LG} surface tension at the interface of liquid/gas.

At equilibrium contact angle θ, liquid spreads an infinitesimal amount further covering extra area of solid surface, dA. The increase in liquid/gas interfacial area is therefore dA cos(θ). Thus, the increase of free energy of the system is:

$$dG = \sigma_{SL}\, dA + \sigma_{LG}\, dA \cos(\theta) - \sigma_{SG}\, dA, \tag{10}$$

and if the system is at equilibrium, dG = 0, and the following equation is obtained, known as Young's equation:

$$\sigma_{SL} + \sigma_{LG} \cos(\theta) - \sigma_{SG} = 0. \tag{11}$$

Critical surface tension σ_c is a parameter characterizing the wettability of solid surface. When a non-polar liquid on a given solid spreads, contact angle decreases as the σ_{LG} decreases, and becomes zero below a certain value of σ_{LG}, which is the critical surface tension (Shaw, 1980). It is the highest value of surface tension of a liquid to completely wet the solid surface (Biolin Scientific, 2018b).

In adhesional wetting, liquid makes contact with the solid substrate and adheres to it (Shaw, 1980). The interfacial area liquid/gas decreases. The work (free energy) of adhesion W_a is given by the Dupré equation:

$$W_a = -\frac{\Delta G_a}{A} = \sigma_{SG} + \sigma_{LG} - \sigma_{SL}, \tag{12}$$

where ΔG_a free energy change due to adhesion.

When combined to Young's equation (11), the following equation is obtained, known as Young-Dupré equation:

$$W_a = \sigma_{LG}(1 + \cos(\theta)). \tag{13}$$

Zero contact angle results that the forces of attraction between liquid and solid are equal or greater than forces between liquid and liquid (completely wetted solid). Finite contact angle

results that the liquid adheres to the solid less than it coheres to itself (partially wetted solid). Contact angle is always less than 180°, because otherwise it would require $W_a = 0$ or $\sigma_{LG} = \infty$.

In immersional wetting, the solid is immersed completely in the liquid (Shaw, 1980). The interfacial are of liquid/gas remains unchanged. The work (free energy) of immersion due to immersion of a solid in liquid is:

$$W_i = -\frac{\Delta G_i}{A} = \sigma_{SG} - \sigma_{SL}\,, \tag{14}$$

where ΔG_i free energy change due to immersion.

When combined to Young's equation (11), the following equation is obtained:

$$W_i = \sigma_{LG}\, cos\theta. \tag{15}$$

If $\sigma_{SG} > \sigma_{SL}$, then $\theta < 90°$ and immersional wetting is spontaneous. If $\sigma_{SG} < \sigma_{SL}$, then $\theta > 90°$ and work must be done to immerse the solid in the liquid.

When studying the equations (9), (12) and (14), it can be noticed that reduction of σ_{SL} facilitates all of these wetting processes (achieving spontaneous spreading and immersion and smaller contact angle). However, reduction of σ_{LG} is not always helpful (Shaw, 1980). In addition to contact angles, capillary phenomenon, where the driving force is pressure difference across the surface, is involved in the basic mechanism of wetting in some cases (Adamson, 1976). Large pressure difference promotes capillarity, and thus wetting. Here, the Young-Laplace equation (8) is derived into the form (Adamson, 1976):

$$\Delta P = \frac{2\,\sigma_{LG}\cos(\theta)}{r}. \tag{16}$$

If θ is not zero, then

$$\Delta P = \frac{2(\sigma_{SG} - \sigma_{SL})}{r}, \quad (17)$$

and if θ is zero, then

$$\Delta P = \frac{2\sigma_{LG}}{r}. \quad (18)$$

Thus, when pursuing large pressure difference, small σ_{SL} is desired, based on equation (17). On the other hand, large σ_{LG} is desired based on equation (18).

Wetting of hydrophobic surface can be remarkably increased by the addition of wetting agents, surface active molecules (Adamson, 1976; Shaw, 1980). Such surfactants are studied more precisely later. Surface roughness has also an effect on contact angle. If $\theta < 90°$, liquid will more likely penetrate into the pores and hollows of the solid surface and if $\theta > 90°$, liquid does not penetrate into the solid.

Surface tension is defined as presence of free energy at the liquid surface. If the interface studied is between liquid and gas, the phenomenon is referred as surface tension. The excess energy is formed, because molecules on the surface of the liquid do not interact equally to all directions but more to the direction of bulk of a liquid (Shaw, 1980). This is illustrated in Figure 10. Intermolecular interactions are mainly van der Waals forces. Liquid surface attempts to minimize its own area. If the interface studied is between two liquids, the phenomenon is referred as interfacial tension. At the interface of two liquids, the imbalance of intermolecular forces is lower (Shaw, 1980). Surface tension can be defined as static or dynamic surface tension. Dynamic surface tension is time-dependent surface tension of the liquid, which approaches the equilibrium values of static surface tension during time. The lower the dynamic surface tension, the easier the wetting. The time for a liquid to achieve static surface tension may vary from seconds to hours.

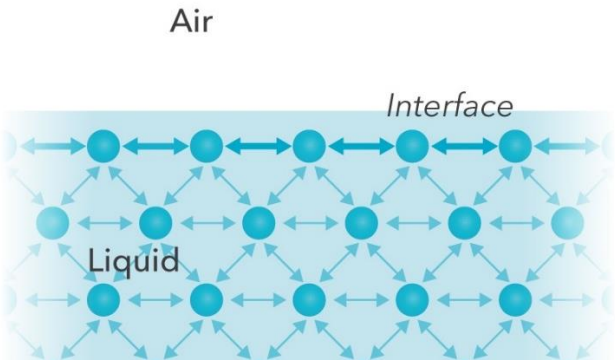

Figure 10 Existing interactions of molecules at the surface of the liquid and in the bulk of the liquid (Biolin Scientific, 2018c).

Critical micelle concentration (CMC) of a surfactant is a point, where physical properties of the liquid, especially surface tension, undergo a remarkable change (Shaw, 1980). Certain molecules, amphiphilic molecules, contain two distinct components differing in their affinity for solutes (Figure 11A). The part of the molecule having affinity for polar solutes is referred as hydrophilic, and the part having affinity for non-polar solutes is referred as hydrophobic. When amphiphilic molecules interact with water, the polar part seeks to interact with water and non-polar part avoids the interaction. There are two ways for amphiphilic molecule to arrange in such situation, which are presented in Figure 11B and Figure 11C. First, at the surface of the water, polar part interacts with water and non-polar part locates above the surface (in air or non-polar liquid). This interrupts the cohesive energy at the surface and thus lowers the surface tension. Such molecules are wetting agents. Second, molecules form aggregates, micelles, where polar part is exposed to water and non-polar parts orient towards the center of the micelle.

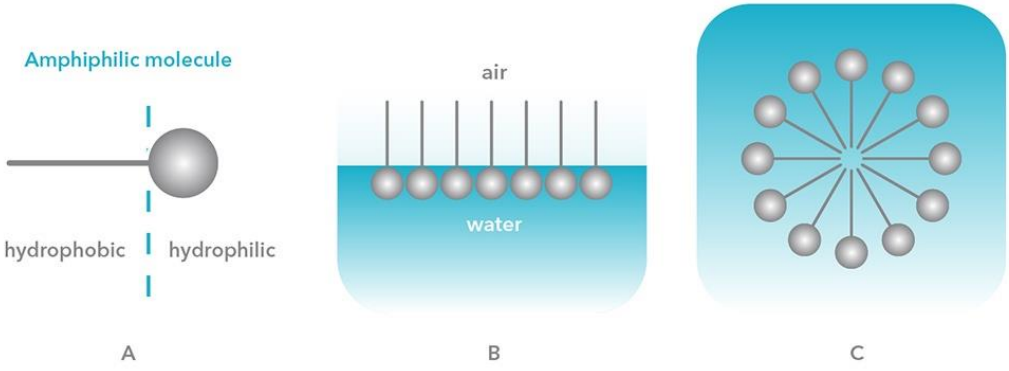

Figure 11 A) Amphiphilic molecule. Arrangement of amphiphilic molecules B) at the surface of water and C) to form micelles. (Biolin Scientific, 2018b)

The proportion of molecules present at the surface or as micelles depend on surfactant concentration. Arrangement at the surfaces is favored at low concentrations, until the surface becomes “full” and more micelles are arranged. The concentration, where the surface is completely loaded with surfactants and any further addition will generate only micelles, is called critical micelle concentration. From this point further, any addition of amphiphilic molecules generates only micelles and do not further lower the surface tension but stays the same. Determined CMC is used for optimization of amount of surfactants used and the change in surface tension after mixing and time required to reach equilibrium can be determined. CMC affects also other physical properties of the liquid, for example conductivity, molar conductivity, osmotic pressure and turbidity of the liquid, like presented in Figure 12. (Shaw, 1980)

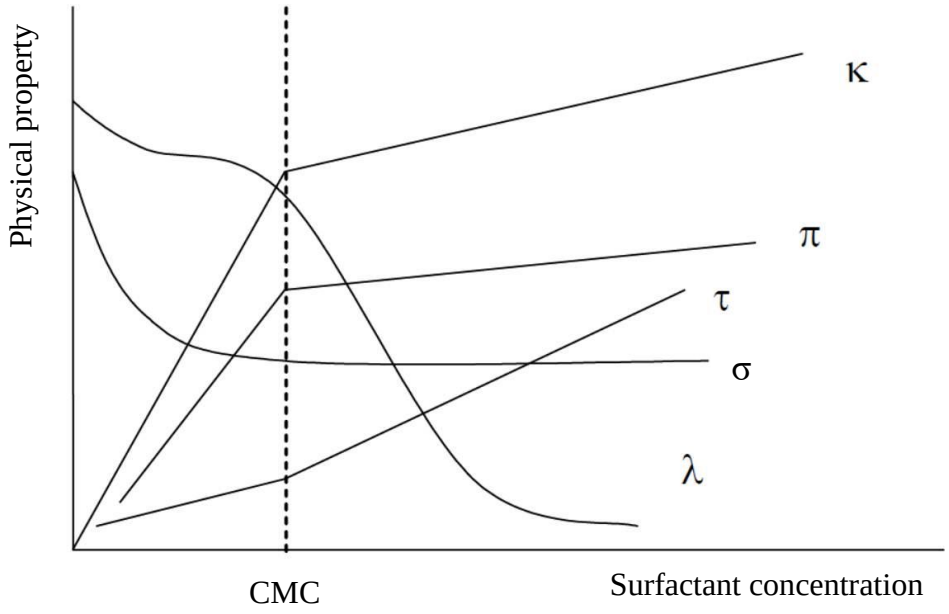

Figure 12 The effect of CMC on liquid physical properties: conductivity (κ), surface tension (σ), osmotic pressure (π), turbidity (τ) and molar conductivity (λ) (Colloid and Surface Chemistry Virtual Lab, 2018).

6.2 Additives to affect surface chemistry of resins

Surfactants are surface active molecules, which can be applied as chemical additives into the plywood resin. Wetting phenomenon (contact angle) and surface tension are the most remarkable surface chemical properties to be modified, and modification can be performed with wetting agents (Adamson, 1976; Birkert et al., 2006). Wetting agents are amphiphilic

molecules, surfactants, promoting displacement of air by liquid at the surface of solid (Shaw, 1980). When surfactants are added to liquid, they spontaneously adsorb at the surface, and decrease the surface energy (Langevin, 2000). A monolayer is formed, with the polar parts of the surfactant molecule in contact with water, and the hydrophobic parts in contact with air (Figure 11b).

Surfactants are classified according to the charge carried by the surface active part of the molecule to anionic, cationic, non-ionic and ampholytic (zwitterionic) surfactants. Particularly anionics are used as wetting agents. Hydrophilic part of effective soluble surfactants is often an ionic group. Ions having a strong affinity for water (electrostatic attraction to water dipoles) are capable of pulling long hydrocarbon chains into solution with them. Non-ionic hydrophilic groups may also be strong as a sum of modest affinities of monomer units in a polymer chain. As an advantage, the lengths of both hydrophilic and hydrophobic groups can be varied. Irregularly shaped surfactant molecules are often very good wetting agents since micelle formation is not desired. Thus, relatively high concentrations of unassociated surfactant molecules can be applied and greater lowering of both liquid/gas surface tension and solid/liquid surface tension are achieved. (Shaw, 1980) In addition, two identical, conventional surfactant molecules can be chemically bonded together by a spacer. Here, even better wetting and lower CMC can be achieved, and especially dynamic surface tension can be reduced. This is referred as Gemini surfactant technology (Louis, 2003).

In curtain coating, surfactants allow air to escape from the plywood adhesive and hold the curtain together for greater distances of fall from the head. 100-460 mm of more falling distance can be achieved. Amount of surfactants is usually less than 1 % of the resin solution. Surfactants usually lower the resin viscosity about 50 mPas. For curtain formation, a) diols, b) 5- to 10-mol ethoxylates which have, or on average have, 8-10 carbons, or c) sodium sulfate salts, such as octyl, hexyl or alkyl, surfactants are recommended. Surfactants may be anionic or non-ionic. (Sellers, 1985) Amount of wetting agent is critical, since high wettability results over-effective soaking into the veneer (Shaw, 1980) and dosage over CMC of surfactant only increases the costs, and does not improve the performance.

Choosing the suitable surfactant is important, since its compatibility to alkaline solutions (Seller, 1985) and to nature of solid surface (side effects such as toxicity and foaming may occur) (Shaw, 1980) must be considered. In addition, variables affecting the performance of surfactants (Triantafillopoulos et al., 2004) are for example:

- chemical structure, chain length and concentration of surfactant molecules
- viscosity of the curtain fluid
- local velocities in the curtain flow field
- age of curtain fluid
- rate at which fresh curtain surface is generated.

As a disadvantage, surfactants may have bubble stabilizing effect called Marangoni effect, which is caused by their linear structure. So, addition of surfactants may cause undesired resin/adhesive foaming (Evonik, 2017a). However, especially non-ionic surfactants (Langevin, 2000) and Gemini surfactants (Louis, 2003) do not favor the foam stabilization. Prevention of foaming is studied later in this work. Also ecological impact of the surfactants must be considered, since their poor biodegradability, aquatic toxicity and bioaccumulating may be remarkable.

Polar liquids (such as water) have strong intermolecular interactions and thus high surface tensions. In addition to surfactants, any factors decreasing the strength of this interaction will lower the surface tension (such as increased temperature and contaminants). (Seller, 1985)

Examples of commercial wetting agents/surfactants available for coatings and adhesives are presented in Table XIII.

Table XIII Commercial wetting agents/surfactants available for coatings and adhesives.

Producer	**Brand**	**Description**	**Reference**
BASF SE	Efka®	Coating additives enabling dispersion of e.g. pigments, foam control at different process stages and the management of coating surface properties.	(BASF, 2018c)
BASF SE	Hydropalat®	Low foaming substrate wetting agents for waterborne applications. Additive for e.g. adhesives and industrial coatings.	(BASF, 2013; 2018c)
BYK Additives & Instruments	BYK-3xxx	Surfactants for aqueous e.g. coatings and adhesives. Reduction of surface tension and improved substrate wetting.	(BYK, 2018)
BYK Additives & Instruments	BYK-DYNWET	Substrate wetting agent for aqueous e.g. coatings and adhesives. Low foam stabilization. Reduces dynamic surface tension and is suitable for high-speed machines.	(BYK, 2018)
DOW Chemical	ECOSURF™	Biodegradable surfactant offering low-foam wetting and additional foam reduction.	(DOW, 2018b)
Evonik Industries	Dynol®	Superwetting surfactants for the most difficult to wet surfaces, coating additive.	(Evonik, 2017b)
Evonik Industries	Syrfynol®	Multi-functional surfactants and defoamers, e.g. low foaming dynamic wetting agents, molecular defoamers and specialty surfactants, coating additive.	(Evonik, 2017b)
Evonik Industries	TEGOPREN® TEGO® Surten	Wetting agents for polymer dispersions with excellent performance at high processing speed. Suitable for water-based adhesives. TEGO® Surten especially for adhesive curtain coating.	(Evonik, 2017a; 2018)
King Industries, Inc.	DISPARLON® AQ-2xx, -5xx and -7xxx, LS	Leveling, recoatability, wetting and anti-cratering for waterborne systems.	(King Industries, 2017)

6.3 Analytical methods

Determination of contact angle is performed for non-porous solids with a goniometry or a tensiometer. Goniometry involves observation of a static or dynamic sessile drop of a test liquid on a solid substrate (Adamson, 1976). Tensiometer is used for dynamic Wilhelmy method, where the forces of interaction, when a solid is contacted with the test liquid, are measured. For porous solids, tensiometer and Washburn's equation capillary rise method are combined to determine the contact angle. However, contact angle determination for porous solids is a challenge due to questioned validity of averaged cos(θ) equation (Adamson, 1976). Contact angle is utilized also for other experimental parameters such as work of adhesion, work of cohesion, work of spreading and spreading coefficient, work of immersion and wetting tension.

In determination of surface free energy, uniform, sufficiently thick layer of resin is dried onto glass piece. Measurement is performed with at least two liquids, which have different polar and dispersive components. Measurement with 3-5 well characterized wetting liquids is practically suggested. Onto solid resin surface, different liquid drops are dropped, and contact angle is measured. Liquids used for measurement may be for example:

- Water: high polar component, low dispersive component
- Ethylene glycol: polar liquid, higher dispersive component than water
- Diiodomethane: polar component zero, high dispersive component

Total surface free energy is determined from the contact angles of different liquids by equations derived by Fowkes, Wu or Van Oss-Chaudhury and Good (Biolin Scientific, 2017b). Extended Fowkes/OWRK calculation is a geometric mean of dispersive and polar component. Wu calculation utilizes the same principle than Fowkes, but harmonic mean is used instead. Theoretically harmonic mean is not as accurate as Fowkes calculation. For these surface energy determination methods, contact angles of two different liquids are required. Lewis acid-base approach (Van Oss-Chaudhury-Good method) further divides the polar component into acid (electron acceptor) and base (electron donor) components. This is the most accurate method, but also the most sensitive for variations in the measurement. Contact angles of three liquids are required.

Critical surface tension is determined by measuring advancing contact angles made by non-polar or weakly polar liquids and the value of σ_{LG} at $\theta = 0$ is found by graphical extrapolation (Shaw, 1980).

Determination of surface and interfacial tensions may be performed based on measurement of forces or pressure, geometrical surveys or dynamic methods. Different methods are listed in Table XIV. Of these methods, capillary rise, ring, plate, maximum bubble pressure, drop weight or volume and shape analysis of pending or sessile drop/bubble methods are reviewed more precisely.

Table XIV Methods for measurement of surface tension and interfacial tension (collected from Adamson (1976) and Weser (1980)).

Measurement of forces	**Measurement of pressure**	**Geometrical surveys**	**Dynamic methods**
De Noüy ring method	Capillary rise method	Shape of pending or sessile drop/bubble methods	Surface/capillary waves
Wilhelmy plate method	Maximum bubble pressure method	Drop weight or drop volume methods	Oscillating liquid jets
Loop method		Spinning drop method	
		Contact angle measurement	

In capillary rise method, a narrow capillary is immersed into the liquid. Liquid surface will rise (or depress) in the capillary when compared to surrounding liquid surface (Figure 13). This is due to balancing hydrostatic pressure of the capillary and surface tension of the liquid (Weser, 1980). Capillary rise method is considered as the most accurate method for determination of surface tension (Adamson, 1976; Shaw, 1980).

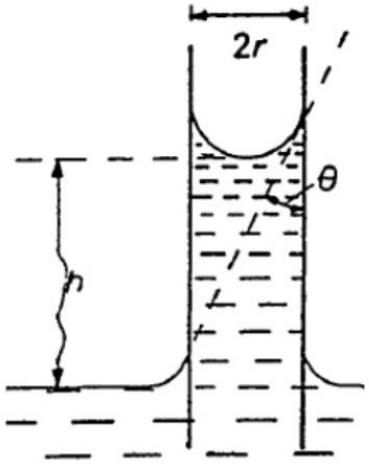

Figure 13 Principle of capillary rise method (Shaw, 1980).

Surface tension can be determined (Adamson, 1976):

$$\sigma = \frac{rh\Delta\rho g}{2\cos(\theta)}, \tag{19}$$

where r radius of the capillary

h height of the liquid rise

Δρ density difference between liquid and gas (surface tension) or liquid and liquid (interfacial tension).

In practice, the capillary rise method is only used when contact angle is zero, since measurement of contact angle is uncertain. Zero contact angle is usually obtained for most liquids by using well-cleaned glass capillary. For accurate work, also meniscus correction should be considered. In a narrow capillary the meniscus is approximately hemispherical, and the following equation can derived:

$$\sigma = \frac{1}{2} r \left(h + \frac{r}{3}\right) \Delta\rho g. \tag{20}$$

Especially for determination of static surface tension, De Noüy ring method and Wilhelmy plate method have gained attention. In De Noüy ring method, maximum force, which applies to the ring, when it is pulled up from the liquid, is measured. Platinum ring is horizontally immersed into the liquid and pulled above the liquid surface (Figure 14).

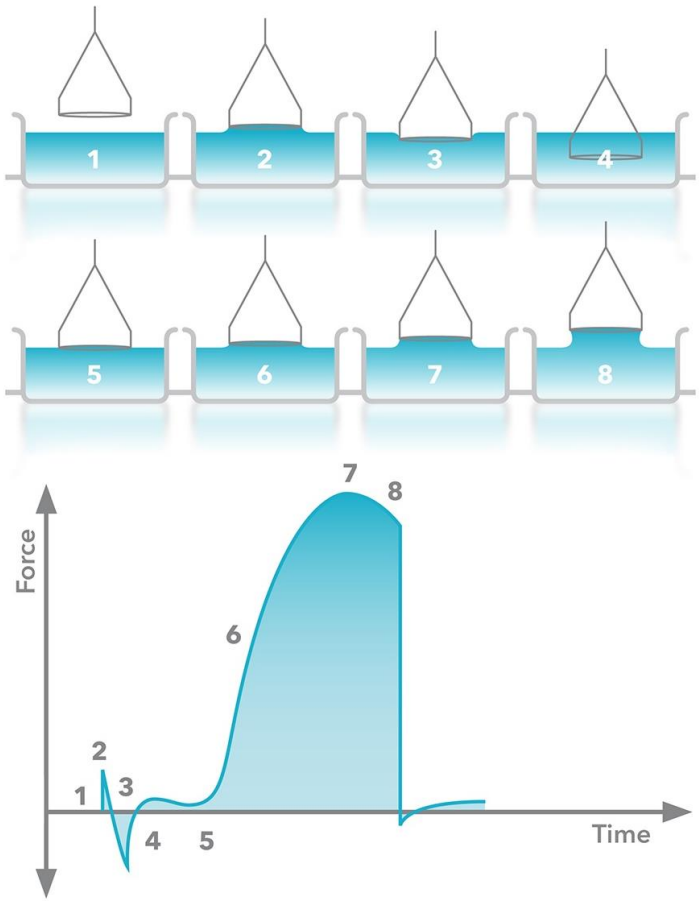

Figure 14 Steps of De Noüy ring method for determination of maximum force of pull on the ring and force measured on each step (Biolin Scientific, 2018c).

Surface tension can be determined (Adamson, 1976; Shaw, 1980):

$$\sigma = \frac{\beta F_{max}}{4\pi r}, \tag{21}$$

where β correction coefficient depending on the shape of the ring and nature of the interface

$F_{\max}$ maximum force of pull on the ring.

In Wilhelmy plate measurement, force, which applies to the plate, when it touches the surface of the liquid, is measured. Platinum plate is vertically immersed to the liquid, but not completely submerged. The plate is pulled up to the surface of the liquid (zero depth of immersion, Figure 15).

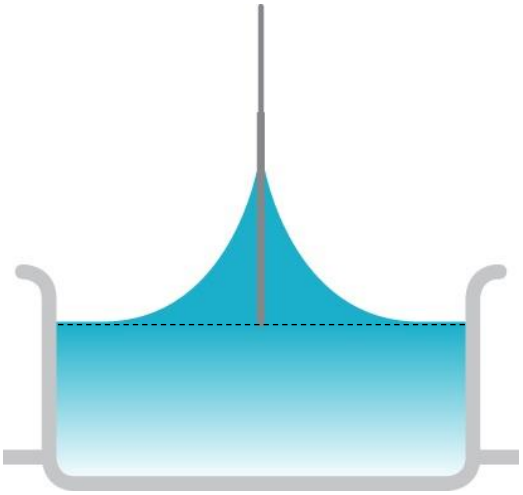

Figure 15 Final step of Wilhelmy plate method for determination of maximum force of the liquid on plate surface (Biolin Scientific, 2018c).

Surface tension can be determined (Adamson, 1976; Shaw, 1980; Weser, 1980):

$$\sigma = \frac{F_w}{l_w \cos(\theta)}, \tag{22}$$

where F_W Wilhelmy force

l_w wetted length

Due to complete wetting of the plate, contact angle can be assumed to be zero. The surface of the plate can also be treated to achieve complete wetting.

For measurement of dynamic surface tension, maximum bubble pressure method is generally utilized. According to the Young-Laplace equation (8), the pressure inside a gas bubble increases with decreasing diameter. When producing an air bubble at the tip of a capillary that is dipped into a liquid, the shape of the bubble changes with the pressure applied to it (Figure 16). The pressure reaches maximum, when the bubble approaches the shape of a hemisphere (bubble radius equal to capillary radius) (Adamson, 1976; Weser, 1980). Dynamic surface tension is obtained as a function of surface age. Viscosity correction may result errors. For the measurement, density of the liquid is required, and capillary viscosity should be determined to ensure correct results.

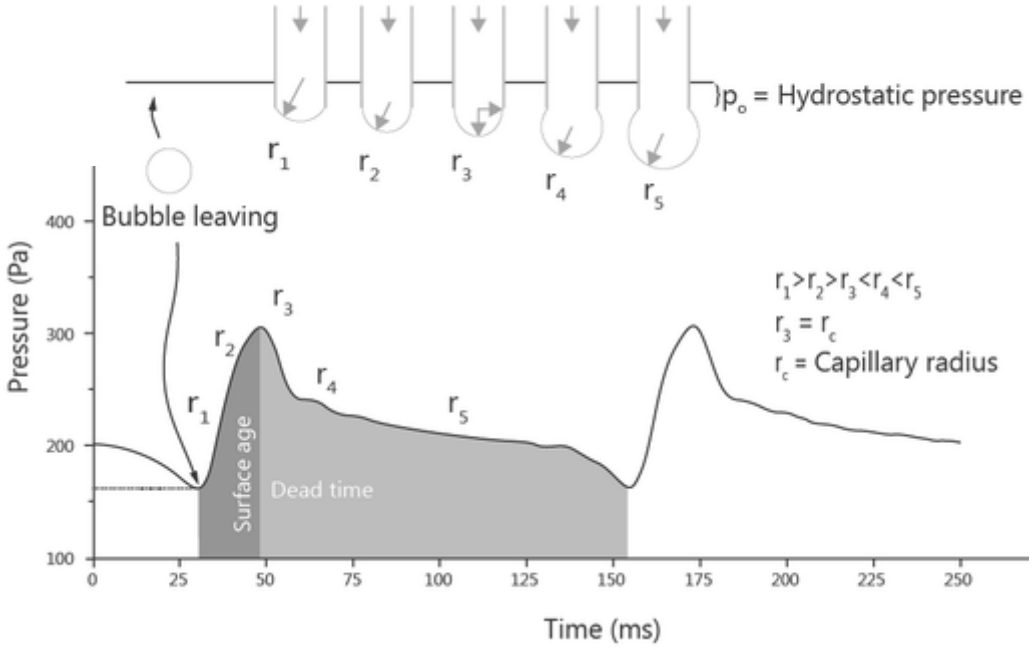

Figure 16 Behavior of a bubble at the tip of capillary in determination of maximum bubble pressure in dynamic surface tension measurement (KRÜSS GmbH, 2018a).

Here, from Young-Laplace equation (8), surface tension is solved. Bubble pressure tensiometer calculation principle is:

$$\sigma = f\frac{r(P_{max} - P_0)}{2} - \Delta\sigma_a - \Delta\sigma_v, \tag{23}$$

where f correction coefficient depending on the capillary

P_{max} maximum pressure inside the bubble

P_0 hydrostatic pressure of the liquid

$\Delta\sigma_a$ coefficient due to aerodynamic resistance of the capillary

$\Delta\sigma_v$ coefficient depending on the viscosity of the liquid.

In the drop weight and drop volume method, drops of a liquid are allowed to detach slowly from the tip of a vertically mounted capillary. At the moment of detaching, equilibrium between the gravitation force (making the drop detach) and the adherence force (making the

drop stay at the tip due to surface tension) is established. The mass or the volume of the drop is measured.

Surface or interfacial tensions can be determined (Adamson, 1976; Shaw, 1980):

$$\sigma = \frac{m_{drop} g}{2\pi r} F_d = \frac{V_{drop} \rho g}{2\pi r} F_d, \quad (24)$$

where m_{drop} mass of the drop

V_{drop} volume of the drop

F_{d} correction coefficient due to detachment.

Correcting factor is required, because at the moment of detachment, the drop does not completely leave the tip, the surface tension forces are seldom vertical and there is a pressure difference across the curved liquid surface (Shaw, 1980).

In drop/bubble shape analysis, either pendant or sessile drop is optically studied. Pendant drop of a liquid is formed at the tip of vertically mounted capillary. The shape of a drop hanging from the tip is determined from the balance of forces which include surface tension of the liquid.

Surface or interfacial tensions can be determined (Adamson, 1976):

$$\sigma = \frac{\Delta \rho g r_0^2}{\beta}, \quad (25)$$

where r^2 radius of drop curvature at apex

β shape factor, defined through Young-Laplace equation.

Sessile drop is fixed to a solid, smooth surface. The height of the drop reaches maximum as the volume of the drop/bubble increases, and it becomes independent of the drop diameter (Weser, 1980).

At this point, surface or interfacial tensions can be simply determined (Adamson, 1976):

$$\sigma = \frac{\Delta \rho g h^2}{2}. \tag{26}$$

Critical micelle concentration (CMC) can be determined manually by measurement of surface tensions of liquids with different concentrations of surfactant. Here, the problem is with waiting a sufficient time for dynamic surface tension to reach static surface tension after addition of surfactant. Another option is using automatic tensiometer with platinum ring or plate (Biolin Scientific, 2018a), which adds new dose of surfactant when desired stability or maximum time of measurement are reached. Surface tension as a function of logarithmic surfactant concentration is obtained.

6.4 Discussion

To summarize the studied surface chemical properties, Figure 17 is presented.

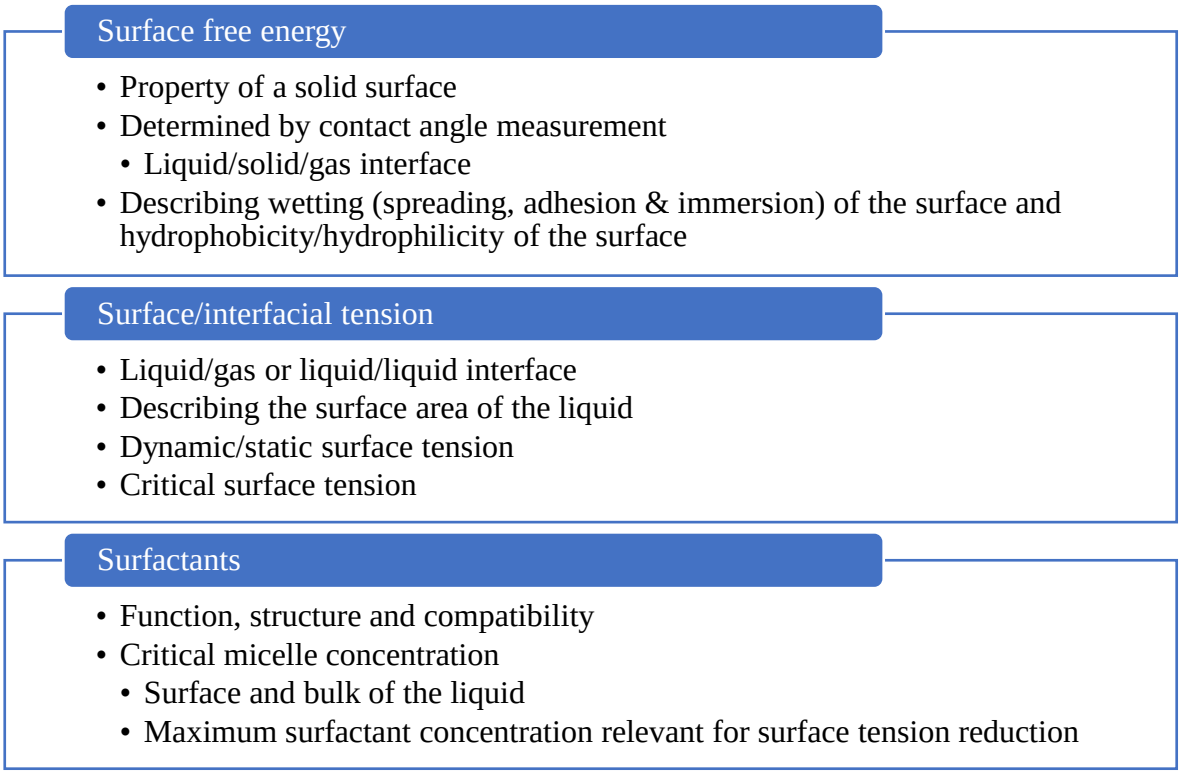

Figure 17 Summary of surface chemical properties studied in this work, the interface where they affect and what they describe.

Via surface free energy determination, interesting wetting phenomena could also be described for resins. This is not widely studied property of coating materials, since coating materials are liquids and surface free energy is a property of a solid surface. However, surface free energy of resins has been studied by Matsushita et al. (2006). Thus, it may be interesting to study surface free energy also in this work.

However, surface tension is widely recognized, interesting property of coating materials. For curtain coating, it has been stated that dynamic surface tension takes into account curtain aging (Triantafillopoulos et al., 2004) and since new area is continuously formed (Louis, 2003), it would be applicable for determination of stability of a curtain. However, with resin as a coating material, it may be irrelevant to measure specifically dynamic surface tension. This is due to high viscosity of the resin, slow speed of the curtain and the conveyor when compared to paper coating, and use of veneer as a substrate material. The speed of the curtain at the moment of collision is slower than in paper coating, and collision itself does not cause curtain rupture. Measurement of dynamic surface tension is also a challenge for resins. Generally used maximum bubble pressure method applies a narrow capillary, which is easily clogged with resin. Surface tension does affect the stability of the curtain, but determination of static surface tension is more practical for resins. In addition, the falling time of the curtain is very short (depending on the curtain height, for 50-350 mm curtain, falling time is 100-270 ms) (Schweizer, 2004). Low surface tension values of the curtain must be reached before or during the free fall and here static surface tension may be more applicable.

7 RHEOLOGY OF RESINS

Rheology is the science of deformation and flow of substance. Viscosity is a property describing substance's resistance to flow. As stated in curtain coating chapter 5, extensional viscosity of the coating material has an essential role in successful formation and stability of the free falling curtain. Rheological properties of plywood resins give also insight about the chemical structure and stability of the material. Thus, also rheology of resins must be studied in order to achieve effective application in curtain coating. Methods to affect these rheological properties and analytical methods to measure these properties are studied. Among the rheological analyses, the most potential are selected for the experimental part of this work.

7.1 Rheological properties

Viscosity is the ratio of shear rate and shear stress (Phan-Thien, 2002). When studying a fluid between two solid plates, and sliding the upper plate with force *F*, shear rate and shear stress can be observed (Figure 18). Fluid moves parallel to upper plate and the speed of the fluid decreases linearly from velocity *U* at the top to zero at the bottom. Friction due to velocity differences between the fluid "layers" gives rise to a force resisting their motion (normal stress). Shear stress is the force which applies to the fluid, when shearing is applied. Shear stress applies to the fluid in the direction of plate movement and normal stress is perpendicular to it. Shear rate is the amount of fluid deformation (strain) over time, when shearing is applied.

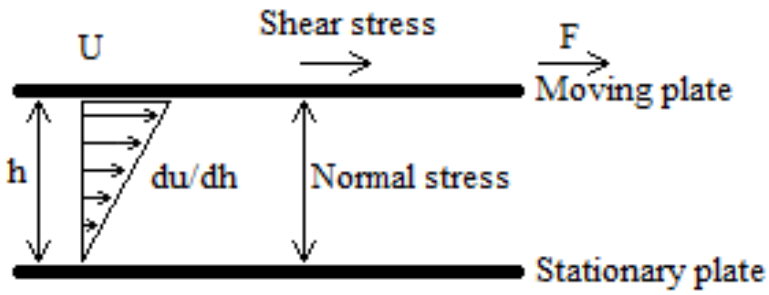

Figure 18 Fluid between two plates, height of the fluid *h*. Upper plate (area *A*) moving at velocity *U*, when slided with external force *F*. Velocity gradient *du/dh*.

Shear stress can be defined (Phan-Thien, 2002; Goodwin and Hughes, 2008):

$$\tau = \frac{F}{A}, \tag{27}$$

where F tangential force on the top plate

A fluid contact area

and shear rate can be defined (Phan-Thien, 2002; Goodwin and Hughes, 2008):

$$\dot{\gamma} = \frac{U}{h}, \tag{28}$$

where U velocity of the top plate

h fluid height,

and finally, viscosity can be defined (Phan-Thien, 2002):

$$\eta = \frac{\tau}{\dot{\gamma}}. \tag{29}$$

Fluid may have Newtonian or non-Newtonian behavior. For a Newtonian fluid viscous stresses are linearly proportional to the local strain rate, so viscosity (equation 29) is constant, depending only on the temperature (Phan-Thien, 2002). Non-Newtonian fluid becomes thinner or thicker when sheared (viscosity changes when strain rate changes). For example, water can be assumed to have Newtonian behavior, but highly viscous fluids are generally non-Newtonian. Rheology focuses on studying non-Newtonian fluids. Pseudoplasticity is similar to shear thinning, but the system flows noticeably only after the shear stress exceeds a certain minimum value, yield value. Thixotropy and rheopexy are time-dependent shear thinning and thickening, respectively. (Shaw, 1980)

In other words, viscosity is Newtonian when the shearing force per unit area (F/A) between two parallel plates of liquid in relative motion is proportional to the velocity gradient (Figure 18) between the planes (Shaw, 1980):

$$\tau = \eta \frac{du}{dh}, \tag{30}$$

where η coefficient of shear viscosity.

Coefficient of shear viscosity is defined for streamlined flows for a given temperature and pressure. For other solutions and dispersions, deviations from Newtonian flow are observed. The main causes for non-Newtonian flow are the formation of a structure throughout the system and orientation of asymmetric particles caused by the velocity gradient (Shaw, 1980). Here, the viscosity studied is precisely called dynamic, shear viscosity. Kinematic viscosity is the ratio of dynamic viscosity and density of the fluid:

$$\nu = \frac{\eta}{\rho}. \tag{31}$$

So, characterization of fluid flow or deformation due to simple shear stress applied is called shear rheology. The study of extensional flows is called extensional rheology. Extensional/elongational flow refers to a flow where velocity gradient is diagonal (accelerating), and it can be planar, uniaxial or biaxial (Barnes et al., 1989). These flows efficiently stretch the fluid elements. The difference between shear and extensional flow is presented in Figure 19.

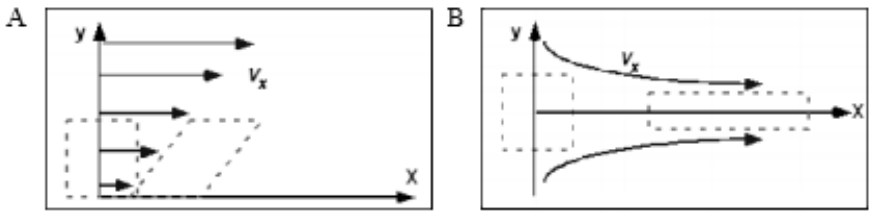

Figure 19 A) Shear flow B) and extensional flow (Willenbacher et al., 2004).

Extensional viscosity (η_E) is a viscosity coefficient when applied stress is extensional stress. It does not usually reach steady-state. For a Newtonian fluid, extensional viscosity is thrice its shear viscosity, but for a polymer solution, extensional viscosity may be much higher than shear viscosity. (Phan-Thien, 2002) The Trouton ratio defines the ratio of extensional viscosity to the shear viscosity of the fluid:

$$Trouton\ ratio = \frac{\eta_E}{\eta_0}, \tag{32}$$

where η_0 zero-shear viscosity.

Rheological behavior occurs with Newtonian viscous fluids and with Hookean elastic solids. Most materials exhibit combination of both viscous and elastic characteristics. This mechanical behavior is called viscoelasticity. Elastic solid deforms by an amount proportional to the applied stress and maintains a constant deformation as long as the stress remains constant (Hooke's law). On removal of stress, the elastic energy stored in the solid is released and the solid immediately recovers to its original shape. Newtonian liquids do

not recover when the stress is removed. When viscoelastic materials are stressed, some of the energy involved is stored elastically, and the rest is dissipated as heat. So, the system is partly deformed into non-equilibrium position and partly flowing into new equilibrium position. (Shaw, 1985)

Viscoelasticity is described by shear modulus (G), which can be defined (Mezger, 2014):

$$G = \frac{\tau}{\gamma}, \tag{33}$$

where γ shear strain.

Shear strain describes deformation of the system and is defined (Mezger, 2014):

$$\gamma = \frac{s}{h}, \tag{34}$$

where s deflection path.

The higher the value of G the stiffer the material, since the deformation of the material is small. When a sample is sheared, ideally elastic material (solid) has no time lag between the applied deformation and resulting shear stress. Viscoelastic material has, however, a time lag for response signal, which can be measured by oscillatory test producing shear strain and shear stress sine curves (Figure 20). The time lag is called the phase shift (δ), and it is always between 0 º and 90 º. Since ideally elastic material has no time lag, δ = 0 º. For ideally viscous material, δ = 90 º. (Mezger, 2014)

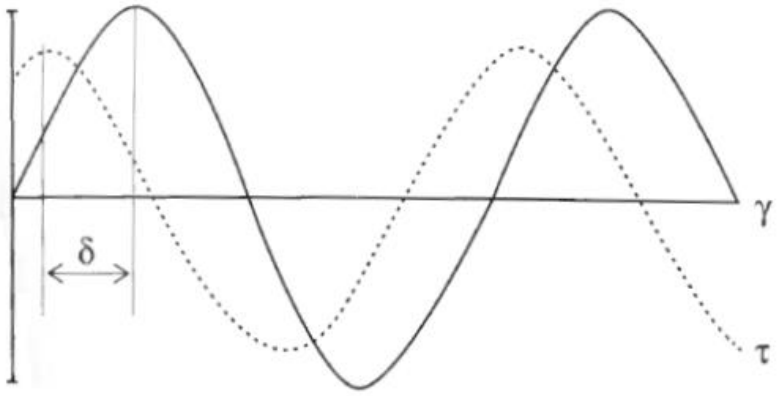

Figure 20 Phase shift (δ) between applied shear strain (γ) and resulting shear stress (τ) (Mezger, 2014).

Complex shear modulus (G^*) describes the entire viscoelastic behavior of a sample, the response of the material to oscillation (deformation/strain) on certain amplitude and frequency of oscillation (Grillet et al., 2012). Loss/viscous (G'') and storage/elastic (G') moduli are fractions of the complex shear modulus, which describe the liquid- or solid-like behavior of the material, respectively. Storage modulus describes the stored deformation energy and loss modulus describes the lost (dissipated) deformation energy. The relationship between phase shift, complex shear modulus, loss and storage moduli are presented in Figure 21 (Mezger, 2014).

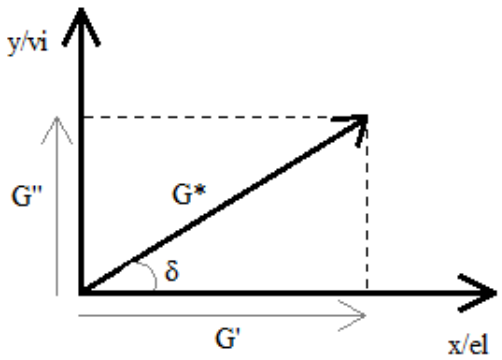

Figure 21 Loss (G'') and storage (G') moduli as fractions of complex shear moduli (G^*), using the phase shift angle (δ). Viscous portion of the viscoelastic behavior is presented on the y-axis and elastic portion on the x-axis. (Mezger, 2014)

Based on Figure 21, the following equation applies:

$$G^{*2} = G'^2 + G''^2. \quad (35)$$

Complex viscosity (η^*) describes the viscosity of viscoelastic material:

$$\eta^* = \frac{G^*}{\omega}, \quad (36)$$

where ω angular frequency of deformation.

Zero-shear viscosity (η_0) is the plateau value of complex viscosity at low frequency region. It is used in calculation of Trouton ratio (equation 32) for viscoelastic material. Zero-shear viscosity is proportional to molar mass of the polymer.

For viscoelastic solids, storage modulus is higher than loss modulus, thus $G' > G''$. This is due to links inside the material, chemical bonds or physical-chemical interactions. For viscoelastic liquids, loss modulus is higher than storage modulus, thus $G'' > G'$. Viscoelastic liquids do not contain such strong bonds between the molecules. Phase transition in the sample means that samples deforms during the measurement from liquid state to solid state or vice versa. Phase transition happens in gel point/crossover point, where loss and storage moduli are equal, $G'' = G'$.

Viscoelasticity is linear when the time-dependent compliance (stress/strain) of a material is independent of the magnitude of the applied stress (Shaw, 1980). This means, that for linear viscoelastic materials, the response (e.g. stress) is directly proportional to applied signal (e.g. strain) at any time (Barnes et al., 1989). Linear viscoelasticity has been modeled most knowingly by Maxwell and Kelvin-Voigt (Barnes et al., 1989; Phan-Thien, 2002). In linear viscoelastic region, the structure of the sample is not destroyed due to too large deformation applied (Mezger, 2014). In linear viscoelastic region, G' (and G'') are constant regardless of the strain applied. Limiting value, linearity limit (γ_L), of linear viscoelastic region is the highest value of strain (%) before change in constant value of G'.

Viscoelastic phenomena are described by Phan-Thien (2002). Normal stress difference (unequal normal stresses in a shear flow) causes:

- Weissenberg rod-climbing effect
    - Viscoelastic fluid climbs the rod whereas Newtonian fluid forms a vortex when stirred.
- die swell
    - Viscoelastic fluid swells remarkably more than Newtonian fluid when exiting a capillary.
- flow down an inclined channel
    - Viscoelastic fluid has a convex surface whereas Newtonian fluid has a flat surface when flowing in a channel.

Transient responses (quantification of relaxation time scale) cause:

- small strain oscillatory flow
    - Functions of the frequency, dynamic properties.
- stress overshoot
    - Shear stress overshoot before steady-state values, start-up of shear flow.
- stress relaxation
    - Shear stress relaxation after steady-state values, stop of shear flow.
- relaxation modulus
    - Shear stress relaxation after applying large strain rate over a small interval.
- recoil
    - Viscoelastic liquid retracts partly to some previous shape after removing a load. Newtonian liquid does not remember the previous shape and the motion of liquid stops immediately upon removal of loads. On the other hand, elastic solid remembers the previous shape perfectly and returns to the shape upon removal of loads.

Another way of describing viscoelasticity is studying interfacial rheology. This is particularly important for systems with high specific area, such as liquid films, emulsions and foams, and systems with surfactants (Ravera et al., 2010). In interfacial rheology, the surface is modified by shear or dilatational stresses. Dilatational stress is compression/expansion of the liquid, surface modification as the area of the surface decreases and increases, and thus variation to the interfacial tension of the liquid. Here, dilatational viscoelasticity, or complex viscoelastic modulus (E^*), is the quantity expressing the relationship between the surface modification of an interfacial layer and the related

dilatational stress (Ravera et al., 2010; Karbaschi et al., 2014). Dilatational viscoelasticity is the relaxation behavior of the fluid after external mechanical stress.

Complex surface elasticity modulus (E^*) of the interface is defined by Gibbs as a relation of interfacial/surface tension change ($d\sigma$) and surface area change (dA/A_0) (Biolin Scientific, 2017a; KRÜSS GmbH, 2018b):

$$E^* = \frac{d\sigma}{dA/A_0}. \tag{37}$$

As for complex shear modulus, only pure elastic interfaces response to mechanical stress without a phase lag. So in general, the interfacial tension follows the area change with a delay, which is due to relaxation processes in the interfacial layer and between the interface and the bulk system. Also complex surface elasticity composes of elastic/storage modulus (E') and viscous/loss modulus (E''). E' describes the impact of the changed area on the concentration change and is considered as pure dilatational elasticity. E'' describes the viscous contribution, and time-dependent change due to gradual concentration equilibration. (Biolin Scientific, 2017a)

For systems with surfactants, studying the dynamic interfacial layers is important for understanding the surfactant function at the fluid interface. Surfactants adsorb at the fluid interface. When expanding the interface, concentration of surfactant molecules with respect to the area decreases and thus the interfacial/surface tension increases. This is the elastic behavior of the interface (E') and it is reversible, so the initial value of surface tension is reached when the initial area of the interface is reached. However, as the interface expands, the free surfactant molecules in the bulk phase diffuse to the interface and adsorption occurs when the molecules fill the space at the interface. This process leads to time-dependent irreversible decrease of surface/interfacial tension and is referred as viscous behavior (E'') of the fluid. Both elastic and viscous processes take place at the interface of a system with surfactants, and the system response to dilatation is thus called viscoelasticity. (KRÜSS GmbH, 2018b)

Mechanism of adsorption and interactions between the molecules affect the properties of the absorbed layer and it can be studied simply via interfacial tension and dilatational viscoelasticity (Karbaschi et al., 2014). For example, molecular re-orientation, conformational changes and aggregation processes affect the properties of the interfacial layer. Thus, the surface kinetics are important in development and characterization of surfactants. Viscoelastic properties of the adsorbed interfacial layer correlate to emulsion and foam stability. Strongly viscoelastic interfacial layer stabilizes well thin films (Langevin, 2000).

Rheology of polymer systems, such as resins, is highly dependent on polymer characteristics such as molecular weight, molecular size and structure (chain length). These properties and in addition temperature and concentration of polymer molecules in solution affect the rheology of the polymer systems (Barnes et al., 1989). Chemically crosslinked polymers form strong networks. Network strength is described with equilibrium modulus (G_e), which is proportional to density of crosslinks. High equilibrium modulus corresponds to stiff systems. Polymer system can be made softer by increasing the space between crosslinks or by increasing defects to polymer network. Spacing can be done by increasing the molecular weight of the polymer chain connecting the crosslinks or by diluting the system with a liquid. Defects in polymer network are loops and hanging ends of polymer chains that are connected only from the one end of the chain. Defects are formed when in production of polymer system there is an imbalance between the number of polymer chains and crosslinkers. (Grillet et al., 2012) For resins, the crosslink density increases as the formaldehyde:phenol (F:P) molar ratio increases and the curing temperature increases (Halász et al., 2001).

The complex structure of a polymer system causes the wide variety of relaxation times, the time required for a system to relax from deformation. Deformation stretch and align sections of polymers. After deformation, the ends of the polymers can rearrange quickly, but the middle sections must wait the ends to relax before they can relax. The longest relaxation time of a free polymer, which determines the overall rheological behavior, is controlled by the molecular weight of the polymer and the viscosity of the surrounding fluid (Grillet et al. 2012). The final deformation of the polymer system is determined by its equilibrium modulus.

The viscoelastic nature of a polymer system and surface and interfacial tensions of the polymer and substrate play important roles in the characterizing the adhesion properties of the polymer system. Newtonian liquids make poor adhesives because they flow for example under gravity and do not stay in place. On the other hand, stiff elastic rubbers separate from a surface because they cannot deform. To function properly, polymeric adhesives must combine liquid-like characteristics (loss modulus *G*") to form good molecular contact under an applied pressure and solid-like characteristics (storage modulus *G*') to resist an applied stress once the bond has been formed. This combination usually requires a high-molecular-weight polymer to form the backbone of the adhesive and low-molecular-weight fractions which favor flow and deformation. (Grillet et al., 2012)

During the crosslinking/curing process of phenol-formaldehyde (PF) adhesive, the adhesive passes through different physical and relaxation states from the viscous to the rubbery or even glassy state. The transition of adhesive from liquid to solid phase occurs at the gel point ($G'' = G'$) at gel time. When $G' < G''$ viscous properties dominate, and only linear or weakly branched structures are formed. When $G' > G''$ elastic properties dominate, and highly branched network structure is formed. (Halász et al., 2001; Grillet et al., 2012) The gelation time is found to depend greatly on sample conditions, such as the concentration of polymer, the gelling temperature and the solvent conditions.

Dimensionless numbers describing rheological behavior of fluids are for example Deborah and Reynolds numbers. Deborah number is the degree of non-Newtonian behavior in a flow. Small Deborah number represents Newtonian flow, while non-Newtonian (with both viscous and elastic effects present) behavior occurs at intermediate range of Deborah numbers, and high Deborah number indicates an elastic/rigid solid. Reynolds number is a measure of the ratio of inertial forces to viscous forces of the fluid. Under low Reynolds numbers viscous forces dominate and the flow is laminar, and under high Reynolds numbers inertia forces predominates and the flow may be turbulent. (Goodwin and Hughes, 2008)

Rheology has a major role especially in studying the nature of colloidal systems, a mixture of dispersed particles (solid, liquid or gas) and dispersion medium (solid, liquid or gas), which are viscoelastic fluids (Shaw, 1980). Plywood adhesives are colloidal systems. Rheological behavior of colloidal systems depends mainly on:

- viscosity of the dispersion medium
- particle concentration
- particle size and shape
- particle-particle and particle-medium interactions.

7.2 Additives to affect rheology of resins

Additives to affect rheological properties of resins are in general mainly viscosity modifiers, such as thickeners. With water-based systems, for example cellulosics, acrylics and associative rheology modifiers (polyurethane and polyether derivatives) may be used (BASF, 2016). Carboxymethylcellulose (CMC) and acrylate thickeners are widely used in paper coatings (Willenbacher et al., 2004). Other rheological additives are for example defoamers to prevent foam generation during mixing and application of adhesive, and dispersants to prevent settling and clumping of the mixture.

In curtain coating, thickeners improve stretchability of the coating material. Newtonian flow behavior and high shear viscosity are preferred (BASF, 2016). Thickeners are large molecules containing functional groups to interact with the coating material (Birkert et al., 2006). Compatibility of thickeners with other additives, especially surfactants, must be considered. Associative thickeners have somehow similar characteristics as surfactants and use of multiple additives in the same adhesive composition may affect the performance of additives (BASF, 2016).

Methoxy- and hydroxy-celluloses may be used as thickeners in ethyl, propyl or alkyl forms. With cellulose thickeners it is possible to reach viscosities of 2000-4000 mPas. Typical amount of thickeners added is less than 0,5 % of the resin composition. Cellulose modifiers result more flexible film and improve dry-out resistance. However, cold-press tack is reduced due to hydrophilic nature of cellulose modifiers. (Sellers, 1985)

CMC and acrylate thickeners for paper coatings indicate shear thinning flow behavior but with relatively low decrease in viscosity. Acrylate thickeners indicate typical elongational behavior of an elastic fluid as the filament diameter decreases exponentially as the function of time. CMC indicate viscous fluid elongational behavior as the filament diameter decreases

more linearly. Long filament break-up times correlate with higher stretchability of the coating material. (Willenbacher et al., 2004)

The basic structure of polyurethane and polyether derivates consists of polyethylene glycols, hydrophobic alcohols and diisocyanates as linking groups. They are hydrophobically modified but still water-soluble, can give coatings more Newtonian or plastic nature and can be modified by the type of hydrophobic end group, molecular weight and degree of branching. Hydrophobically modified polyurethanes and polyethers are abbreviated HEUR and HMPE, respectively. Also hydrophobically modified alkali swellable emulsions (HASE) are generally used rheological additives. (BASF, 2016)

Examples of commercial thickeners for coatings and adhesives are presented in Table XV.

Table XV Commercial thickeners for coatings and adhesives available.

Producer	**Brand**	**Description**	**Reference**
BASF SE	Sterocoll®	Rheology modifier, thickener. Paper coating additive.	(BASF, 2018b)
BASF SE	Rheovis®	Associative and non-associative thickeners, formulation additive for e.g. adhesives and industrial coatings.	(BASF, 2013; 2016)
BYK Additives & Instruments	OPTIFLO	Associative thickener for aqueous e.g. coatings and adhesives to generate a Newtonian flow behavior.	(BYK, 2018)
DOW Chemical	ACRYSOL™	Rheology modifiers, associative thickeners. Excellent flow and levelling, improved viscosity stability.	(DOW, 2018a)
Evonik Industries	TEGO® Rheo	Thickeners for polymer dispersions to obtain Newtonian or pseudoplastic flow behavior. Suitable for water-based adhesives.	(Evonik, 2017a; 2018)
Evonik Industries	TEGO® ViscoPlus	Associative thickeners for waterborne systems to obtain Newtonian, Newtonian with high shear rate, pseudoplastic or strongly pseudoplastic flow behavior. Coating additive.	(Evonik, 2015)
King Industries, Inc.	DISPARLON® AQ-6xx, AQH-8xx	Associative thickeners, anti-settling and anti-sagging. Post-addable.	(King Industries, 2017)
King Industries, Inc.	K-Stay® 700	Thickeners to obtain pseudoplastic and shear thinning flow behavior. Addition during fluid preparation.	(King Industries, 2017)

However, in general adhesive fillers and extenders are used as thickening agents. They are low cost powders, such as wheat flour, corn cob, soda ash (sodium carbonate), lime (calcium carbonate) and mixtures thereof. Fillers and extenders are used to adjust adhesive viscosity and dry matter content. Commercial rheological additives are more expensive and thus rarely used, but could be applied to give adhesive certain type of flow properties.

Resin cooking properties to increase viscosity are high solids content, high temperature and varying reaction time of polymerization. Thus, the degree of polymerization can be affected (Sellers, 1985). Lignin is generally applied as high-molecular-weight (HMW) polymer into the resin composition, which increases the viscosity of the resin more rapidly when compared to conventional PF resins.

Foam generation is one of the operational challenges in plywood production. Foaming causes defects on adhesive surface and thus adhesive application onto veneer is not uniform. Foaming is particularly problematic for high viscous and high solids liquids (Evonik, 2015). Adhesive mixing and the adhesive pumping up to the applicator in curtain coating are the main points where foam may be generated.

Foaming can be prevented or generated foam can be broken by anti-foaming agents, defoamers. Defoamers cause air bubbles to burst and release the air. When surfactants are used, the surface of the liquid is filled with surfactants. Surfactants may stabilize the foam bubble by retarding the coalescence of the bubbles (BASF, 2018a). Defoamers enter the foam bubble surface, spread and cause an opposite Marangoni effect. Fast thinning foam bubble collapses. Defoamers are required to have lower surface tension than surfactants. They may be of insoluble or partially soluble in the medium, and they have positive entering and spreading coefficient (BASF, 2013). In general, defoamers can be classified into three groups; silicone, mineral oil and polymer defoamers.

Incompatibility of the defoamer and the binder material may cause surface defects such as cratering or wetting problems, but foaming is well prevented. On the other hand, too good compatibility/solubility does not accomplish anti-foaming function, but there are no undesired influences on the surface of the material. (BASF, 2018a) Defoamers have surface

active properties, which may counteract with surfactants required for surface tension reduction and curtain formation (Sellers, 1985).

In this work, defoamers are considered as rheological additives even though their functionality at the surface of the material is described. Defoamers affect the rheology of the material, since removal of air bubbles from the liquid affects the flowing properties. Also surface viscosity and elasticity may be decreased if they disrupt the surface structure formed by adsorbed surfactant molecules. In addition, the selected defoamers used in the experimental part of the work, are mainly oil-based defoamers which do not remarkably affect the surface tension of the resin.

Examples of commercial defoamers for coatings and adhesives are presented in Table XVI.

Table XVI Commercial defoamers for coatings and adhesives available.

Producer	**Brand**	**Description**	**Reference**
BASF SE	FoamStar®	Defoamers for water-based formulations, adhesives and sealants. Silicone and polymer-based, emulsion and powder defoamers.	(BASF, 2013; 2018a)
BASF SE	Foamaster®	Defoamers for water-based formulations, adhesives and sealants. Oil-based (mineral, native and white oil), blends and organic.	(BASF, 2013; 2018a)
BASF SE	Etingal®	Defoamer for coatings. Prevention and elimination of surface foam.	(BASF, 2018b)
BYK Additives & Instruments	BYK-0xx	Defoamers for coatings, adhesives and sealants. Optimized compatibility. Silicone-free (polymer), silicone and mineral oil-based.	(BYK, 2018)
DOW Chemical	DOWFAX®	Non-ionic surfactants as foam control agents, low foam characteristics.	(DOW, 2018c)
DOW Chemical	PxxxxE	Defoamers to prevent and eliminate foam in aqueous systems. Water insoluble polypropylene glycols.	(DOW, 2018c)
Evonik Industries	AIRASE®	Defoamers and deaerators for waterborne applications, optimum compatibility. A coating additive. Polyether siloxanes and organic polymer-based.	(Evonik, 2017b)
Evonik Industries	TEGO® Foamex	Prevents foam formation in waterborne coatings and printing inks. For high solids coatings too. Pre-existing foam is destroyed and air inclusions are prevented. Optimized particle size for optimized compatibility. Polyether siloxanes, mineral oils and organic polymer-based.	(Evonik, 2015; 2017b)
Evonik Industries	TEGO® Antifoam	Defoamer additive for water-based formulations/adhesives/polymer dispersions. Provides long term stability. Optimized compatibility. Polyether siloxanes, polyether + siloxine, paraffinic oil and vegetable oil-based.	(Evonik, 2017a; 2018)

7.3 Analytical methods

Rheometers are used for characterizing especially non-Newtonian fluids without a constant viscosity. The non-Newtonian fluids cannot be described by a single number, because they exhibit a variety of different correlations between shear stress and shear rate under different flow conditions. There are two main types of rheometers; rotational (shear) and extensional rheometers based on the type of stress they apply.

Commonly used shear rheometers apply rotation of a spindle, a concentric cylinder or cone and plate combinations in a fluid (Figure 22). Applied shear stress, shear rate, strain and temperature can be constant or variable and the behavior of the fluid in set parameters is measured as viscosity, strain or as storage (G') and loss modulus (G''). To characterize viscoelastic properties of the fluid, for example creep and relaxation measurements (Shaw, 1985; Barnes et al., 1989; Grillet et al., 2012), viscosity measurement (Willenbacher et al., 2004), strain and frequency sweeps and time and temperature sweeps (Grillet et al., 2012; Moubarik, 2014) may be performed.

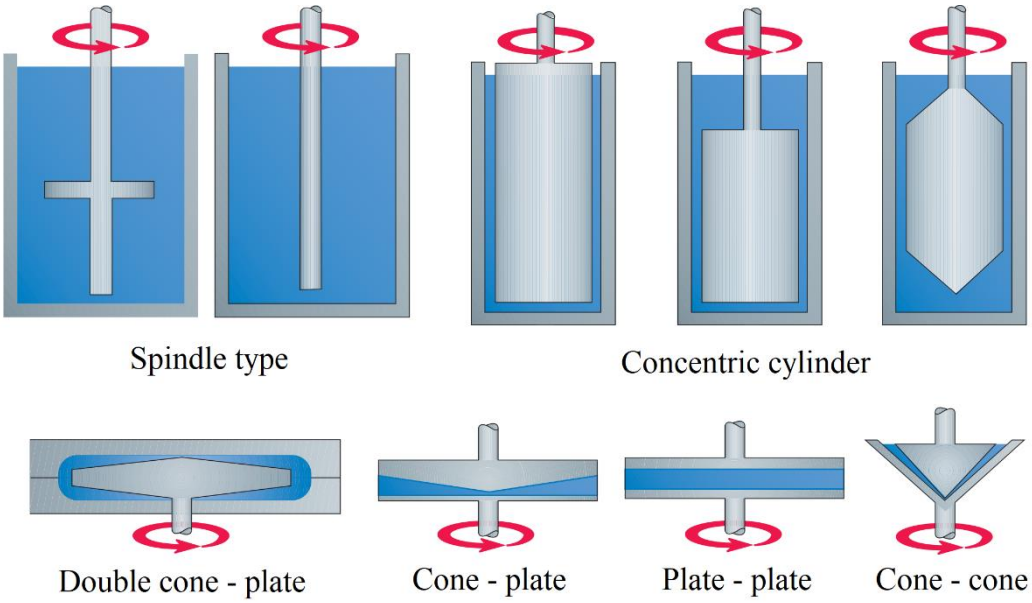

Figure 22 Rotational rheometer equipment options (Tetra Pak, 2018).

Suitable for resins, with narrow-gap concentric cylinder rheometer, shear rate is applied as rotation of cylinder, and can be determined (Barnes et al., 1989):

$$\dot{\gamma} = \frac{r_o \omega}{r_o - r_i}, \tag{38}$$

where ω angular velocity of the inner cylinder
r_o radius of the outer cylinder
r_i radius of the inner cylinder.

When the fluid rotates, it attempts to drag the outer, stationary cylinder around with it. The torque applying to the outer cylinder when it is held in place, is measured and can be converted to shear stress (Barnes et al., 1989):

$$\tau = \frac{M}{2\pi r_i^2 l}, \tag{39}$$

where M torque
l length of the inner cylinder.

Finally, the viscosity is measured as a ratio of shear stress to shear rate as in equation (29).

Static methods to characterize viscoelasticity of a fluid are creep and relaxation measurements (Barnes et al., 1989). In creep measurement, constant shear stress is applied, and strain (deformation) is measured as a function of time, which gives insight about the flow behavior after shearing (recovery after shearing). A polymer liquid or other viscoelastic liquid will eventually reach a constant strain rate. A polymer gel or other viscoelastic solid is subjected to a constant stress, it will eventually reach a constant strain. (Grillet et al., 2012) Viscosity curve describes also the Newtonian/shear thinning/shear thickening flow behavior. Here, viscosity is measured as a function of shear rate or shear strain. In relaxation measurement, constant strain is applied, and relaxation of stress is measured as a function of time. Relaxation behavior of the fluid is more challenging to measure than strain, which is why relaxation measurement is not as common as creep measurement (Barnes et al., 1989).

Oscillatory tests (sweep measurements) are dynamic methods to characterize viscoelasticity of a fluid (Barnes et al., 1989). Oscillation is applied on certain amplitude and frequency (Grillet et al., 2012). Linear viscoelasticity region of the fluid is determined by

strain/amplitude sweep (constant frequency (*Hz* or ω), strain varies (%), Figure 23A). Polymer network properties are characterized in the linear domain, where *G*' is constant. From strain sweep, strain value of linearity limit (γ_L) can be determined. Gel point, where phase transition takes place, is determined by time sweep (constant frequency and strain, behavior of both moduli (*G*' and *G*'') as a function of time). Time sweep may also be performed in higher temperature to study the gelation in industrially interesting temperature (for example curing behavior of plywood adhesive (Moubarik, 2014)). Gel point may also occur in frequency sweep. Frequency sweep (constant strain or stress, frequency varies, Figure 23B) is used to characterize different relaxation times and to determine equilibrium modulus. For polymer systems, the elastic response depends on the frequency of oscillation. At low frequencies, the system has time to rearrange but with higher frequencies not. Here, the stiffness of the system can be determined which gives insight of the degree of crosslinking of the polymer. Highly crosslinked polymers have longer relaxation times. Gel point is proportional to molar mass of the polymer (Mezger, 2014). System relaxation time (λ) can be determined from gel point frequency. As the frequency approaches to zero, elastic modulus reaches a constant value, which is the equilibrium modulus (G_e). (Grillet et al., 2012)

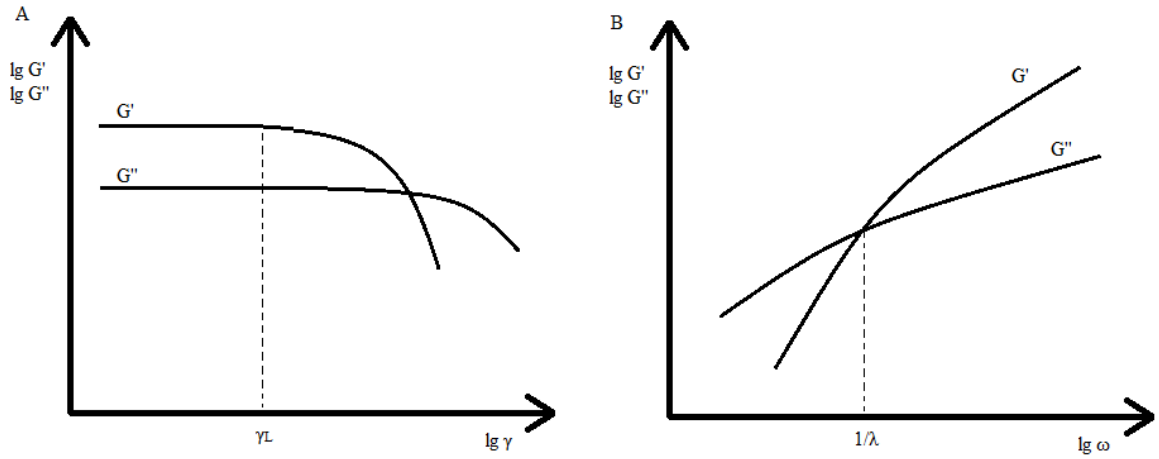

Figure 23 A) Strain/amplitude sweep and B) frequency sweep examples, logarithmic storage (*G*') and loss (*G*'') plotted as a function of logarithmic strain or angular frequency, respectively. Determination of strain value of linearity limit (γ_L) and relaxation time (λ).

Extensional rheometers are less common. Two interesting extensional rheometers for liquids apply filament stretching and break-up studies. HAAKE™ CaBER™ (capillary break-up

extensional rheometer) is a commercial rheometer by Thermo Fisher Scientific (Willenbacher et al., 2004) used for measurement of extensional viscosity of for example paper coatings (Voss & Tadjbach, 2004; Birkert et al., 2006). CaBER^{TM} can be used for characterization of fluids and semi-solids with shear viscosity range of 10-10^{6} mPas (Thermo Fisher Scientific, 2018). Operating principle of the rheometer is based on stretching a drop of fluid between two parallel plates (uniaxial extensional flow). Upper plate is moved up rapidly (50 ms), so the sample elongates and produces a liquid filament (Figure 24). The diameter of the filament as the necking proceeds is measured by laser micrometer as a function of time until the filament breaks-up (Figure 25). Long break-up time correlates with high extensional viscosity.

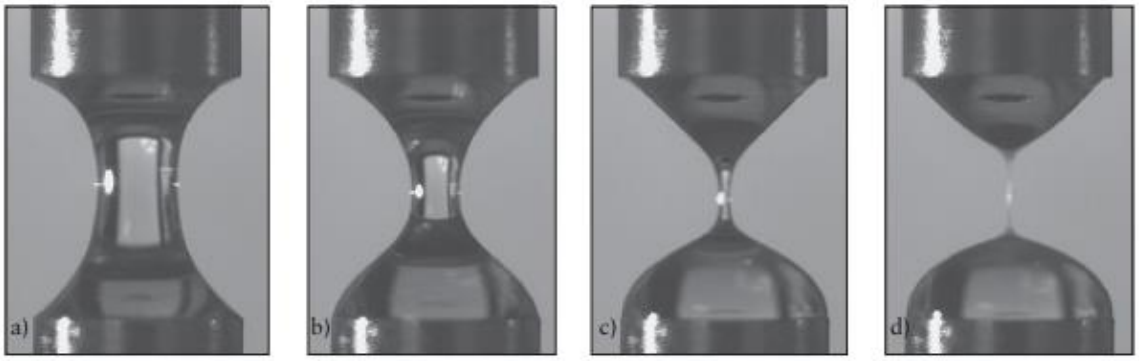

Figure 24 Example of CaBER^{TM} measurement. A) Filament forming. B-C) Filament necking. D) Filament break-up. (Willenbacher et al., 2004)

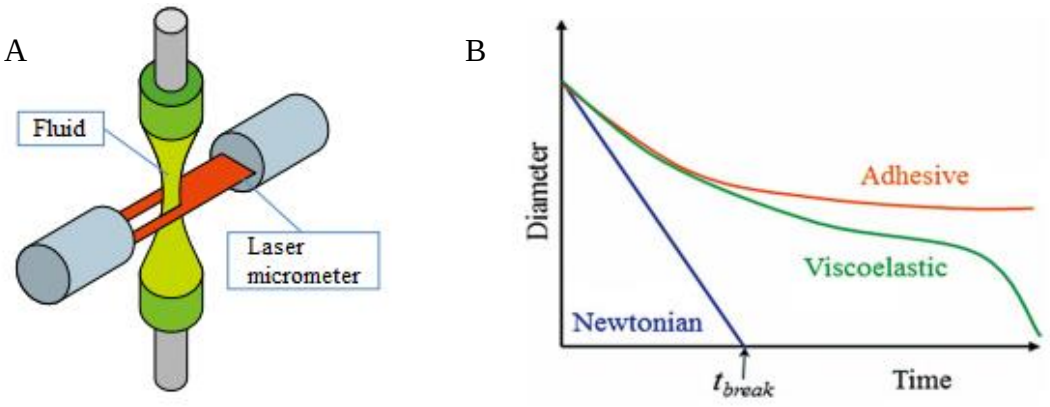

Figure 25 Measurement of filament diameter as a function of time with CaBER^{TM} extensional rheometer. A) Sample stretched between two parallel plates and laser micrometer measuring the diameter of the fluid. B) Typical behavior of adhesive, viscoelastic fluid and Newtonian fluid in CaBER^{TM} extensional rheometer. (Willenbacher et al., 2004)

If the surface tension of the sample is known, apparent extensional viscosity can be determined. Midfilament diameter can be measured by CaBER^{TM} (Cambridge Polymer Group, 2013):

$$d_{mid}(t) = \frac{-\sigma}{\eta_E}. \tag{40}$$

For viscoelastic liquids, the break-up time increases dramatically as the polymer weight increases (Anna & McKinley, 2001). For Newtonian liquids, the filament thinning is linear with time. Here, equation (40) is also the slope of the curve. σ/η_E may here be termed capillary velocity, so it is the absolute value of slope (McKinley & Tripathi, 2000).

Apparent extensional viscosity can be solved (Anna & McKinley, 2001; Yesilata et al., 2006):

$$\eta_E(t) = \frac{-\sigma}{d d_{mid}/dt}. \tag{41}$$

Apparent extensional viscosity is plotted as a function of Hencky strain (also known as true strain and logarithmic strain, ε) (Anna & McKinley, 2001; Yesilata et al., 2006):

$$\varepsilon(t) = 2 \ln\left(\frac{d_0}{d_{mid}(t)}\right), \tag{42}$$

or as a function of Hencky strain rate ($\dot{\varepsilon}$):

$$\dot{\varepsilon}(t) = -2\frac{dln(d_{mid}/d_0)}{dt}, \tag{43}$$

where d_0 initial sample diameter between the plates in the beginning of the measurement.

Apparent extensional viscosity of Newtonian liquids is constant over Hencky strain and approximately three times its shear viscosity. For viscoelastic polymer solutions, the

apparent extensional viscosity increases as the strain increases. For adhesives, the apparent extensional viscosity diverges as the adhesive starts to solidify over time. (Cambridge Polymer Group, 2013)

Elongational relaxation time (λ_E) can be calculated from equation (Yesilate et al., 2006):

$$d_{mid}(t) \approx \exp\left(-\frac{t}{3\lambda_E}\right). \quad (44)$$

Elongational relaxation time dependence to relaxation time obtained from oscillatory shear rheology (λ) varies depending on the fluid material. For viscoelastic fluids, relaxation times are approximately equal. Strain rate and elongational relaxation time can be utilized in calculation of dimensionless Deborah number, known as stretch rate. (Anna & McKinley, 2001)

CaBER™ assumes axial symmetry of filament thinning. However, gravitational effects break this symmetry, and cause weak axial flow downwards. Relative magnitude of the effect compared to opposing capillary forces can be described by dimensionless Bond number (McKinley & Tripathi, 2000; Anna & McKinley, 2001):

$$Bo = \frac{\rho g d_0^2}{4\sigma}. \quad (45)$$

The gravitational effect can be neglected if Bond number is much less than 1 (McKinley & Tripathi, 2000).

Surface tension, viscosity, elasticity and mass transfer affect the filament stretching phenomenon (Willenbacher et al., 2004). By monitoring the dynamics of the fluid filament break-up following a rapid extensional deformation of the sample, information about relaxation times, non-Newtonian flow behavior and break-up time of the fluid can be obtained (Cambridge Polymer Group, 2013).

Cambridge Polymer Group has developed another filament stretching applying extensional rheometer (FiSER™), which has provided wide applicability in characterizing viscous

polymers fluids and melts with true uniaxial extensional flow. During the measurement, FiSER^{TM} elongates the sample continuously, whereas CaBER^{TM} rapidly elongates the sample once in the beginning of the measurement. The limitation of the device is incompatibility with low viscosity fluids, relatively high cost and no commercial availability.

For solid samples, there are extensional viscosity accessories to be attached to shear rheometers available. These optional accessories in general apply horizontal elongation of the sample, which is loaded between two drums.

Viscometers measure fluid properties under only one flow condition and provide a single value of shear viscosity. They are most applicable for characterizing of Newtonian fluids with constant viscosity but are generally used also for non-Newtonian fluids to obtain overall conception of viscosity of the analyzed fluid. Viscometers can be for example rotational or glass capillary viscometers. Brookfield is very common viscometer manufacturer (Beneventi & Guerin, 2005), which apply rotation of for example a spindle or cone into fluid.

To determine dilatational interfacial viscoelastic properties of the fluid, forced oscillation of a bubble/drop at broad frequency range is a well-known analysis (Ravera et al., 2010; Karbaschi et al., 2014). Here, the interfacial tension and the surface area change of the drop is measured while the drop is pulsating at determined frequency. The pulsation/deformation of the interfacial layer is caused by expansion/compression of a hanging drop. The surface/interfacial tension is determined by pendant drop shape analysis method with Young-Laplace fit (KRÜSS GmbH, 2018b). The method is simple, but possibly occurring deviations from sphericity, caused by gravity, lead to unwanted overtones in the experiment and thus deviations from an ideal shape of drops must be considered (Karbaschi et al., 2014).

7.4 Discussion

To summarize the studied rheological properties, Figure 26 is presented.

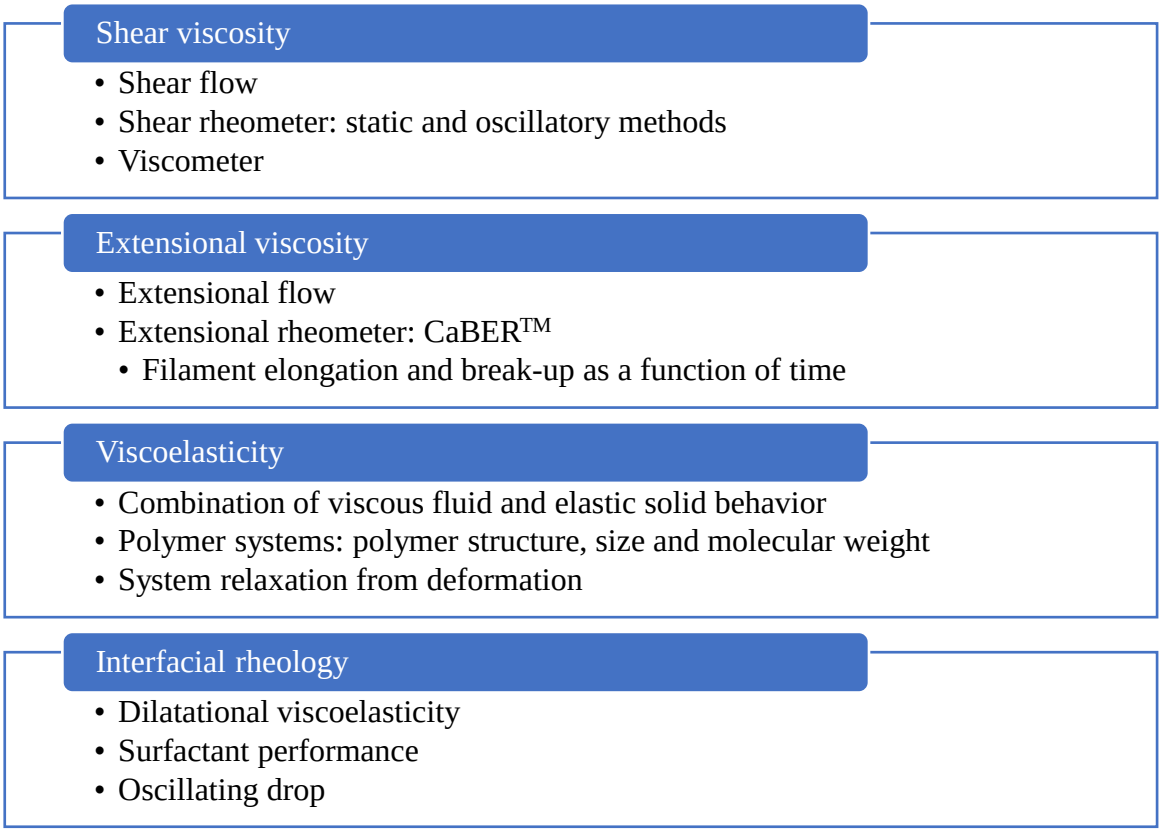

Figure 26 Summary of rheological properties studied in this work and methods to measure the properties.

Flow behavior of the resins can be determined by shear rheometer. As stated, Newtonian flow behavior is desired for curtain coating materials, and by rheological thickeners flow behavior can be changed. Resins are polymer systems and thus viscoelastic properties measured by shear rheometer oscillatory methods are interesting to be determined. Viscoelasticity gives insight about the structural stability of the coating material.

In curtain coating, if the coating material contains long flexible molecules (polymers), viscoelastic tensile stress will appear. Strong planar extensional flow occurs due to the liquid acceleration as it flows down the curtain (Figure 27). The effect of viscoelastic behavior on liquid curtain stability was investigated by Becerra and Carvalho (2011). They have shown that the presence of small amount of high molecular weight polymer in the liquid, which leads to high extensional viscosity, can remarkably increase the stability of the curtain.

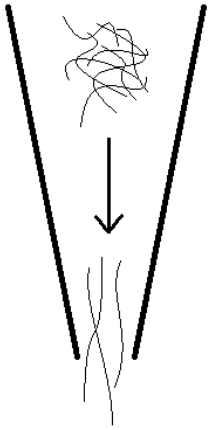

Figure 27 Polymer chains of the fluid are stretched in extensional flows.

Also studying the interfacial rheology and more precisely dilatational viscoelasticity as a measure for surfactant performance is interesting, since surfactants are going to be used in the experimental part of this work. This measurement can be interesting to be compared to frequency sweep of oscillatory tests, since in both determinations frequency is varied.

EXPERIMENTAL PART

In the experimental part of the work, surface chemical and rheological properties of resins are determined. In the experiments, commercial phenol-formaldehyde (PF) resins for roller and curtain coating and lignin-phenol-formaldehyde (LPF) resin are used as reference resins. It can be assumed, that the commercial PF curtain resin contains unknown additives, and it has different properties than roller coating resin. To the LPF resin, commercial surfactants and defoamers are added to obtain similar surface chemical and rheological properties than commercial PF curtain resin has. This gives insight about the applicability of LPF resin in curtain coating of veneer.

Used analytical methods are surface tension, surface free energy, shear rheology, extensional rheology and interfacial viscoelasticity. Suitability of the analytical method to be used in determination of resin properties is reviewed. Additive performance is evaluated.

Final aim of the experimental part of this work is to determine operational windows for additive dosing for LPF resin to be applied in curtain coating of veneer. Operational windows are determined for two surfactants with all defoamers, based on elongation property target.

8 MATERIALS

Next, resins, surfactants and defoamers used in this work are reviewed. Resin and additive combinations are presented as experiments.

8.1 Resins

In the experiments, commercial plywood phenol-formaldehyde (PF) resins for roller and curtain coating are used as reference resins. PF resin for roller coating is further referred as PF resin and PF resin for curtain coating is further referred as PF curtain resin.

Lignin-phenol-formaldehyde (LPF) resin produced by UPM. LPF resin contains 50 % of lignin of the amount of phenol. Preparation of LPF adhesive is performed in Figure 28.

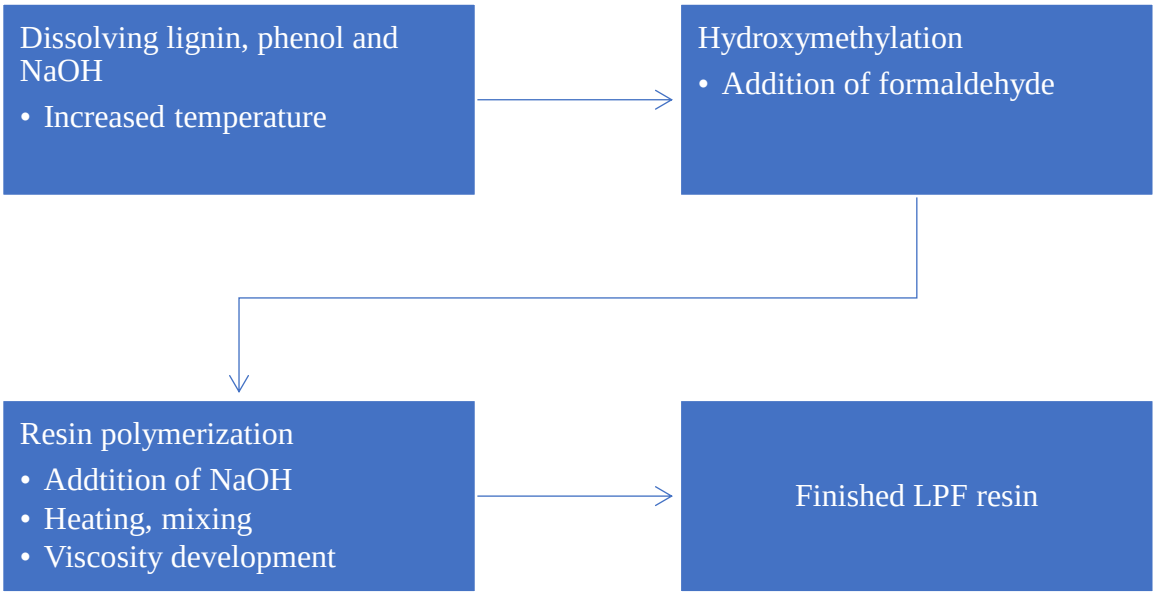

Figure 28 Lignin-phenol-formaldehyde resin and adhesive preparation.

Resins used in this work are stored frozen in a freezer (temperature -19 ºC). Before using them for analyses, the resins are completely melted. Liquid resins are stored in a fridge (temperature + 5-7 ºC) for a week at longest. Prior to use, resins are mixed for 5 minutes to obtain homogenous composition.

8.2 Additives

Surfactants used in this work are all produced by Evonik Industries AG. All surfactants are suitable for water-based coating and adhesive formulations. Surfactants are:

- Surfactant 1 is non-ionic superwetter utilizing Gemini surfactant technology. Non-persistent foam generation.
    - Concentration: 100 %.
- Surfactant 2 is non-ionic dynamic wetting agent and in some applications molecular defoamer.
    - Concentration: component A 50-70 %, component B 10-25 %.
- Surfactant 3 is non-ionic dynamic wetting agent. Low foaming.
    - Concentration: component A 100 %.
- Surfactant 4 is non-ionic, organic wetting agent. Low foaming.
    - Concentration: 100 %.

In addition, one additive working as a surfactant and defoamer produced by Evonik Industries AG is studied:

- Surfactant/Defoamer 1 is non-ionic wetting agent utilizing Gemini surfactant technology and molecular defoamer.
    - Concentration: component B 70-90 %, component C 20-35 %.

Surfactant 1 was chosen because of its superwetting ability. Surfactant 2 was chosen because of its additional nonfoaming or in some cases defoaming ability. Surfactant 3 was chosen because it composes of component A of surfactant 2. Surfactant 4 was chosen because of its remarkably different chemical composition. Surfactant/defoamer 1 was chosen because of its additional defoaming ability and it mostly composes of component B of surfactant 2.

Different surfactants have been tested previously in curtain coating trials. Based on trials, surfactants 1-3 are considered as good additives for achieving a stable curtain. Surfactant 4 has given varying results depending on surfactant dosage. Performance of surfactant/defoamer 1 has not been desired in trials at dosages typical for surfactants. At lower dosages it has shown defoaming ability. In this work, effect of surfactants on LPF resin properties is determined.

Surfactants are added preliminary at three dosages; 0,2 %, 0,4 % and 0,6 % of the weight of resin. Surfactant amount 0,6 % is considered maximum dosage based on economic point of view of industrial scale production process. Even lower dosages than 0,2 % of the weight of resin are interesting, but this dosage is preliminary considered as a minimum amount for achieving a stable curtain based on previous curtain coating trials.

Defoamers used in this work are:

- Defoamer 1 is organic oil defoamer produced by Evonik Industries AG. Controlling and eliminating foam.
- Defoamer 2 is vegetable oil defoamer produced by Evonik Industries AG. Avoiding premature coagulation.
- Defoamer 3 is non-ionic surfactant and defoamer produced by Dow Chemical.

All three defoamers have performed defoaming ability in previous laboratory foaming tests. In curtain coating trials, performance of defoamer 1 has not been desired. In this work, effect of defoamers on LPF resin properties is determined. Dosages of 0,03 % and 0,05 % of the weight of resin are considered relevant for industrial scale production process, but also amount of 0,10 % of the weight of the resin is partly studied. Compatibility of surfactants and defoamers have also been tested previously, but not with a systematic approach.

All additives are presented in Appendix I (classified).

To add additives to a resin sample, average weight of a drop of each additive was determined by weighing (accuracy 0,1 mg) 10 separate drops of an additive formed with 1 ml pipette. Desired dosage of an additive was added to resin sample at the precision of a drop. After the addition, resins were mixed and stored for at least 24 h, and mixed again prior to analyses. Storage of resins allows additives to affect the solution.

8.3 Experiments

Final experiments of the work are presented in Appendix II, Table I and Table II. Visual presentation of the experiments is presented in Figure 29 and Figure 30. In total the work includes 79 experiments.

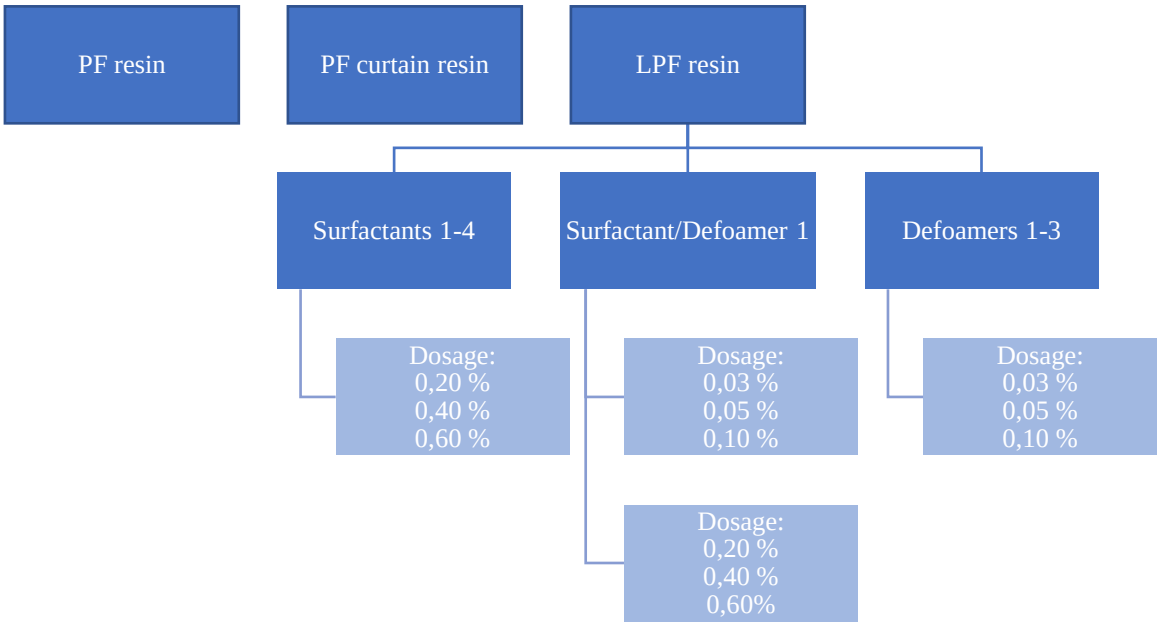

Figure 29 Experiments of the work. PF resin, PF curtain resin and LPF resin as the reference resins. To LPF resin, in total 8 additives are added at different dosage levels, surfactants primarily 0,20 %, 0,40 % and 0,60 % and defoamers 0,03 %, 0,05 % and 0,10 %. Surfactant/defoamer 1 was added at all dosage levels.

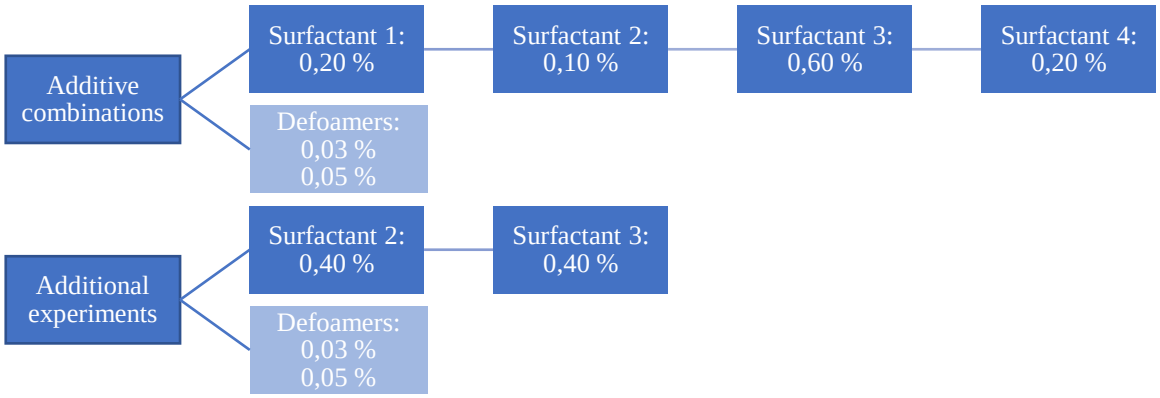

Figure 30 Additive combinations and additional experiments of the work. Surfactant dosage level selected based on surface tension results so that the surface

tension at the same level with PF curtain reference resin. Additional experiments added based on results from extensional rheology.

9 METHODS

Next, the analytical methods, used devices and operation conditions, to determine general, surface chemical and rheological properties of the resins performed in this work are reviewed.

9.1 Determination of general properties of resins

General properties of the reference resins (PF resin, PF curtain resin and LPF resin) were determined, including the following properties:

- Dry matter content, [%]
- pH, [-]
- Conductivity, [mS/m]
- Alkalinity, [%]
- Free formaldehyde content, [%]
- Gel time, [min]
- Viscosity, [cP] and [s]
- Molar mass, [-]

Dry matter content of the resins was determined by measuring approximately 1 g of resin and drying it in the temperature 105 ºC for 3 h. pH and conductivity were determined by Mettler Toledo SevenCompact pH/Ion S220 and SevenEasy S230 devices, respectively. Alkalinity and free formaldehyde content were determined by internal titration methods. Gel time was determined by setting the resin sample in a test tube into 100 ºC water and measuring the time for resin to form gel-like structure. Viscosity was determined by Brookfield DV1 digital viscometer (plate spindle, speed of 50 rpm) and flow viscosity cup (FC) DIN53211 (6 mm hole) in temperatures 20 ºC and 25 ºC. Polymer molar masses (number average and weight average), polydispersity index (PDI, M_w/M_n) and peak maximum were determined by Thermo Dionex size exclusion chromatography (SEC) device.

9.2 Determination of surface chemical properties of resins

Attension Theta optical tensiometer manufactured by Biolin Scientific was used for determination of surface tension of the experiments. Theta tensiometer utilizes pendant drop shape analysis method for surface tension determination. In calculation of results, LPF resin density 1,2073 g/cm^3 was used. A drop was formed with a micropipette of 200 µl and the drop volume was 4 µl in all but one experiment with drop volume of 3,5 µl. Drop volume of 4 µl (or 3,5 µl) was the maximum for resins including surfactants to be formed and not to drop during the measurement. For PF resin and LPF resin, larger drops could have been formed, but the drop volume effect on obtained surface tension values was not remarkable. The measurement was started when the drop was formed. Surface tension value after 3 seconds of the beginning of the measurement was selected. At least 5 replicates were done for each sample and the repeatability was good. An average surface tension value was calculated for each sample. The accuracy of the device was 0,01 mN/m. The device was calibrated daily prior to use. Measurements were performed in temperature of 23 ± 2 ºC.

For comparison, surface tension of the reference resins was also determined with De Noüy ring method. Manual Force Tensiometer K6 manufactured by KRÜSS GmbH was used. At least 3 replicates were done for each sample and the repeatability of the measurement was good. The accuracy of device utilizing the ring method was approximately 0,5 mN/m. The device was calibrated by using water. The scale of the device was adjusted for each sample.

Attension Theta optical tensiometer was also used for contact angle measurements to determine surface free energy of the resins. For the measurements, sufficient amount of resin was dried in room temperature onto piece of glass. Contact angles between the solid resin surface and sessile drop of water, ethylene glycol and diiodomethane were determined. Drop volumes used were 3 µl for water and ethylene glycol and 1 µl for diiodomethane. The measurement was started when the drop was detached from the capillary. Contact angle values after 0,5 and 1 second of the beginning of the measurement were selected. At least 5 replicates were done for each sample, but the repeatability was not good. An average contact angle value was calculated for each liquid for each sample based on at least 4 replicates. The accuracy of the device was 0,01 º. The device was calibrated daily prior to use. Measurements were performed in temperature of 23 ± 1 ºC and relative humidity of 50 ± 2

%. Total surface free energy and its components were calculated with Steven Abbott calculator (Abbott, 2018).

9.3 Determination of rheological properties of resins

MCR302 shear rheometer manufactured by Anton Paar GmbH was used for determination of shear viscosity, structural and viscoelastic properties of the reference resins. CC27 concentric cylinder (inner cylinder effective length 40,024 mm and diameter 26,665 mm; outer cylinder positioning length 72,5 mm and diameter 28,920 mm) was mainly used but also ST-24 paddle spindle stirrer was tested. Viscosity curve, amplitude sweep to determine the linear viscoelastic region of the resins and frequency sweep were performed. For viscosity curve, shear rate was varied first from 1 to 100 1/s and then from 100 to 1 1/s. Shear rate was also varied from 1 to 500 1/s and from 500 to 1 1/s. For amplitude sweep, strain varied from 0,01 to 100 % and frequencies of 15, 10 and 1 rad/s were used. For frequency sweep, angular frequency varied from 500 to 0,5 rad/s and strains of 1, 0,5 and 0,1 % were used. Measurements were performed in temperature of 25 ºC.

HAAKE™ CaBER™ 1 capillary break-up extensional rheometer manufactured by Thermo Fischer Scientific Inc. was used for determination of elongational properties of the experiments. Plates of 6 mm were used, so also the sample diameter was 6,0 mm. Initial and final aspect ratios defining the sample elongation were 1,00 and 2,75, respectively, so the sample initial height and final heights were 2,99 mm and 8,24 mm, respectively. System imposed axial Hencky strain (ε_f) was 1,01, which is between the optimal range ($1 < \varepsilon_f < 2$) determined by Anna & McKinley (2001). Measurement duration was 2 s and sampling rate 4000 Hz. For each experiment, at least 6 replicates were done and for each replicate 2 elongations. The repeatability was good. The resin filament diameter was measured as a function of time and the break-up time determined. The diameter was normalized for scale 0-1. Apparent extensional viscosity curves were plotted as a function of strain. Plotting was performed by V4.50 CaBER Data Analysis software. An average curve for filament elongation was calculated for each sample based on at least 5 replicates. Average apparent extensional viscosity curves were calculated for part of the experiments, and in calculations, LPF resin density 1,2073 g/cm^3 and surface tension determined by pendant drop method were used. Measurements were performed in temperature of 25 ± 2 ºC.

Effect of additive dosage increase was studied and working curve coefficients were computed via regression analysis (multiple linear regression, MLR), tool available in Microsoft Excel Data Analysis Add-Inns. Regression analysis models the relationship between multiple explanatory variables and a response variable by fitting a linear equation to observed data (Montgomery et al., 2012).

Interfacial viscoelastic properties of the experiments were determined by using CAM 200 optical contact angle and surface tension meter manufactured by KSV Instruments Ltd and PD-100 pulsating drop module. LPF resin density 1,2073 g/cm^3 was used in heavy phase settings and air as light phase. Drop volumes used were 27 µl, 11 µl and 15 µl for PF resin, PF curtain resin and LPF resin, respectively, which were the maximum to be formed and not to drop during the measurement. Measurements were performed at frequencies of 0,05 Hz, 0,10 Hz and 0,25 Hz. Frame interval of 1 second and 50 frames were recorded at frequencies of 0,10 Hz and 0,25 Hz and frame interval of 2 seconds and 30 frames were recorded at frequency of 0,05 Hz. OscDrop software were used in calculation of results. At least 3 replicates were performed at each frequency for each sample. For every measurement, a new drop was formed. The repeatability was variable. Average values were calculated at each frequency for each sample. Measurements were performed in temperature of 23 ± 1 ºC and relative humidity of 50 ± 2 %.

10 RESULTS AND DISCUSSION

Next, the results of the analyses are performed and discussed. In addition to general properties of the resins, surface tension was determined by pendant drop shape analysis method and De Noüy ring method, surface free energy was determined via contact angle measurements, shear (viscosity curve, amplitude sweep and frequency sweep) and extensional rheological properties (filament break-up time and capillary velocity, apparent extensional viscosity) were determined and interfacial viscoelasticity by oscillating pendant drop shape analysis method was determined. Properties of LPF resin were modified with commercial additives.

Based on these measurements, Table XVII and Table XVIII can be presented. Table XVII summarizes the suitability of the measurement for determination of resin properties. Table XVIII summarizes the performance evaluation of the additives to modify resin properties.

Table XVII Review of analytical methods performed in this work.

Analytical method	**Suitability**	**Comments**	**Reference to this work**
Surface tension	+	Clear differences between the resins obtained. Pendant drop method simple, reliable and accurate.	Chapter 10.2, Appendix III
Surface free energy	-	Drying of resins not applicable, repeatability not good.	Chapter 10.5, Appendix III
Shear rheology	+/-	Viscosity curves applicable, results of oscillatory measurements unexpected. No characteristic differences between the resins obtained.	Chapter 10.3, Appendix IV
Extensional rheology	+	Clear differences between the resins obtained in filament break-up and capillary velocity. Extensional rheometer reliable and good repeatability.	Chapter 10.4, Appendix IV
Interfacial viscoelasticity	-	Additive performance evaluation challenging, uncertain applicability with resins.	Chapter 10.5, Appendix IV

Table XVIII Review of additives used in this work.

Additive	**Studied dosage, % of the weight of resin**	**Surface tension**	**Elongational properties**
Surfactant 1	0,2; 0,4; 0,6 Elongation: 0,2	Efficient ST reduction, higher dosage possible. Dosage to reach PF curtain resin ST: 0,16 %	Slight improvement in filament break-up time obtained. Capillary velocity remarkably affected.
Surfactant 2	0,1; 0,2; 0,4; 0,6 Elongation: 0,1	ST reduced, CMC achieved: 0,40 %. Dosage to reach PF curtain resin ST: 0,13 %	Excellent improvement in filament break-up time obtained. Capillary velocity remarkably affected.
Surfactant 3	0,2; 0,4; 0,6 Elongation: 0,6	ST reduced, higher dosage possible. Dosage to reach PF curtain resin ST: 0,75 %	Excellent improvement in filament break-up time obtained. Capillary velocity remarkably affected. Best.
Surfactant 4	0,2; 0,4; 0,6 Elongation: 0,2	Efficient ST reduction, higher dosage possible. Dosage to reach PF curtain resin ST: 0,29 %	Good improvement in filament break-up time obtained. Capillary velocity remarkably affected.
Surfactant/ Defoamer 1	0,03; 0,05; 0,1; 0,2; 0,4; 0,6	ST reduced, CMC achieved: 0,40 %. Dosage to reach PF curtain resin ST: 0,11 %	Excellent improvement in filament break-up time obtained. Capillary velocity remarkably affected.
Defoamer 1	0,03; 0,05; 0,10	No major effect on ST, some type of CMC obtained: 0,05 %.	Filament break-up time and capillary velocity slightly improved, some type of CMC obtained: 0,05 %
Defoamer 2	0,03; 0,05; 0,10	No major effect on ST.	Filament break-up time and capillary velocity poorly improved. No differences between dosage levels.
Defoamer 3	0,03; 0,05; 0,10	ST slightly reduced with highest dosage.	Filament break-up time and capillary velocity poorly improved. Slight differences between dosage levels.

Additive combinations were analyzed with extensional rheometer. Based on multiple linear regression (MLR) analysis results, surfactant/defoamer 1 was considered the best, since increased dosing was mainly important/reasonable in order to achieve desired elongational properties. Defoamer 3 was considered poor, since increased dosing was mainly not important. Defoamers 1 and 2 had relatively same type of performance. Surfactant 1 and 4 performances varied depending on the defoamers, the best combination was achieved with surfactant/defoamer 1 and other defoamers provided poor results. Surfactants 2 and 3 had relatively same type of performance, combination with all but defoamer 3 provided good results. Operational windows were calculated to surfactants 2 and 3 in combination with all defoamers. From the operational window, the additive dosage combination may be selected in order to achieve the desired elongational property, as long or longer break-up time than break-up time of PF curtain resin.

10.1 General properties of resins

General properties of the reference resins without any additives are presented in Table XIX.

Table XIX General properties of PF resin, PF curtain resin and LPF resin.

Property	**Unit**	**PF resin**	**PF curtain resin**	**LPF resin**
Dry matter content	%	47,6	47,1	45,2
pH	-	12	12,2	12,6
Conductivity	mS/m	1807	1677	2050
Alkalinity	%	7,1	7,1	6,8
Free formaldehyde content	%	0,07	0,10	0,05
Gel time	min	30	26	63
Viscosity - Brookfield, 20 ºC	cP	473	550	442
Viscosity - Brookfield, 25 ºC	cP	332	400	312
Viscosity – FC 6, 20 ºC	s	20	24	20
Viscosity – FC 6, 25 ºC	s	14	19	16
Molar mass - M_W	-	5371	6740	8357
Molar mass - M_N	-	1221	1402	1228
PDI (M_W/M_N)	-	4	5	7
Peak max.	-	3296	3823	2686

The most remarkable difference between the resins is in the viscosity of the PF curtain resin. Viscosity of the curtain resin is higher (400 cP, Brookfield 25 ºC) than the viscosity of PF resin and LPF resin (332 cP and 312 cP, respectively). For LPF resins, longer gel time is

typical. This commonly is due to lower degree of polymerization than PF resins, which affects the curing of the resin. This has been described earlier in LPF resin chapter 4.

10.2 Surface tension

Surface tension of the reference resins was determined with pendant drop shape analysis method and De Noüy ring method. For PF resin and LPF resin the surface tensions determined with both methods were in good relation. For PF curtain resin the surface tension value obtained with ring method was higher than with pendant drop method. Surface tension of PF curtain resin was however still lower than surface tension of LPF resin. The surface tensions determined with both methods are presented in Table XX.

Table XX Surface tensions of the reference resins, determined by pendant drop shape analysis method and De Noüy ring method.

Resin	**Surface tension, pendant drop method, mN/m**	**Surface tension, De Noüy ring method, mN/m**
PF resin	71,28	72,2
PF curtain resin	36,09	43,5
LPF resin	46,52	45,7

Pendant drop shape analysis method was selected for further surface tension measurements due to its higher accuracy and suitability to resins. When using the ring method device, the ring does not rapidly rise from the viscous resin when the maximum force is reached, but slowly starts moving when the force is increased. Even though the repeatability was good, the device was considered not to work completely as it should. Surface tension of the experiments are plotted as a function of surfactant and defoamer dosage in Figure 31 and Figure 32.

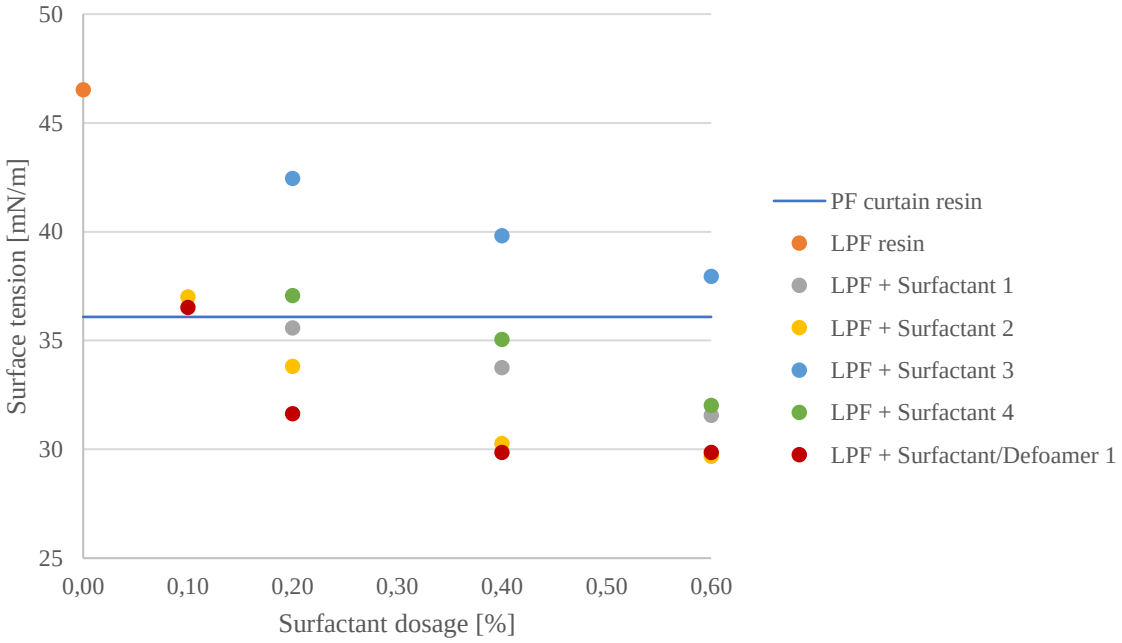

Figure 31 Surface tension of experiments plotted as a function of surfactant dosage. Surface tension determined by pendant drop shape analysis method with Attension Theta optical tensiometer, in temperature of 23 ± 2 ºC. Drop (volume 4 µl, except for LPF + 0,60 % Surfactant 2 experiment 3,5 µl) formed with 200 µl micropipette, and resin density used 1,2073 g/cm^3. Values obtained after 3,0 s from the beginning of the measurement.

As seen from Figure 31, all surfactants remarkably lowered the surface tension of LPF resin. Surfactants 1 and 4 performed relatively similar, efficient lowering of the surface tension of LPF resin. With dosage of 0,2 % of the weight of the resin, the surface tension was able to be lowered approximately to the level of PF curtain resin. Further addition of both surfactants would be possible, since critical micelle concentration (CMC) was not yet achieved with dosage of 0,6 %. Surfactant 3 also lowered the surface tension of LPF resin and further addition would be possible. However, the performance was not as strong as with surfactants 1 and 4. With dosage of 0,6 % of the weight of resin the surface tension was able to be lowered to the level of PF curtain resin. For surfactant 2 and surfactant/defoamer 1 additional experiments with dosage of 0,1 % were added, since the dosage of 0,2 % already lowered the surface tension below the level of PF curtain resin. CMC was achieved with dosage of 0,4 % of the weight of resin for both additives. Higher dosing than 0,4 % of the surfactant 2 or surfactant/defoamer 1 is not reasonable, since further lowering of the surface tension is not possible with these additives.

The accurate required dosages of different surfactants to obtain PF curtain resin surface tension (36,09 mN/m), estimated graphically from the surface tension curves in Figure 31, are:

- Surfactant 1: 0,16 % of the weight of resin
- Surfactant 2: 0,13 % of the weight of resin
- Surfactant 3: 0,75 % of the weight of resin
- Surfactant 4: 0,29 % of the weight of resin
- Surfactant/Defoamer 1: 0,11 % of the weight of resin.

Based on chemical composition of the surfactants, surfactants 2 and 3 and surfactant/defoamer 1 are somehow similar, but surfactant 3 does not have special defoaming ability. This may be the reason, why CMC is achieved for surfactant 2 and surfactant/defoamer 1, but for surfactant 3 a higher dosage is required. Surfactant 1 is reported as superwetter utilizing Gemini technology, which could imply that large reductions to surface tension can be achieved and thus CMC is not yet achieved. Surfactant 4 remarkably different chemistry seem to function in resin solution relatively well, based on this analytical method.

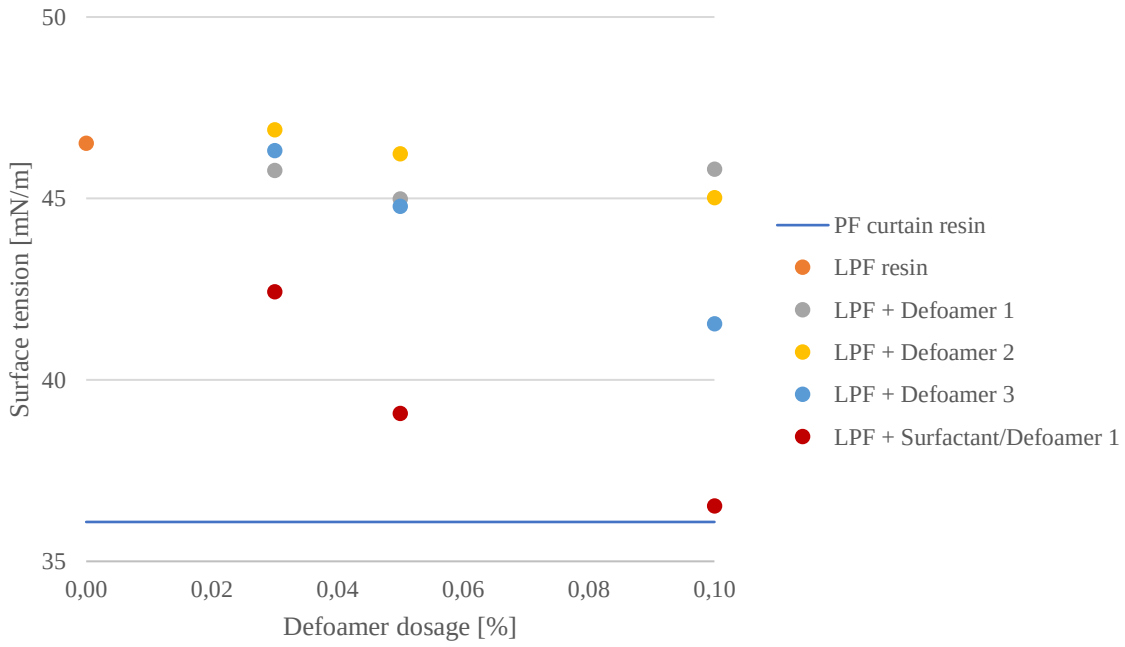

Figure 32 Surface tension of experiments plotted as a function of defoamer dosage. Surface tension determined by pendant drop shape analysis method with Attension Theta optical tensiometer, in temperature of 23 ± 2 ºC. Drop

(volume 4 µl) formed with 200 µl micropipette, and resin density used 1,2073 g/cm^3. Values obtained after 3,0 s from the beginning of the measurement.

As seen from Figure 32, the effect of defoamers on surface tension with dosing of 0,03 % and 0,05 % of the weight of resin is not remarkable. Defoamers 1 and 2 do not much lower the surface tension even with the highest dosage of 0,10 %. For defoamer 1 the CMC was achieved with dosage of 0,05 %. With dosage of 0,10 % of defoamer 3, surface tension of LPF is lowered. However, its performance is not as strong as the performance of surfactant/defoamer 1, which remarkably lowers the surface tension of LPF resin even with the dosage of 0,03 %. Both defoamers 1 and 2 are oils based on their chemical composition, which would imply that they do not affect the surface tension as much as defoamer 3 or surfactant/defoamer 1, which are reported non-ionic surfactants and defoamers.

The complete surface tension results determined by pendant drop method and expanded uncertainty of experiments are presented in Appendix III, Table I. Expanded uncertainty between the replicates was determined based on equation on level of confidence of 95 %:

$$Expanded\ uncertainty = \pm 2\ \frac{Standard\ deviation}{\sqrt{n}}, \qquad (46)$$

where n the number of replicates.

Expanded uncertainty between the replicates was in general minor, there were only a few experiments of which the expanded uncertainty exceeded 0,6.

Surface tensions of PF resins have been analyzed by Hse (1972). In the research, variable properties were differentiating NaOH/P molar ratio (0,4; 0,7 and 1,0), solids content (37, 40 and 43 %) and F/P molar ratio (1,6; 1,9; 2,2 and 2,5), and their effects on surface tensions of resins were determined. Surface tensions were measured by Du Noüy ring method and ranged from 68,4 to 79,9 mN/m. It was revealed, that surface tension was the most affected by NaOH/P ratio, next by F/P ratio and the least by solids content. Surface tension increased as the molar ratios of NaOH/P and F/P increased. Shear strength, wood failure and delamination of the finished plywood glue joint were also analyzed. The bond quality

decreased as the surface tension increased but may be partly due to difficulties in adhesive spreading. (Hse, 1972)

Yang and Frazier studied the influence of organic fillers on surface tension (2016b) and rheology (2016a) of PF adhesives (the latter reviewed later). Here, PF resole resins are used for production of veneer-based wood composites such as plywood and laminated veneer lumber. Adhesive contains PF resin, water, sodium hydroxide, wheat flour extender, sodium carbonate and different organic fillers. In their studies, the used organic fillers were flours of walnut shell, red alder bark and corn cob residue.

Surface tension of the adhesive affects wettability of the surface and adhesive penetration, but also glue joint water retention, prepress tack and final bond quality (Yang and Frazier, 2016b). Methods used to determinate the surface tension were drop weight method with two corrections and drop shape analysis. All methods were in reasonable agreement. PF resin had surface tension of 67,1-69,0 mN/m. Wheat flour extender and organic fillers all reduced the surface tension of PF adhesive (Table XXI). Surface tension reduction can be explained by the chemical composition of the extender and fillers. Alkaline resin releases the components of extender (lipids, polysaccharides and proteins) and extractives of fillers (e.g. xylan and lignin) in the substances, which act as surface active compounds and reduce surface tension. The influence of adhesive viscosity on surface tension measurement when using different size syringe needles for formation of the drop was also analyzed. Viscosity was found to affect the surface tension, but not significantly. Age of the adhesive affected the surface tension remarkably, since the viscosity of the adhesive increased during storage. Most change occurred within the first 8 hours of storing (Table XXI). However, as conclusions it can be stated that drop shape analysis and the two largest needles (inner radius 0,4 mm and 0,6 mm) provided the most systematic and reliable results.

Table XXI Surface tension of PF resin and PF adhesives with wheat flour extender and organic fillers after preparation and after 8 h of storing in room temperature (combined from Yang and Frazier (2016b)).

Sample	**Surface tension, mN/m, 0 h**	**Surface tension, mN/m, 8 h**
PF resin	67,1-69,0	N.A.

PF adhesive including wheat flour extender	60,8-62,8	N.A.
PF adhesive including wheat flour extender + alder bark filler	50,2-51,3	48,3-50,5
PF adhesive including wheat flour extender + walnut shell filler	51,4-53,8	48,8-51,6
PF adhesive including wheat flour extender + corn cob filler	54,9-58,0	52,4-54,8

Reviewed in curtain coating resin/adhesive chapter 5.3, Bond and Moehl (1975) reported PF resin without additives having surface tension of 69,7 mN/m. Surface tension of PF resin determined in this work is in good agreement with surface tension results determined by Hse (1972), Yang and Frazier (2016b) and Bond and Moehl (1975). Schweizer (2004) concluded that for paper curtain coatings, surface tension must be below 40 mN/m to achieve stable curtain. The studied patents by Järvi (1969) and Bond and Moehl (1975) concluded that surface tension of 30-55 mN/m is required to obtain a good curtain. PF curtain resin surface tension is in line with both requirements. However, in previous curtain coating trials it has been noticed, that LPF resin surface tension (46,52 mN/m) is not sufficient for successful curtain formation. This strengthens the validity for surface tension requirement presented by Schweizer (2004).

10.3 Shear rheology

Reference resins were analyzed with shear rheometer. In Figure 33, viscosity curves of reference resins are performed.

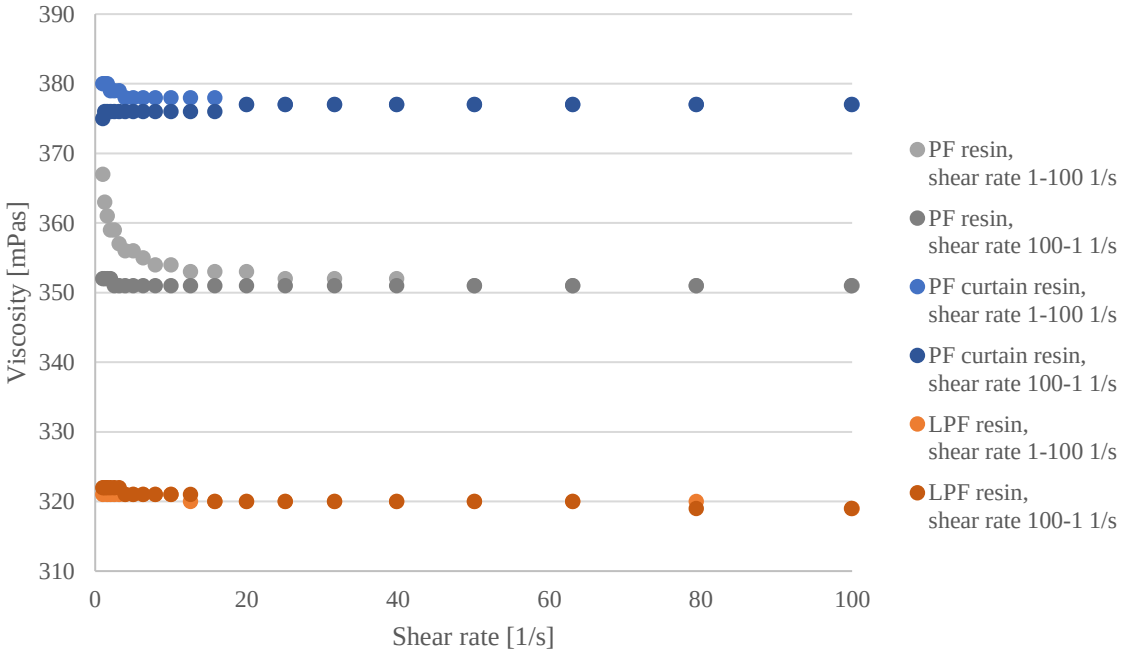

Figure 33 Viscosity curves of the reference resins, viscosity as a function of shear rate, determined by MCR302 shear rheometer and CC27 cylinder, in temperature of 25 ºC. Shear rate varied first from 1-100 1/s (lighter curves) and then from 100-1 1/s (darker curves).

As seen from Figure 33, behavior of the resins is almost Newtonian. When studying the curves where shear rate varied from 1-100 1/s, a slight shear thinning at low shear rates (especially with PF resin) can be noticed. At shear rates higher than 20 1/s, viscosity remains constant, which implies Newtonian liquid type of behavior. Same observation was also done by Domínguez et al. (2013) and Yang and Frazier (2016a).

After shearing, no remarkable structural deformation can be noticed. This can be concluded, since the curves where shear rate varied from 100-1 1/s, are very close to first curves (Yang and Frazier, 2016a). Also higher shear rates were tested, up to 500 1/s. This was performed to ensure, that the viscosity remains constant even at higher shear rates, and it did. Viscosity levels of the resins are in line with resin viscosities measured by Brookfield 25 ºC. PF curtain resin has the highest viscosity, PF resin the second highest and LPF resin the lowest.

Further results from shear rheometer, amplitude and frequency sweep curves of the resins, are presented in Appendix IV, Figure 1 and Figure 2. Results are presented and discussed in Appendix IV, because they were unexpected based on literature (Domínguez et al. 2013;

Moubarik, 2014; Yang and Frazier, 2016a) and did not imply differences between the resins. The results from amplitude and frequency sweeps imply that all resins are ideally Newtonian liquids, since storage modulus was not plotted in any of the measurements, even though measurement variables were changed. Since storage modulus was not plotted, also further calculations based on frequency sweep results (complex shear modulus (G^*) and further complex viscosity (η^*) and zero-shear viscosity (η_0), and relaxation time (λ)) could not been performed reliably.

10.4 Extensional rheology

With extensional rheometer, the reference resins and additive performance were studied based on elongational properties. Based on pendant drop surface tension determinations, the following surfactant dosages for LPF resin were primarily selected for extensional rheometer analyses:

- Surfactant 1: 0,20 % of the weight of resin (experiment 4)
- Surfactant 2: 0,10 % of the weight of resin (experiment 7)
- Surfactant 3: 0,60 % of the weight of resin (experiment 13)
- Surfactant 4: 0,20 % of the weight of resin (experiment 14)
- Surfactant/Defoamer 1: 0,10 % of the weight of resin (experiment 19)

By selection of these experiments, the surface tension of all experiments was approximately the same and on the same level to commercial PF curtain resin, 35-38 mN/m. Defoamer dosages without surfactants were 0,03 %, 0,05 % and 0,10 % and with surfactants 0,03 % and 0,05 %, of the weight of LPF resin. Surfactant/defoamer 1 was considered as a defoamer in additive combinations.

Filament elongation as a function of time and break-up time of reference resins are presented in Figure 34. Bond numbers (equation 45) for the reference resins are 1,50; 2,95 and 2,29, respectively for PF resin, PF curtain resin and LPF resin. To neglect the gravitational effects, the Bond number should be much less than 1, for example < 0,1 (McKinley & Tripathi, 2000). When solving the diameter from equation (45), the resulting diameter is the upper limit for validity of data. Those diameters are 1,55 mm, 1,10 mm and 1,25 mm, respectively for PF resin, PF curtain resin and LPF resin, and cover approximately 40 ms from the beginning of the measurement. Limiting diameter is approximately the same for resins including surfactants, since the surface tension is approximately the same.

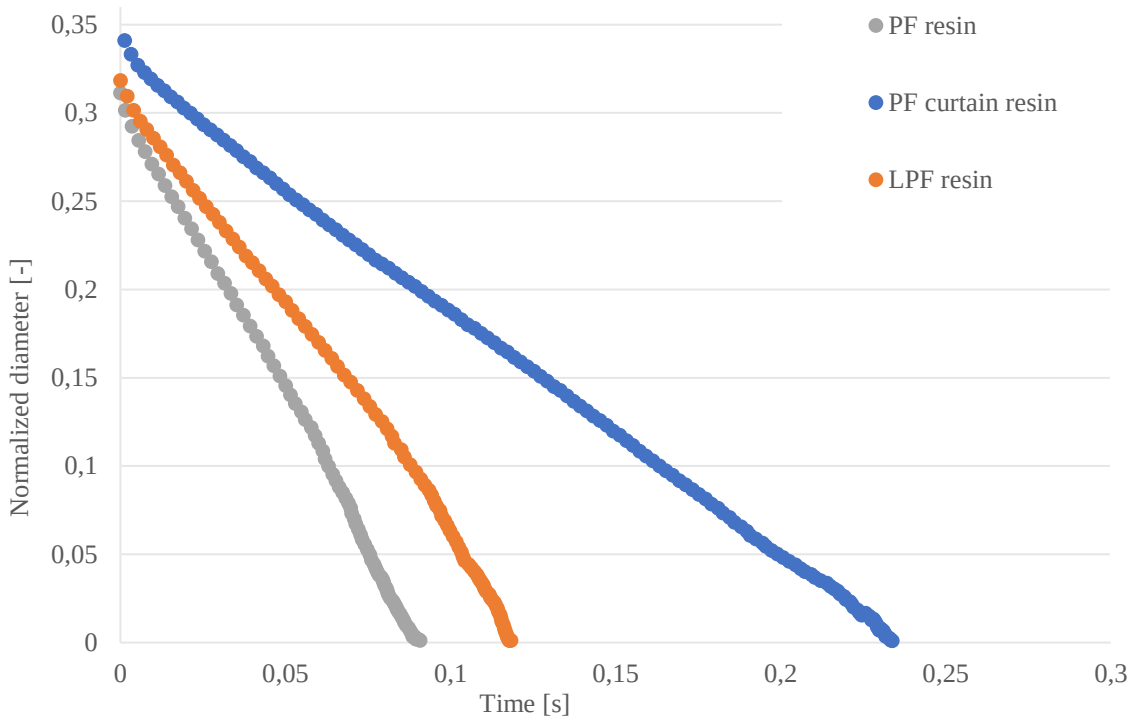

Figure 34 Elongational properties of the reference resins. Normalized diameter of filament elongation and break-up as a function of time determined by HAAKE™ CaBER™ 1. Measurement was performed with 6 mm plates with initial and final aspect ratio of 1,00 and 2,75, respectively, and in temperature of 25 ± 2 ºC.

As seen from Figure 34, all resins perform Newtonian liquid behavior by linear curves. However, the difference in filament break-up time (when diameter is zero) and capillary velocity (absolute value of slope of the curve) between the PF curtain resin and PF and LPF resins is remarkable. Surface tension does give insight about the elongation behavior, since the break-up time extends as the surface tension lowers. However, extensional viscosity does also affect the break-up time, since otherwise break-up time of LPF resin would be closer to PF curtain resin as its surface tension is closer to PF curtain resin than to PF resin. Based on Figure 34, when pursuing the properties of PF curtain resin, long break-up time and small capillary velocity are desired.

In Figure 35, the effect of surfactants on LPF resin elongational properties are presented.

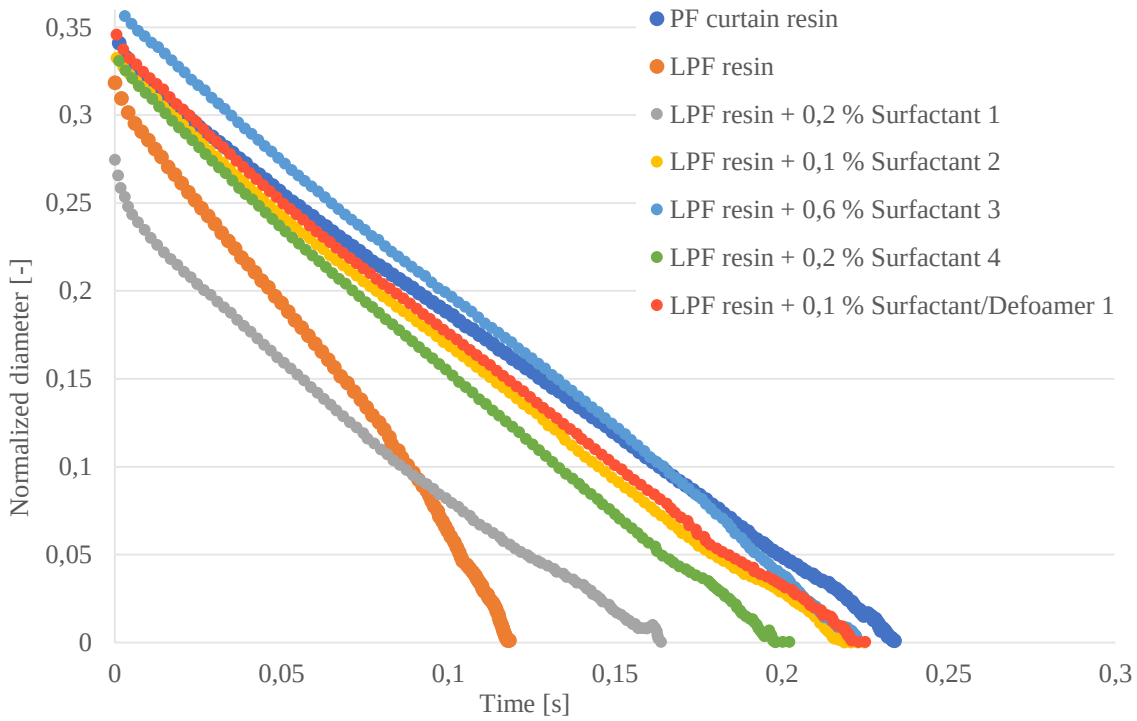

Figure 35 Effect of surfactants (varying dosage 0,2 %, 0,1 %, 0,6 %, 0,2 % and 0,1 % of the weight of resin for surfactants 1-4 and surfactant/defoamer 1, respectively) on LPF resin elongational properties. Normalized diameter of filament elongation and break-up as a function of time determined by HAAKE™ CaBER™ 1. Measurement was performed with 6 mm plates with initial and final aspect ratio of 1,00 and 2,75, respectively, and in temperature of 25 ± 2 ºC.

As seen from Figure 35, all surfactants affect the elongation of LPF resin. Surfactant 1 remarkably changes the capillary velocity to match the velocity of PF curtain resin. However, the break-up time is still remarkably lower than break-up time of PF curtain resin. Surfactants 2-4 and surfactant/defoamer 1 match the curve of PF curtain resin better than surfactant 1. Also surfactants 2-4 and surfactant/defoamer 1 change the capillary velocity of the resin. With surfactants 2 and 3 and surfactant/defoamer 1 the break-up time is almost as long as the break-up time of PF curtain resin. Surfactant 4 does not longer the break-up time as much, but still more than surfactant 1. The performance of surfactant 1 may be due to its primary superwetting ability and may thus not affect the elongation so remarkably.

In Figure 36, Figure 37, Figure 38 and Figure 39, the effect of defoamers and defoamer dosages on LPF resin elongational properties are presented.

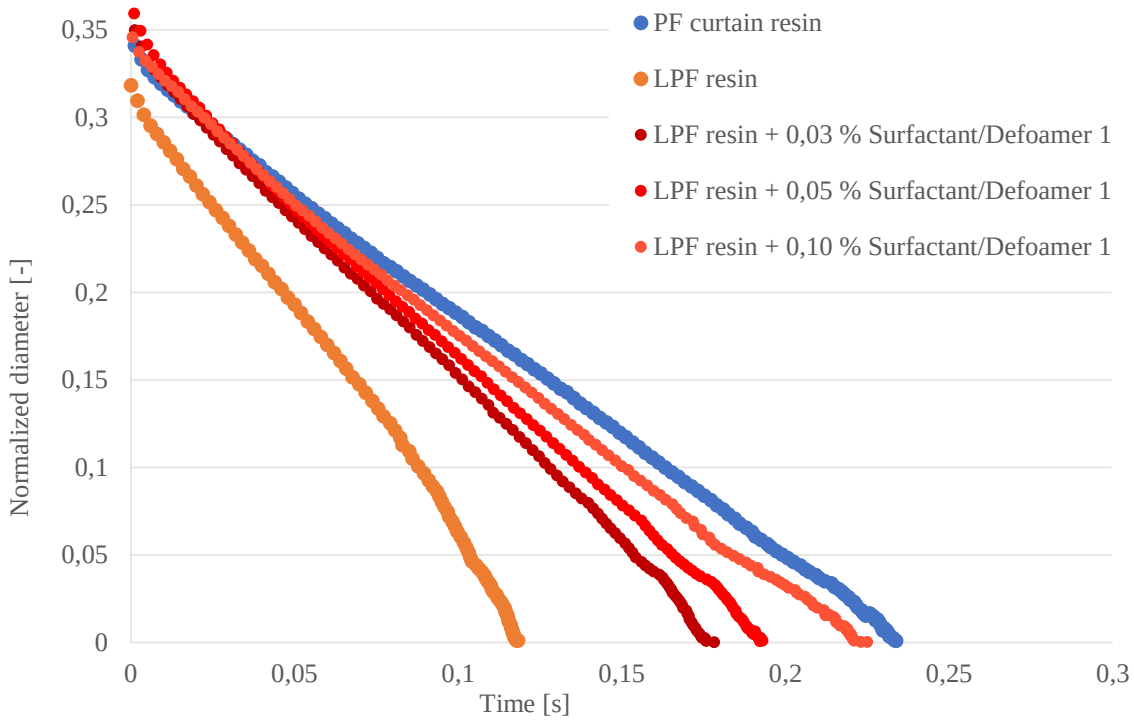

Figure 36 Effect of surfactant/defoamer 1 on LPF resin elongational properties. Normalized diameter of filament elongation and break-up as a function of time determined by HAAKE™ CaBER™ 1. Measurement was performed with 6 mm plates with initial and final aspect ratio of 1,00 and 2,75, respectively, and in temperature of 25 ± 2 ºC.

As seen from Figure 36, the performance of surfactant/defoamer 1 is very good. Increasing the dosing gradually and proportionally affects the LPF resin curve, when considering the filament break-up time and the capillary velocity (absolute value slope of the curve) of the resin. Already with dosages of 0,03 % and 0,05 % of the weight of resin a remarkable affect can be noticed, and with dosage of 0,10 % very similar curve to PF curtain resin is obtained.

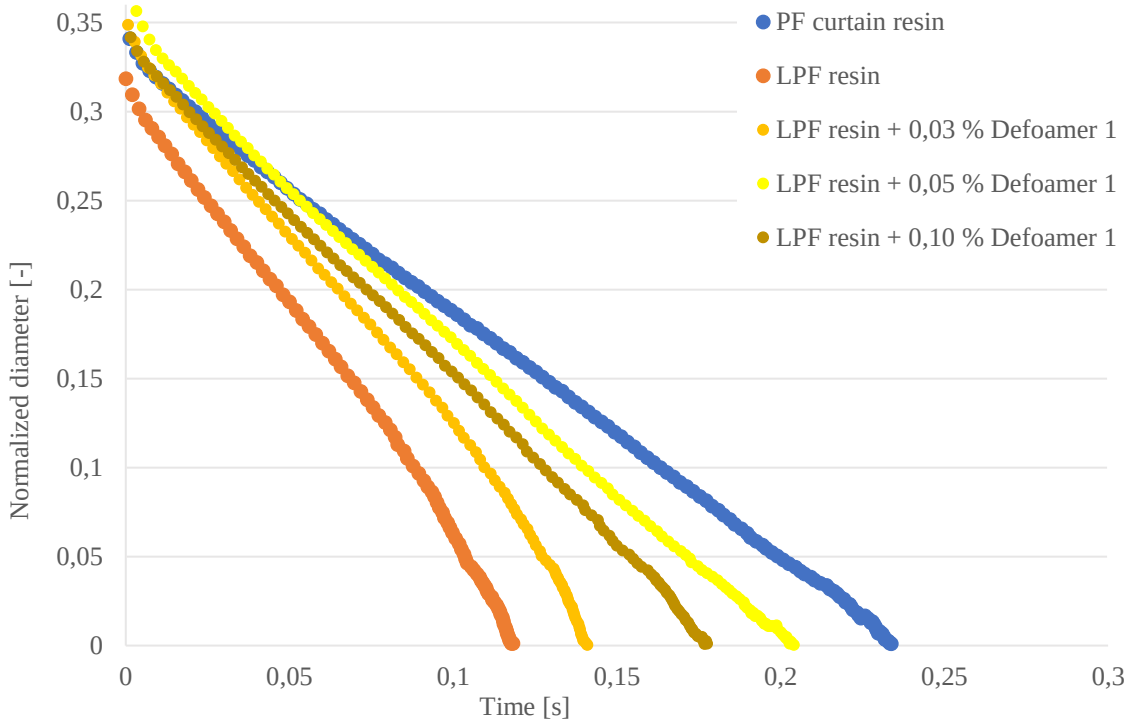

Figure 37 Effect of defoamer 1 on LPF resin elongational properties. Normalized diameter of filament elongation and break-up as a function of time determined by HAAKE™ CaBER™ 1. Measurement was performed with 6 mm plates with initial and final aspect ratio of 1,00 and 2,75, respectively, and in temperature of 25 ± 2 ºC.

As seen from Figure 37, the performance of defoamer 1 is variable. Dosage of 0,03 % of the weight of resin affect the LPF resin only slightly. Dosage of 0,05 % has relatively good performance when compared to PF curtain resin curve. Dosage of 0,10 % again worsen the performance, since the break-up time is shorter than with the dosage of 0,05 %. Also in surface tension results, CMC was noticed for defoamer 1 between 0,05-0,10 %.

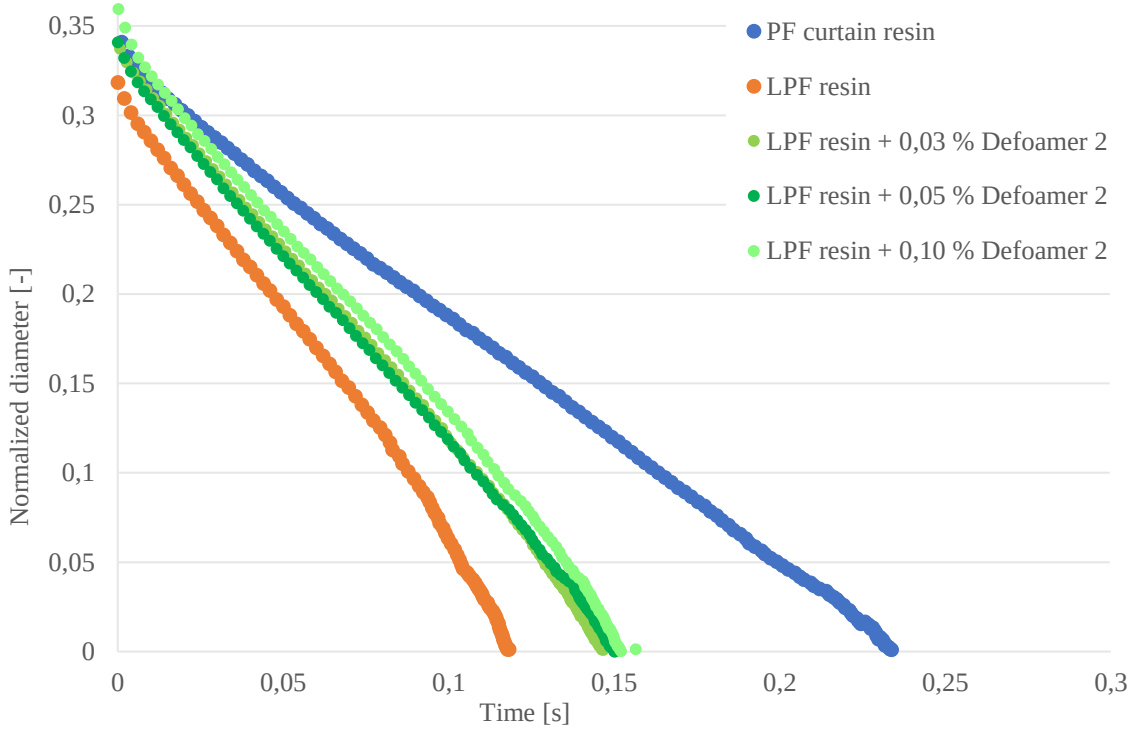

Figure 38 Effect of defoamer 2 on LPF resin elongational properties. Normalized diameter of filament elongation and break-up as a function of time determined by HAAKE™ CaBER™ 1. Measurement was performed with 6 mm plates with initial and final aspect ratio of 1,00 and 2,75, respectively, and in temperature of 25 ± 2 ºC.

As seen from Figure 38, the dosing of defoamer 3 does not affect the performance of the additive. The elongation of LPF resin is slightly affected, but there is no difference between the dosage levels. Also in surface tension results, dosage levels did practically have no differences.

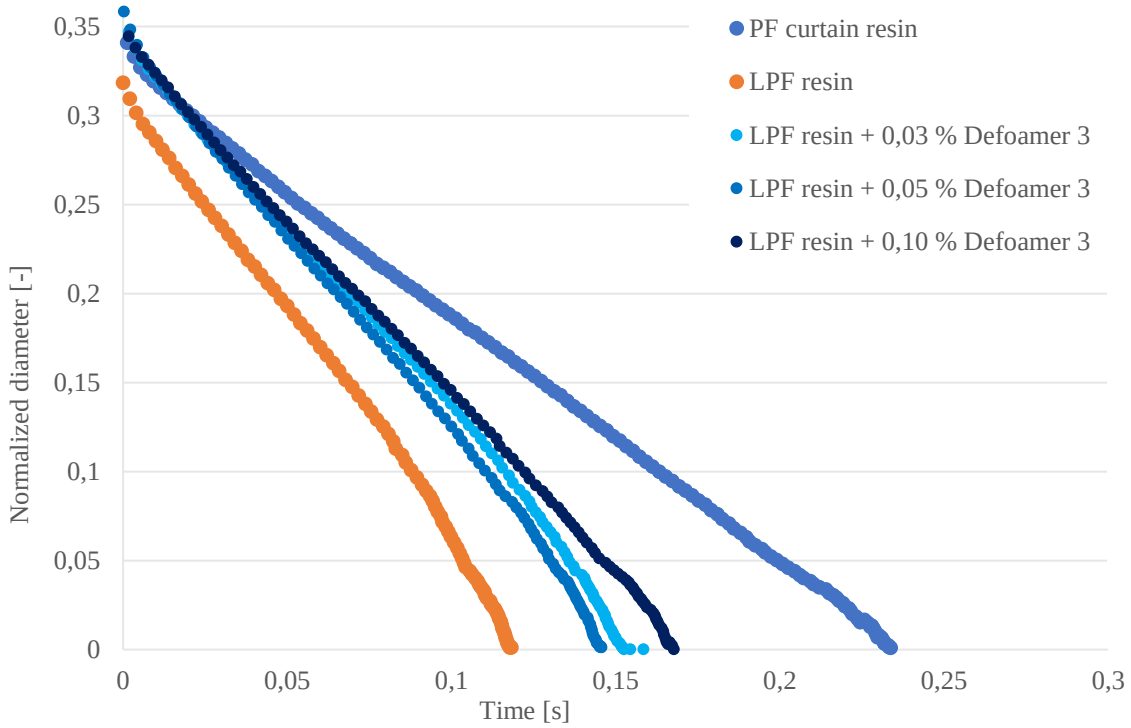

Figure 39 Effect of defoamer 3 on LPF resin elongational properties. Normalized diameter of filament elongation and break-up as a function of time determined by HAAKE™ CaBER™ 1. Measurement was performed with 6 mm plates with initial and final aspect ratio of 1,00 and 2,75, respectively, and in temperature of 25 ± 2 ºC.

As seen from Figure 39, the effect of defoamer 3 on LPF resin is slight. The break-up time and the capillary velocity is gradually and proportionally affected as the dosage level increases, but the difference between the dosage levels is small. Also in surface tension results, only dosage of 0,10 % of the weight of resin had remarkable effect on LPF resin.

Additive combinations, surfactants 1-4 at dosages of 0,2 %, 0,1 %, 0,6 % and 0,2 % of the weight of resin, respectively, with defoamers at dosages of 0,03 % and 0,05 % performed relatively good results. For surfactant 1 and 4, the filament break-up time could be further increased with defoamers, and break-up time of PF curtain resin was achieved with few additive combinations. For surfactants 2 and 3, the addition of defoamers exhibited slightly varying results, but again, break-up time of PF curtain resin was achieved with few additive combinations. In Appendix IV, in Figure 3, Figure 4, Figure 5 and Figure 6 the effect of surfactant and defoamer combinations on LPF resin filament elongation curves are presented. In Appendix IV, Table I, the complete filament elongation results (break-up time

and capillary velocity) of experiments are presented. Expanded uncertainty on level of confidence of 95 % (equation 46) was calculated for normalized diameter at each time point for LPF resin and experiments including only surfactant (Figure 35). Expanded uncertainty of normalized diameter varied between below 0,001 mm to 0,017 mm at each time point, on average 0,005-0,007 mm.

A way of describing the surfactant and defoamer combinations is statistical multiple linear regression (MLR) analysis, computed here with Microsoft Excel Data Analysis Add-Inn. Analysis exhibits, whether it is reasonable to increase the defoamer dosage level. Statistical importance and comparison of dosages are presented via regression coefficients from MLR analysis. Importance of increasing the defoamer dosage levels on filament break-up time and capillary velocity (absolute value of slope of the elongation curve) are presented in Figure 40 and Figure 41, respectively. When pursuing the properties of PF curtain resin, high break-up time and small capillary velocity are desired. In Figure 40, positive bars imply that increasing the defoamer dosage level is important, since an increase in the filament break-up time can be achieved. Negative bars imply, that increasing the defoamer dosage level is not important.

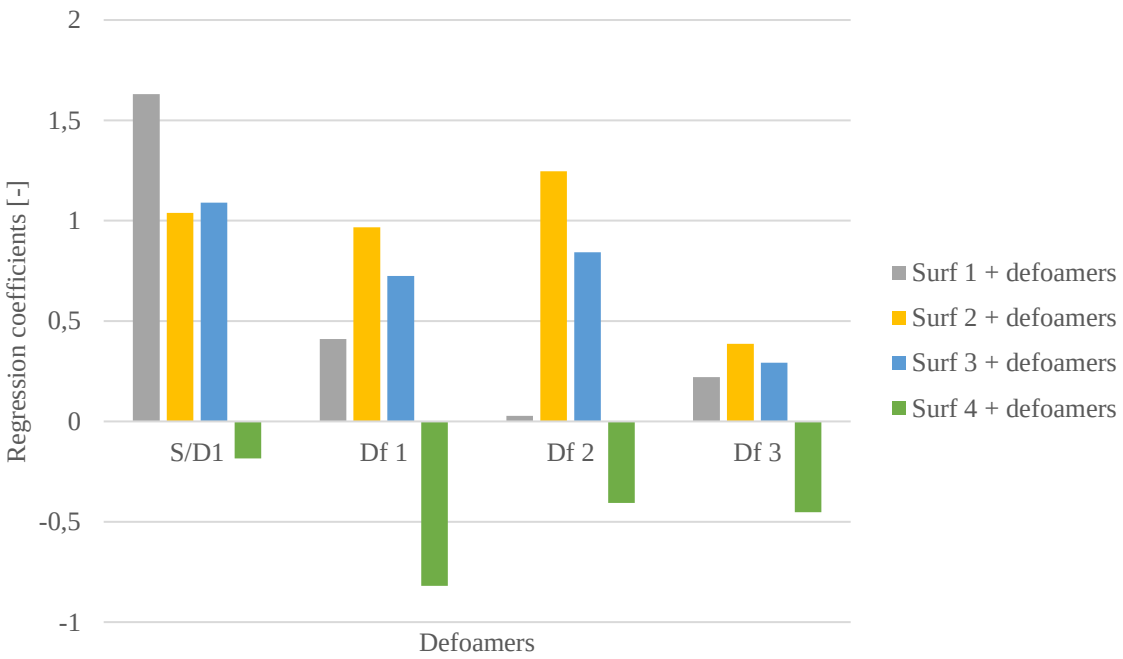

Figure 40 Statistical importance of increasing the defoamer dosage level with surfactants 1-4, when considering the resin filament break-up time, obtained from extensional rheometer analysis. Increased break-up time is desired.

Importance is estimated via statistical MLR analysis. Surf 1-4 = surfactants 1-4, S/D1 = surfactant/defoamer 1 and Df 1-3 = defoamers 1-3.

As seen from Figure 40, increasing the dosage level of surfactant/defoamer 1 and defoamers 1-3 have varying importance on filament break-up time, when combined with surfactants 1-4. For surfactant 1, the importance of increased dosage of surfactant/defoamer 1 is remarkably larger than with defoamers 1-3. For surfactants 2 and 3, the importance of increased dosage of all defoamers is more equal, but with defoamer 3 the least important. For surfactant 4, increasing the dosage of any defoamer is not important. From here it could be concluded, that the remarkably different chemical composition of surfactant 4 may be the cause for poor compatibility with defoamers and is thus undesired. Figure 40 implies, that compatibility of surfactant/defoamer 1 with all surfactants is the best, defoamers 1 and 2 have relatively similar compatibility and defoamer 3 the worst compatibility with surfactants.

In Figure 41, negative bars imply that increasing the defoamer dosage level is important, since a decrease in the capillary velocity can be achieved. Positive bars imply, that increasing the defoamer dosage level is not important.

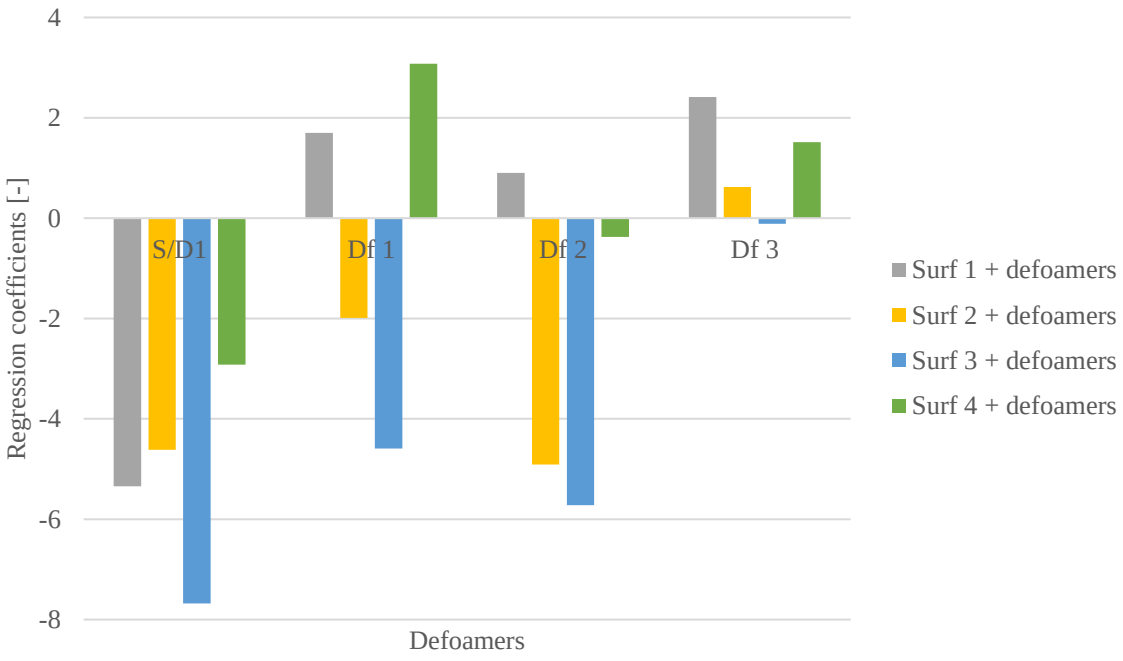

Figure 41 Statistical importance of increasing the defoamer dosage level with surfactants 1-4, when considering the resin capillary velocity, obtained from

extensional rheometer analysis. Decreased capillary velocity is desired. Importance is estimated via statistical MLR analysis. Surf 1-4 = surfactants 1-4, S/D1 = surfactant/defoamer 1 and Df 1-3 = defoamers 1-3.

As seen also from Figure 41, increasing the dosage level of surfactant/defoamer 1 and defoamers 1-3 have varying importance on capillary velocity, when combined with surfactants 1-4. For surfactants 1 and 4, only increased dosage of surfactant/defoamer 1 is important. For surfactants 2 and 3, all but increased dosage of defoamer 3 are important. Also Figure 41 implies, that compatibility of surfactant/defoamer 1 with all surfactants is the best, defoamers 1 and 2 have relatively similar compatibility and defoamer 3 the worst compatibility with surfactants.

When considering the additive combinations and their chemical compositions, based on elongational properties, it could be concluded, that chemical composition of defoamer 3 (non-ionic surfactant and defoamer) does not function with surfactants as desired. Defoamer 3 can be assumed to have more complex chemical composition than defoamers 1 and 2 (oils), and thus their compatibility is better with surfactants 1-4. Surfactant/defoamer 1 has somehow similar chemical composition than surfactants 2 and 3, and may thus strengthen the effect on elongation properties.

Based on these results, surfactants 2 and 3 were considered the best out of the studied four surfactants. The filament break-up time of PF curtain resin was achieved with a few additive combinations, with all surfactants. However, based on MLR analysis, surfactant 1 performed variable and surfactant 4 in general poor combinations with defoamers, and surfactants 2 and 3 performed good compatibility. This means, that increasing the defoamer dosage level further improved the elongational properties of the LPF resin.

An operational window, where the interaction effect of surfactant and defoamer combinations could be detected and specific elongational property of LPF resin could be achieved was desired to obtain for surfactants 2 and 3. Thus, further measurements with extensional rheometer were performed for surfactant 2 and 3 dosages of 0,40 % of the weight of resin (experiments 9 and 12) and combinations with all defoamers. In Appendix IV, in Figure 7 and Figure 8 the effect of surfactant and defoamer combinations on LPF resin

filament elongation curves are presented, and in Table II, the complete filament elongation results (break-up time and capillary velocity) of the additional experiments are presented.

In Figure 42, the effect of surfactants 2 and 3 dosage levels on LPF resin elongational properties is presented.

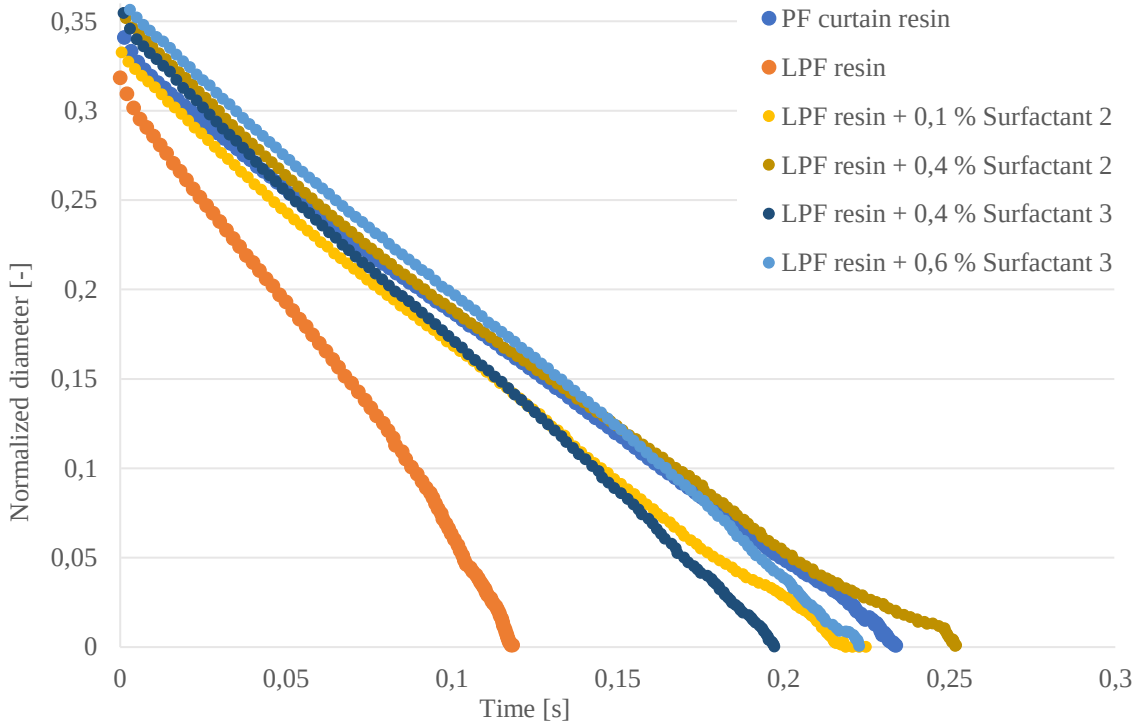

Figure 42 Effect of surfactants (dosage 0,1 % and 0,4 % of the weight of resin for surfactant 2 and 0,4 % and 0,6 % for surfactant 3) on LPF resin elongational properties. Normalized diameter of filament elongation and break-up as a function of time determined by HAAKE™ CaBER™ 1. Measurement was performed with 6 mm plates with initial and final aspect ratio of 1,00 and 2,75, respectively, and in temperature of 25 ± 2 ºC.

As seen from Figure 42, increase of surfactant 2 dosage level further increases the filament break-up time and decrease of surfactant 3 dosage level decreases the filament break-up time. This result was expected based on the surface tension results, since the surface tension is further decreased for surfactant 2 and increased for surfactant 3.

From the surfactant and defoamer combinations it can be noticed, that for surfactant 2, the break-up time could be further increased with defoamers with dosage 0,03 %, but with

dosage 0,05 % no further increases were noticed. Surfactant 3 performed relatively similar behavior with defoamer dosage of 0,03 %, and dosage 0,05 % further improved the break-up time with all but defoamer 2. These observations can also be noticed in MLR analyses. Statistical importance of increasing the dosage level is presented in Figure 43 and Figure 44. In Figure 43, increase to filament break-up time is desired, and thus positive bars imply that increasing the defoamer dosage level is important. In Figure 44, decrease to filament capillary velocity is desired, and thus negative bars imply that increasing the defoamer dosage level is important. From here it can be concluded, that for surfactant 2 with dosage of 0,4 % of the weight of resin, defoamer dosage level should be maximum 0,03 %.

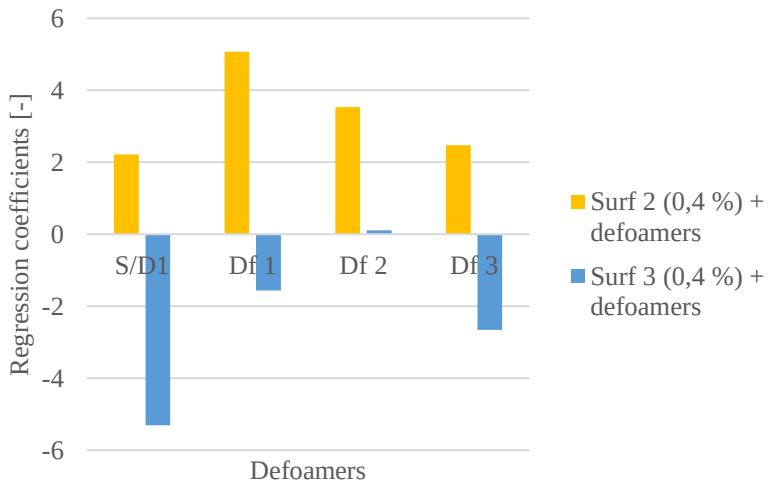

Figure 43 Statistical importance of increasing the defoamer dosage level with surfactants 2 and 3 with dosage of 0,4 % of the weight of resin, when considering the resin filament break-up time, obtained from extensional rheometer analysis. Increased break-up time is desired. Importance is estimated via statistical MLR analysis. Surf 2-3 = surfactants 2-3, S/D1 = surfactant/defoamer 1 and Df 1-3 = defoamers 1-3.

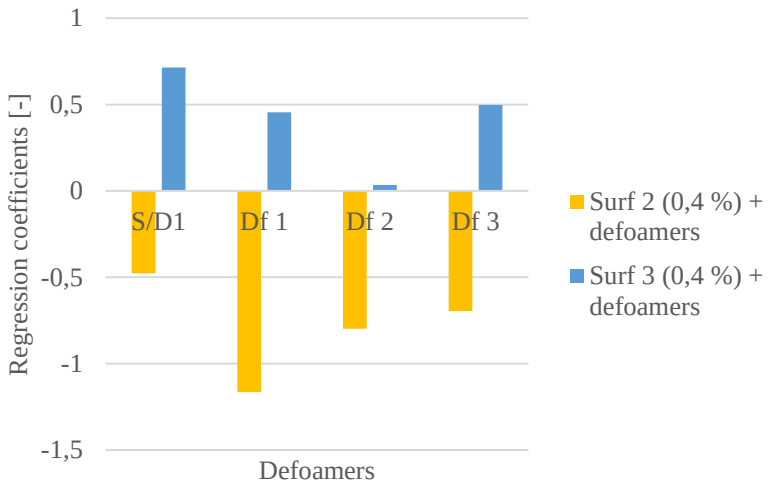

Figure 44 Statistical importance of increasing the defoamer dosage level with surfactants 2 and 3 with dosage of 0,4 % of the weight of resin, when considering the resin capillary velocity, obtained from extensional rheometer analysis. Decreased capillary velocity is desired. Importance is estimated via statistical MLR analysis. Surf 2-3 = surfactants 2-3, S/D1 = surfactant/defoamer 1 and Df 1-3 = defoamers 1-3.

Working curves for operational windows were obtained for additive combinations from interaction effect analysis, modelled with MLR method. Working curves are computed based on second-order model with interaction (Montgomery et al., 2012):

$$y = b_0 + b_1 * x_1 + b_2 * x_2 + b_3 * x_1 * x_2 + b_4 * x_1^2 + b_5 * x_2^2, \quad (47)$$

where y response variable to be modelled (filament break-up time)

b regression coefficients

x_1 explanatory variable in regression (surfactant dosage)

x_2 explanatory variable in regression (defoamer dosage).

Interaction coefficients were obtained from MLR analysis, computed here with Microsoft Excel Data Analysis Add-Inn, possibly not significant variables (based on *P*-value) were deleted and MLR analysis was computed again. Final regression results are presented in Appendix V. Surfactant dosage was extrapolated for defoamer dosages of 0-0,05 %, when target break-up time (y) value was 234 ms (filament break-up time of PF curtain resin). Model was evaluated by comparing the measured and estimated break-up times of

experiments and fitting a linear trendline to the plot. Fit of the model, R^2-value, was for working curves (the higher the better, max 100 %):

- Surfactant 2 + Surfactant/Defoamer 1: 85,29 %
- Surfactant 2 + Defoamer 1: 80,82 %
- Surfactant 2 + Defoamer 2: 95,73 %
- Surfactant 2 + Defoamer 3, 95,11 %
- Surfactant 3 + Surfactant/Defoamer 1: 72,61 %
- Surfactant 3 + Defoamer 1: 52,10 %
- Surfactant 3 + Defoamer 2: 92,68 %
- Surfactant 3 + Defoamer 3: 79,52 %.

Working curves for LPF resin with surfactant 2 and defoamers are presented in Figure 45 and working curves for LPF resin with surfactant 3 and defoamers are presented in Figure 46. Operating areas are marked with diagonal lines. It should be noted, that generally considered maximum dosage level of surfactants is 0,6 % of the weight of resin (0,05 % for defoamers), so the dosing is economically applicable. The required dosage of surfactant 2 is well in line with the economical point of view, and thus the maximum surfactant dosage limit (0,6 %) is not plotted in Figure 45. With surfactant 3, the only applicable additive combination, from the economical point of view, would be surfactant 3 and surfactant/defoamer 1.

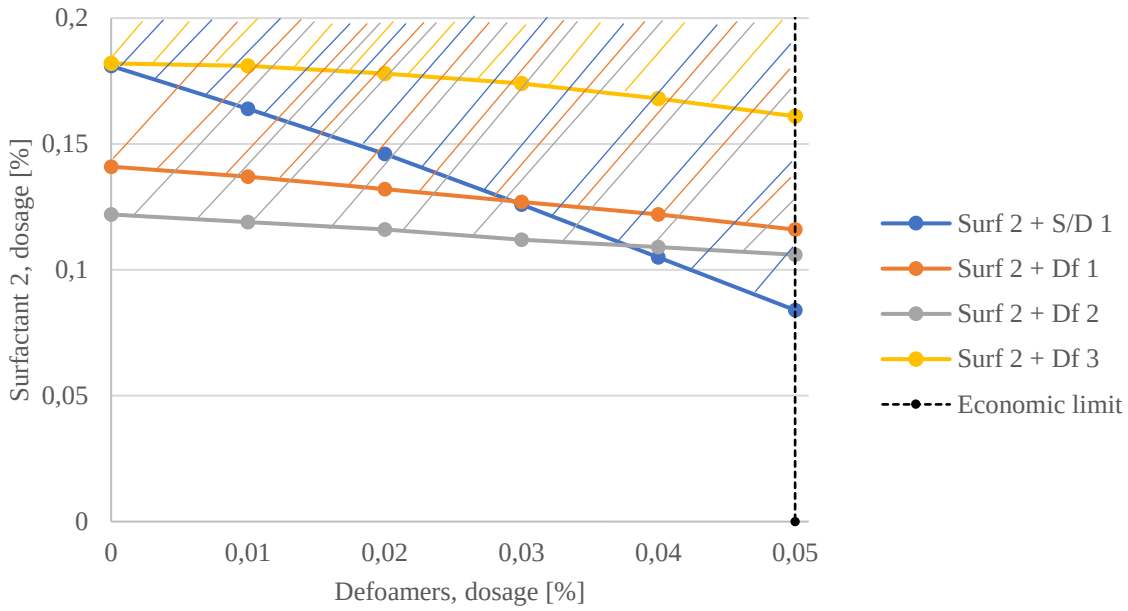

Figure 45 Operational window for LPF resin with surfactant 2 and defoamer combinations. Required dosage of both additives plotted, when the target filament break-up time is 234 ms. For working curves, data obtained from extensional rheometer analysis and model coefficients computed via statistical MLR analysis. Operating area marked with diagonal lines. Surf 2 = surfactant 2, S/D1 = surfactant/defoamer 1 and Df 1-3 = defoamers 1-3.

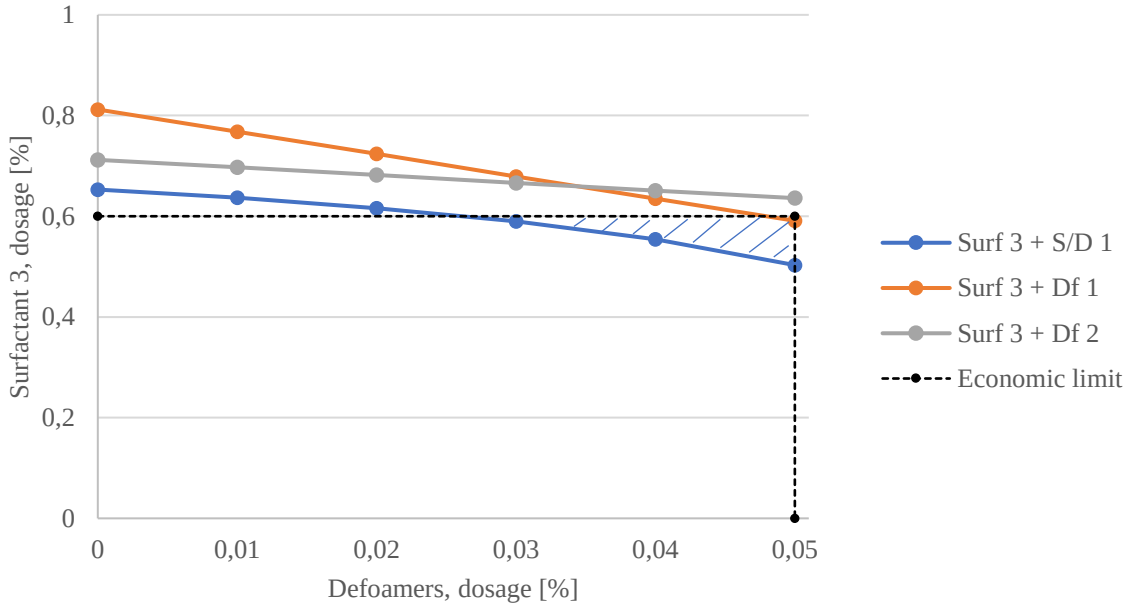

Figure 46 Operational window for LPF resin with surfactant 3 and defoamer combinations. Required dosage of both additives plotted, when the target filament break-up time is 234 ms. For working curves, data obtained from extensional rheometer analysis and model coefficients computed via

statistical MLR analysis. Operating area marked with diagonal lines. Surf 3 = surfactant 3, S/D1 = surfactant/defoamer 1 and Df 1-2 = defoamers 1-2.

Working curves seem reliable based on the measured results. As seen from Figure 45, especially with surfactant/defoamer 1, surfactant 2 dosage is highly dependent on surfactant/defoamer 1 dosage. For other defoamers, surfactant 2 dosage does not vary as much. Highest dosage of surfactant 2 is required for defoamer 3. As seen from Figure 46, the surfactant 3 dosage level does not vary that much either, when combined with defoamers. With surfactant/defoamer 1 and defoamer 1 a small decrease in surfactant 3 dosage can be obtained when defoamer dosage level is increased. Working curve was not obtained for surfactant 3 and defoamer 3 combination, since filament break-up time target was not achieved in extrapolation, and further deletion of variables was not possible. Overall, working curve models were less fitting for surfactant 3 models than for surfactant 2 models.

Thermo Fischer Scientific HAAKE™ CaBER™ 1 device has been commercially available since 2002. There are no scientific research papers regarding elongation properties of resins. Paper coatings, and specifically the effect of thickeners on the coating properties and polymer elongation properties have been reported to some extent. In these studies, filament break-up time is generally mentioned but capillary velocity is not mentioned as a remarkable factor for stable curtain formation.

Birkert et al. (2006) studied the stretchability of paper coating colors. Stretchability can be affected by thickeners. On molecular level, large molecules (extended polymer chains), hyperstructure with pigment (pigment-polymer interaction/compatibility) and water binding ability by hydrogen donor/acceptor interaction are favored. Polyacrylamide thickeners performed the highest extensional viscosity, when qualitatively compared to polyethylene glycol and polyacrylic acid thickeners. They found out, that in paper coating, both too low and too high extensional viscosity lead to coating defects.

Voss & Tadjbach (2004) studied paper coating colors, which indicated via shear rheology analysis practically identical behavior. Characteristic differences between the coating colors which would indicate advantages and disadvantages regarding the successful curtain formation or stability were not observed. However, via extensional rheology analysis, clear differences in filament break-up time (range of 50-200 ms) were observed. Extensional

rheology characteristics correlation to curtain formation and stability were studied in pilot trials. Dynamic surface tension of the coating colors (determined by bubble pressure tensiometer) were 54 mN/m (at 50 ms) and 32 mN/m (at 3000 ms, close to equilibrium/static surface tension). Also effect of natural and synthetic co-binders and special, acrylic acid/acrylamide-based special thickeners on extensional rheology was studied. Conventional thickeners showed only minimum effect on stretchability of the coating color (break-up time 50 ms). Special thickeners enabled much higher elongation/stretchability, and indicated positive effects also in coating trials at high speeds (lowered spot index). Here, the filament break-up time was increased up to 300 ms. Trouton ratio was calculated for conventional co-binders to be 3-6, and for efficient special thickeners to be 10.

Becerra & Carvalho (2011) studied stability of viscoelastic curtain composing of polyethylene glycol (PEG) and high molecular weight polyethylene oxide (PEO) was added into the solution. PEO addition of 0,05 % of the weight of PEG resulted filament break-up time of approximately 300 ms and was reported to stabilize the curtain remarkably.

PF curtain resin break-up time is 234 ms, which is relatively close to break-up time (300 ms) of the best curtain coating color studied by Voss & Tadjbach (2004) and formed stable curtain studied by Becerra & Carvalho (2011). Filament break-up time of 300 ms was not achieved with any of the additive combinations. Closest break-up time to this, with surfactant 2 (0,40 % of the weight of resin) and surfactant/defoamer 1 (0,03 % of the weight of resin) combination, break-up time of 280 ms was achieved. However, in this work, the results are in general compared to properties of PF curtain resin, since it is a commercial product and working. In addition, paper coatings go through more extreme elongation as the conveyor speeds in paper production are faster.

From CaBER^{TM} measurement, also apparent extensional viscosity curves are obtained as a function of Hencky strain. Apparent extensional viscosities of the reference resins are presented in Figure 47 and effect of surfactants on LPF resin apparent extensional viscosity is presented in Figure 48.

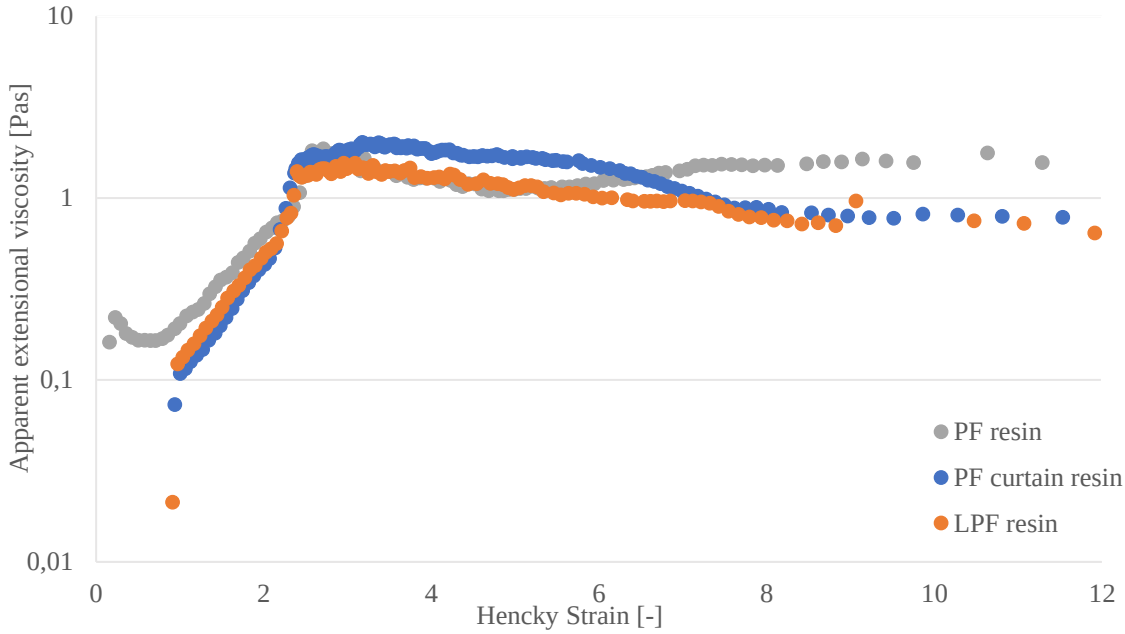

Figure 47 Apparent extensional viscosity of the reference resins as a function of Hencky strain, determined by HAAKE™ CaBER™ 1. Measurement was performed with 6 mm plates with initial and final aspect ratio of 1,00 and 2,75, respectively, and in temperature of 25 ± 2 ºC.

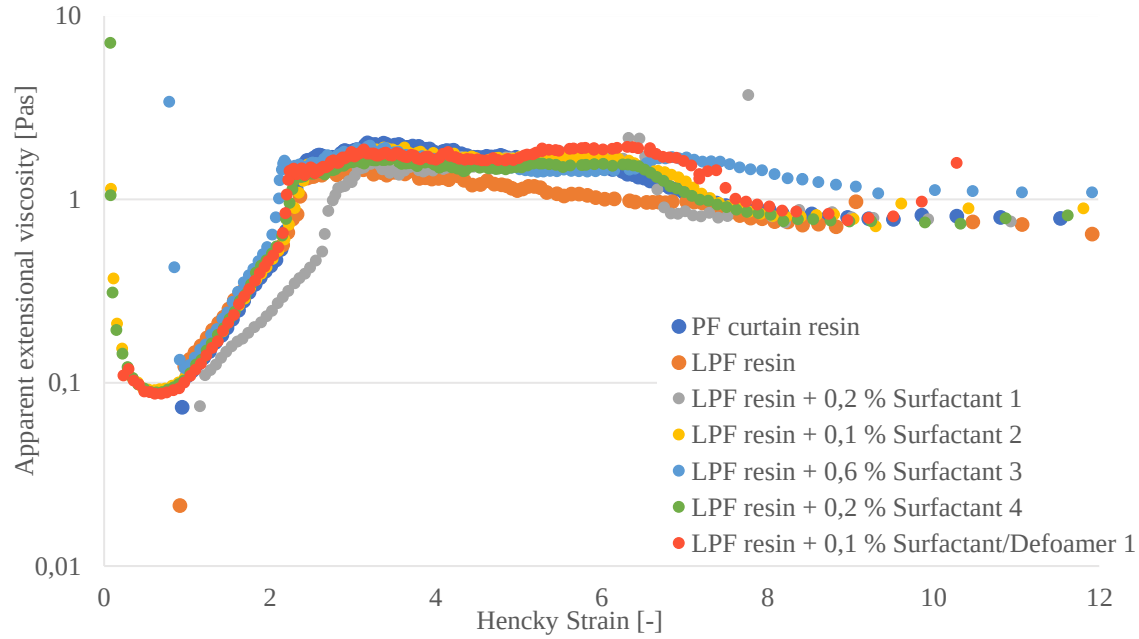

Figure 48 Effect of surfactants on LPF resin apparent extensional viscosity as a function of Hencky strain, determined by HAAKE™ CaBER™ 1. Measurement was performed with 6 mm plates with initial and final aspect ratio of 1,00 and 2,75, respectively, and in temperature of 25 ± 2 ºC.

As seen from Figure 47 and Figure 48, the apparent extensional viscosity curves are very similar, differences between the reference resins and effect of surfactants are not significant. Curves approach constant value, which would imply about the Newtonian liquid behavior (Cambridge Polymer Group, 2013), but not ideally. To combine shear and extensional rheology results, further calculations would include determination of Trouton ratio for resins. Thus, differences between the resins could probably be detected more easily. From shear rheology, complex shear modulus (G^*) and complex viscosity (η^*) could be calculated based on equations (35) and (36), respectively, and plotted as a function of angular frequency. Zero-shear viscosity (η_0) could be determined from complex viscosity curve. Trouton ratio could be calculated based on equation (32), and plotted as a function of Hencky strain as Anna & McKinley (2001), Yesilata et al. (2006), Becerra & Carvalho (2011) and Hussainov et al. (2012) did. From Trouton ratio curve, possible extensional thickening could be detected. Trouton ratio approaches constant steady-state value, which could also be determined. Elongational relaxation time (equation 41) could be determined and compared to shear relaxation time (Anna & McKinley, 2001; Yesilata et al., 2006). However, relaxation time was not obtained from shear rheology, since crossover point for loss and storage moduli was not observed.

In Appendix IV, these further calculations are presented as a test, when neglecting the absence of storage modulus and determining the zero-shear viscosity based on the available data.

10.5 Other analyses

Surface free energy determination was tested for LPF resin and PF curtain resin. The results and discussion in detail are presented in Appendix III. The obtained results are in line with surface tension results, since PF curtain resin has higher surface free energy than LPF resin. The higher surface free energy of a solid, the easier wetting, and the lower surface tension of a liquid, the easier wetting. However, the standard deviation between the replicate contact angle determinations was remarkable (even over 7 º), and determinations especially with water was challenging due to fast absorption into the solid resin. Matsushita et al. (2006) did not report to face these kind of issues.

As the water evaporates from resin during drying, it may cause undesired crosslinking in the resin structure. This may vary also the surface chemical properties of the resin. Since surface tension results gave reliable and accurate results, surface free energy determinations were not continued.

Interfacial viscoelasticity determination was tested for the reference resins and for surfactant 1 and 4, and defoamer 3. The determination should give insight about the surfactant performance in the solution, and thus surfactants with remarkably different chemical composition and defoamer described as non-ionic surfactant and defoamer were chosen. The results and discussion are presented in Appendix IV. Standard deviation between the replicate oscillating drop determinations at each frequency was variable and sometimes remarkable. Frequency range used in this work was relatively narrow due to practical issues, and the range should be wider (Ravera et al., 2010; Karbaschi et al., 2014). Lower frequencies were not applicable due to drying of the resin drop during a long measurement. Camera of the device was not able to record frames faster, and thus higher frequencies could not be applied.

Differences between the LPF resin and PF resins and additives were able to detect. However, due to lack of reference results from literature, evaluation of the additive performance was challenging. In the scope of this work, the determination was not considered as valuable as the other analytical methods determining surface tension and rheological properties of the resins.

11 CONCLUSIONS

In this thesis, the surface chemical and rheological properties of phenol-formaldehyde (PF) and lignin-phenol-formaldehyde (LPF) resins used in plywood adhesive preparation were determined. Curtain coating as an adhesive application method in plywood production requires specific resin properties, since formation of a stable and uniform curtain is a challenge. Curtain coating of paper is commonly studied, and it has been concluded that surface tension reduction and extensional viscosity increasement correlate with successful curtain formation. Curtain coating of veneer and surface chemical and rheological properties

of resins are not as widely studied. The objective of the work was to develop LPF resin composition for curtain coating of veneer.

In the experimental part of this work, it was discovered that surface tension of resins can be determined via pendant drop shape analysis method simply and reliably. Pendant drop shape method was in good correlation with De Noüy ring method, and provided more accurate results. Surface free energy determination via contact angle measurements was not applicable for resins. Drying of resins may cause structural changes, and reliability and repeatability of the determination were poor.

Rheological properties of the resins were determined via shear, extensional and interfacial rheology. Viscosity curves determined by shear rheometer were reliable, but oscillatory tests provided unexpected results based on literature and differences between resins, which would indicate advantages and disadvantages for curtain coating, were not observed. Elongational properties, determined via capillary break-up extensional rheometer (CaBER^{TM}), provided clear differences between the resins. Interfacial viscoelasticity measurement for studying the surfactant function faced some operational issues and due to lack of reference results, evaluation of surfactant performance was not considered reliable.

In this thesis, properties of a commercial PF resin for curtain coating were considered desirable. With commercial additives, surfactants and defoamers, the properties of LPF resin were modified. Surface tension of LPF resin was reduced from 46,52 mN/m to 36,09 mN/m (PF curtain resin) with surfactant dosing of 0,11-0,75 % of the weight of resin, depending on the surfactant. From both shear and extensional rheology analyses it was concluded, that resins exhibit Newtonian flow behavior. Both filament break-up time and capillary velocity were describing elongational properties obtained from extensional rheometer measurement.

PF curtain resin exhibited long filament break-up time (234 ms) and slow capillary velocity (1,39 mm/s) and LPF resin short filament break-up time (118 ms) and fast capillary velocity (2,60 mm/s). As the surface tension of LPF resin was adjusted with each surfactant to the level of PF curtain resin, a remarkable difference in elongation properties was obtained. Also performance of defoamers was able to be evaluated with extensional rheometer. With additive combinations (both surfactants and defoamers) as long or longer break-up time and

as slow or slower capillary velocity, than PF curtain resin exhibited, were obtained for LPF resin.

Statistical importance of defoamer level increasement was studied via multiple linear regression analysis and it was considered to correlate with surfactant and defoamer compatibility. Based on compatibility, two best surfactants were selected. Further measurements were performed to obtain an operational window to correlate LPF resin filament break-up time to dosage of both surfactant and defoamer. Operational windows were obtained for two surfactants in combination with all defoamers.

Further studies regarding the topic of this work include industrial trials to determine correlation between the laboratory analyses and curtain coating of veneer. Based on this work it can be concluded that surface tension and elongational properties of the coating material are essential for successful curtain formation, since differences between the resins were noticed. Those properties can be suggested to be measured in the future, when studying resins for curtain coating and for evaluation of additives. In the future, operational windows could be determined with additional variables and limitations. To fully confirm the performance of the additive combinations, curtain coating trials are required.

REFERENCES

Abbott, S. (2018). *Surface Energy Calculator*. [online] Prof Steven Abbott Apps. Available at: https://www.stevenabbott.co.uk/abbottapps/SEC/index.html [Accessed 17 Oct. 2018].

Adamson, A. (1976). *Physical Chemistry of Surfaces*. 3rd ed. New York: John Wiley & Sons, Inc.

Alén, R. (2011). Biorefining of forest resources. *Papermaking Science and Technology - Book 20*. Helsinki: Finnish Paper Engineers Association.

Anna, S. and McKinley, G. (2001). Elasto-capillary thinning and breakup of model elastic liquids. *Journal of Rheology*, 45(1), pp.115-138.

Barnes, H., Hutton, J. and Walters, K. (1989). *Rheology Series vol. 3: An Introduction Rheology*. Amsterdam: Elsevier Science Publishers B.V.

BASF (2013). *Additives for Adhesives and Sealants*. [online] Available at: http://www.dispersions-pigments.basf.com/portal/load/fid793202/Booklet_%20Additives%20for%20adhesives%20and%20sealants.pdf [Accessed 8 Aug. 2018].

BASF (2016). *Practical Guide to Rheology Modifiers.* [online] Formulation Additives by BASF. Available at: https://www.dispersions-pigments.basf.com/portal/load/fid806722/RheologyModifiers-Brochure.pdf [Accessed 26 Jul. 2018].

BASF (2018a). *A Practical Guide to Defoamers.* [online] Formulation Additives by BASF. Available at: https://www.dispersions-pigments.basf.com/portal/load/fid807410/BASF%20Defoamers%20Practical%20Guide.pdf [Accessed 15 Aug. 2018].

BASF (2018b). *Paper & Board - Coating Additives*. [online] BASF Dispersions & Pigments. Available at: http://www.dispersions-pigments.basf.com/portal/basf/ien/dt.jsp?setCursor=1_832005 [Accessed 8 Aug. 2018].

BASF (2018c). *Practical Guide to Wetting Agents and Surface Modifiers.* [online] Formulation Additives by BASF. Available at: https://www.dispersions-pigments.basf.com/portal/load/fid831592/Wetting%20Agents%20and%20Surface%20Modifiers.pdf [Accessed 8 Aug. 2018].

Becerra, M. and Carvalho, M. (2011). Stability of viscoelastic liquid curtain. *Chemical Engineering and Processing: Process Intensification*, 50(5-6), pp.445-449.

Beneventi, D. and Guerin, D. (2005). Physical chemistry, rheology and curtain formation ability of surfactant-starch solutions. [conference material] *22. PTS Streicherei-Symposium, Baden-Baden, September 2005*.

Biolin Scientific (2017a). *Pulsating drop technique to characterize surfactant behavior in flotation process*. Attension - Application Note 11. [online] Available at: https://cdn2.hubspot.net/hubfs/516902/Pdf/Attension/Application%20notes/AT-AN-11-Pulsating-drop-surfactant-in-flotation.pdf?t=1539950841852 [Accessed 22 Oct. 2018].

Biolin Scientific (2017b). *Surface free energy - theory and calculation*. Attension - Technology Note 4. [online] Available at: https://cdn2.hubspot.net/hubfs/516902/Pdf/Attension/Tech%20Notes/AT-TN-04-Surface-free-energy-theory.pdf?t=1535604088175 [Accessed 31 Aug. 2018].

Biolin Scientific (2018a). *Measurements - Contact Angle*. [online] Available at: https://www.biolinscientific.com/measurements/contact-angle [Accessed 6 Jul. 2018].

Biolin Scientific (2018b). *Measurements - Critical Micelle Concentration*. [online] Available at: https://www.biolinscientific.com/measurements/critical-micelle-concentration [Accessed 6 Jul. 2018].

Biolin Scientific (2018c). *Measurements - Surface Tension*. [online] Available at: https://www.biolinscientific.com/measurements/surface-tension [Accessed 6 Jul. 2018].

Birkert, O., Hamers, C., Krumbacher, E., Schachtl, M., Gane, P., Gerteiser, N., Ridgway, C., Fröhlich, U. and Tietz, M. (2006). Curtain Coating of Pigment Coats. *Professional Papermaking*, 2, pp.56-71.

Bond, W. and Moehl, T. (1975). *Plywood Adhesive*. Georgia-Pacific Corporation. US1976/3931070.

BYK (2018). *Additives for Adhesives & Sealants.* [online] BYK Additives. Available at: https://www.byk.com/en/additives/applications/adhesives-sealants/aqueous.php [Accessed 8 Aug. 2018].

Calvo-Flores, F. and Dobado, J. (2010). Lignin as Renewable Raw Material. *ChemSusChem*, 3(11), pp.1227-1235.

Cambridge Polymer Group (2013). *The Capillary Breakup Extensional Rheometer (CABER™)*. Filament Breakup Rheometry. Cambridge Polymer Group. [online] Available at: http://www.campoly.com/files/3913/7122/7764/007_New.pdf [Accessed 27 Jul. 2018]

Clausen, V., Järvi, R. and Zweig, A. (1965). *Curtain Coating Apparatus*. Simpson Timber Company. US1969/3451374.

Colloid and Surface Chemistry Virtual Lab. (2018). *Determination of Critical Micelle Concentration (CMC) of a Surfactant*. [online] Available at: https://csc-iiith.vlabs.ac.in/exp14/index.html [Accessed 6 Jul. 2018].

Danielson, B. and Simonson, R. (1998). Kraft lignin in phenol formaldehyde resin. Part 1. Partial replacement of phenol by kraft lignin in phenol formaldehyde adhesives for plywood. *Journal of Adhesion Science and Technology*, 12(9), pp.923-939.

Doering, G. (1992). *Lignin Modified Phenol-Formaldehyde Resins*. Georgia-Pacific Resins, Inc. US1993/005202403A.

Domínguez, J., Oliet, M., Alonso, M., Rojo, E. and Rodríguez, F. (2013). Structural, thermal and rheological behavior of a bio-based phenolic resin in relation to a commercial resol resin. *Industrial Crops and Products*, 42, pp.308-314.

Dow (2018a). *ACRYSOL™ Rheology Modifiers*. [online] Dow Coating Materials. Available at: https://www.dow.com/en-us/coatings/products/acrysol [Accessed 8 Aug. 2018].

DOW (2018b). *ECOSURF™ Surfactants.* [online] Dow Coating Materials. Available at: https://www.dow.com/en-us/coatings/products/ecosurf [Accessed 8 Aug. 2018].

DOW (2018c). *Foam Control - Polypropylene Glycols and Copolymers Europe*. [online] Available at: https://www.dow.com/polyglycols/ppgc/europe/apps/foamcon.htm [Accessed 15 Aug. 2018].

Dunky, M. (2003). Adhesives in the Wood Industry. In: A. Pizzi and K. Mittal, ed., *Handbook of Adhesive Technology*, 2nd ed. New York: Marcel Dekker, pp.887-956.

Evonik (2015). *TEGO Product Overview*. Evonik Coatings.

Evonik (2017a). *Additives for Water Based Adhesives*. Evonik Polymer Dispersions.

Evonik (2017b). *One partner. Many experts. Product Reference Guide*. Evonik Coatings.

Evonik (2018). *Product Overview - Additives for Polymer Dispersions*. Evonik Polymer Dispersions.

Glazer, A. and Nikaido, H. (1995). *Microbial Biotechnology: fundamentals of applied microbiology*. San Francisco: W. H. Freeman.

Goodwin, J. and Hughes, R. (2008). *Rheology for Chemists*. 2nd ed. Cambridge: Royal Society of Chemistry.

Grillet, A., Wyatt, N. and Gloe, L. (2012). Polymer Gel Rheology and Adhesion. In: J. Vicente, ed., *Rheology*. Rijeka: InTech.

Halász, L., Vorster, O., Pizzi, A. and Guasi, K. (2001). Rheology study of gelling of phenol-formaldehyde resins. *Journal of Applied Polymer Science*, 80(6), pp.898-902.

Holladay, J., Bozell, J., White, J. and Johnson, D. (2007). *Top Value-Added Chemicals from Biomass: Volume II - Results of Screening for Potential Candidates from Biorefinery Lignin*. Pacific Northwest National Laboratory for the United States Department of Energy.

Hse, C. (1972). Surface Tension of Phenol-Formaldehyde Wood Adhesives. *Holzforschung*, 26(2), pp.82-85.

Hu, L., Pan, H., Zhou, Y. and Zhang, M. (2011). Methods to Improve Lignin's Reactivity as a Phenol Substitute and as a Replacement for Other Phenolic Compounds: a Brief Review. *BioResources*, 6(3), pp.3515-3525.

Hussainov, M., Tätte, T. and Hussainova, I. (2012). Technique for extensional rheology characterization of highly reactive viscoelastic liquids. *Rheologica Acta*, 51(8), pp.729-742.

Järvi, R. (1969). *High Molecular Weight/Low Molecular Weight Phenol-Formaldehyde Curtain Coating Adhesive Composition*. Simpson Timber Company. US1971/3591535.

Karbaschi, M., Lotfi, M., Krägel, J., Javadi, A., Bastani, D. and Miller, R. (2014). Rheology of interfacial layers. *Current Opinion in Colloid & Interafce Science*, 19(6), pp.514-519.

King Industries (2017). *K-Stay Rheology Modifiers & DISPARLON for Solventborne and Solventless Systems*. [online] Available at: http://www.kingindustries.com/assets/1/7/K-STAY_DISPARLON_Combined.pdf [Accessed 8 Aug. 2018].

Koponen, H. (2002). *Puutuoteteollisuus 4: Puulevytuotanto*. 3rd ed. Helsinki: Opetushallitus.

KRÜSS GmbH (2018a). *Bubble Pressure Tensiometer*. [online] Available at: https://www.kruss-scientific.com/services/education-theory/glossary/bubble-pressure-tensiometer/ [Accessed 10 Jul. 2018].

KRÜSS GmbH (2018b). *Interfacial rheology*. [online] Available at: https://www.kruss-scientific.com/services/education-theory/glossary/interfacial-rheology/ [Accessed 22 Oct. 2018].

Langevin, D. (2000). Influence of interfacial rheology on foam and emulsion properties. *Advances in Colloid and Interface Science*, 88(1-2), pp.209-222.

Laurichesse, S. and Avérous, L. (2014). Chemical modification of lignins: Towards biobased polymers. *Progress in Polymer Science*, 39(7), pp.1266-1290.

Louis, C. (2003). *Importance of Surfactants in Dynamic Applications of Waterborne Pressure Sensitive Adhesives*. Air Products and Chemicals, Inc.

Mankar, S., Chaudhari, A. and Soni, I. (2012). Lignin in phenol-formaldehyde adhesives. *International Journal of Knowledge Engineering*, 3(1), pp.116-118.

Matsushita, Y., Wada, S., Fukushima, K. and Yasuda, S. (2006). Surface characteristics of phenol–formaldehyde–lignin resin determined by contact angle measurement and inverse gas chromatography. *Industrial Crops and Products*, 23(2), pp.115-121.

Mattinen, M. (2016). *Lignin-based polymer blends and biocomposite materials*. [lecture material] School of Chemical Technology. Aalto University.

McKinley, G. and Tripathi, A. (2000). How to extract the Newtonian viscosity from capillary breakup measurements in a filament rheometer. *Journal of Rheology*, 44(3), pp.653-670.

McVay, T., Baxter, G. and Dupre, Jr., F. (1993). *Reactive Phenolic Resin Modifier*. Georgia-Pacific Resins, Inc. US1999/005866642A.

Merck KGaA (2017a). *Formaldehyde solution 37% (stabilized with about 10% methanol) for synthesis*. Safety Data Sheet. Darmstadt: Merck KGaA.

Merck KGaA (2017b). *Phenol for Synthesis*. Safety Data Sheet. Darmstadt: Merck KGaA.

Mezger, T. (2014). *Applied Rheology - With Joe Flow on Rheology Road*. Anton Paar GmbH.

Montgomery, D., Peck, E. and Vining, G. (2012). *Introduction to linear regression analysis*. 5th ed. Hoboken: John Wiley & Sons, Inc.

Morrel, S. (2014). *Oxidizable Phenolic-Based Urethanes.* [online] PCI - Paint & Coating Industry. Available at: https://www.pcimag.com/articles/98855-oxidizable-phenolic-based-urethanes [Accessed 15 Jun. 2018].

Moubarik, A. (2014). Rheology Study of Sugar Cane Bagasse Lignin-Added Phenol–Formaldehyde Adhesives. *The Journal of Adhesion*, 91(5), pp.347-355.

Peng, W. and Riedl, B. (1994). The chemorheology of phenol-formaldehyde thermoset resin and mixtures of the resin with lignin fillers. *Polymer*, 35(6), pp.1280-1286.

Phan-Thien, N. (2002). *Understanding viscoelasticity: basics of rheology*. Berlin: Springer.

Pietarinen, S., Valkonen, S. and Ringena, O. (2014). *A Method for Increasing the Reactivity of Lignin*. UPM-Kymmene Corporation. US2016/0237194A1.

Pizzi, A. (1994). *Advanced Wood Adhesives Technology*. New York: Marcel Dekker.

Pizzi, A. (2003a). Natural Phenolic Adhesives II: Lignin. In: A. Pizzi and K. Mittal, ed., *Handbook of Adhesive Technology*, 2nd ed. New York: Marcel Dekker, pp.589-598.

Pizzi, A. (2003b). Phenolic Resin Adhesives. In: A. Pizzi and K. Mittal, ed., *Handbook of Adhesive Technology*, 2nd ed. New York: Marcel Dekker, pp.541-571.

Pizzi, A., Ibeh, C. (2014). Phenol-Formaldehydes. In: H. Dodiuk and S. Goodman ed., *Handbook of Thermoset Plastics*, 3rd ed. William Andrew, pp.13-44.

Raskin, M., Ioffe, L., Pukis, A. and Wolf, M. (2001). *Resin Material and Method of Producing Same*. Cellutech LLC. US2002/0065400A1.

Ravera, F., Loglio, G. and Kovalchuk, V. (2010). Interfacial dilational rheology by oscillating bubble/drop methods. *Current Opinion in Colloid & Interface Science*, 15(4), pp.217-228.

Robitschek, P., Chappelie, N. and Lorimer, J. (1974). *Liquid Phenol-Aldehyde Adhesive for Use in Curtain-Coating Adhesive Applicators*. Chembond Corporation. US1976/3966658.

Schweizer, P. (2004). Curtain coating – stability a critical operating parameter. *Paper Technology*, 45(2), pp.28-35.

Sellers, T. (1985). *Plywood and adhesive technology*. New York: Marcel Dekker.

Shaw, D. (1980). *Introduction to Colloid and Surface Chemistry*. 3rd ed. Oxford: Butterworth-Heinemann Ltd.

Tetra Pak (2018). *Chapter 3: Rheology*. [online] Dairy Processing Handbook. Available at: http://dairyprocessinghandbook.com/chapter/rheology [Accessed 17 Sep. 2018].

Thermo Fisher Scientific (2018). *HAAKE™ CaBER™ 1 Capillary Breakup Extensional Rheometer*. [online] Rheometers & Viscometers. Available at: https://www.thermofisher.com/order/catalog/product/398-0001?SID=srch-srp-398-0001 [Accessed 27 Jul. 2018].

Triantafillopoulos, N., Grön, J., Luostarinen, I. and Paloviita, P. (2004). Operational issues in high speed curtain coating of paper, Part 1: The principles of curtain coating. *Tappi Journal*, 3(11), pp.6-10.

UPM Biochemicals. (2018). [website] Available at: http://www.upmbiochemicals.com [Accessed 4 Jun. 2018].

UPM Biofore. (2018). *Bonding breakthrough: the new life of lignin*. [online] Available at: https://www.upmbiofore.com/plywood/bonding-breakthrough-the-new-life-of-lignin/ [Accessed 4 Jun. 2018].

UPM Kaukas. (2018). [website] Available at: http://www.upmpulp.fi/upm-kaukas/ [Accessed 4 Jun. 2018]

UPM-Kymmene Oyj (2018). *Annual Report 2017*. [online] Available at: http://assets.upm.com/Investors/2017/Reports%20and%20Presentations%202017/UPM_Annual%20Report_2017.pdf [Accessed 7 Jun. 2018].

Valmet. (2018). *Valmet LignoBoost - lignin extraction*. [online] Available at: https://www.valmet.com/more-industries/bio/lignin-separation/ [Accessed 20 Jun. 2018].

Voss, M. and Tadjbach, S. (2004). Extensional Rheology of Coating Colours for Curtain Application. [conference material] *TAPPI Coating and Graphic Arts Conference, Baltimore, May 2004*.

Weser, C. (1980). Measurement of Interfacial Tension and Surface Tension - General Review for Practical Man. *GIT Fachzeitschrift für das Laboratorium*, 24, pp.642-648, 734-742.

Willenbacher, N., Benz, R., Ewers, A. and Nijman, J. (2004). *The influence of thickeners on the application method of automotive coatings and paper coatings – rheological investigations with the HAAKE CaBER 1*. Rheology Application Notes. Thermo Fisher Scientific.

Winterowd, J., Zhang, C. and Neogi, A. (2010). *Utilization of Kraft Lignin in Phenol/Formaldehyde Bonding Resins for OSB*. Weyerhaeuser NR Company. US2011/0245381A1.

WISA BioBond. (2018). *WISA BioBond - The most sustainable plywood bonding technology*. [online] Available at: http://www.wisabiobond.com/ [Accessed 4 Jun. 2018].

Yang, X. and Frazier, C. (2016a). Influence of organic fillers on rheological behavior in phenol-formaldehyde adhesives. *International Journal of Adhesion and Adhesives*, 66, pp.93-98.

Yang, X. and Frazier, C. (2016b). Influence of organic fillers on surface tension of phenol-formaldehyde adhesives. *International Journal of Adhesion and Adhesives*, 66, pp.160-166.

Yesilata, B., Clasen, C. and McKinley, G. (2006). Nonlinear shear and extensional flow dynamics of wormlike surfactant solutions. *Journal of Non-Newtonian Fluid Mechanics*, 133(2-3), pp.73-90.

APPENDIX II: EXPERIMENTS

In Table I and Table II, final experiments of this work are presented. The reference resins are commercial phenol-formaldehyde (PF) resins for roller and curtain coating and lignin-phenol-formaldehyde (LPF) resin for roller coating. For experiments 32-63, surfactant dosage is selected based on surface tension results, so that the surface tension is at the same level with PF curtain resin.

Table I Experiments of the work. PF resin and PF curtain resin are commercial phenol-formaldehyde resins to be used in roller and curtain coating applications, respectively. LPF resin is a lignin-phenol-formaldehyde resin developed by UPM. Surf = surfactants 1-4, dosage varying 0,10-0,60 % of the weight of resin. Surf/Df = surfactant/defoamer 1, dosage varying 0,03-0,60 % of the weight of resin. Df = defoamers 1-3, dosage varying 0,03-0,10 % of the weight of resin.

EXP	Resin	Surf dosage	Surf	Surf/Df dosage	Surf/ Df	Df dosage	Df
1	PF resin						
2	PF curtain resin						
3	LPF resin						
4	LPF	0,20 %	1				
5	LPF	0,40 %	1				
6	LPF	0,60 %	1				
7	LPF	0,10 %	2				
8	LPF	0,20 %	2				
9	LPF	0,40 %	2				
10	LPF	0,60 %	2				
11	LPF	0,20 %	3				
12	LPF	0,40 %	3				
13	LPF	0,60 %	3				
14	LPF	0,20 %	4				
15	LPF	0,40%	4				
16	LPF	0,60 %	4				
17	LPF			0,03 %	1		
18	LPF			0,05 %	1		
19	LPF			0,10 %	1		
20	LPF			0,20 %	1		
21	LPF			0,40 %	1		
22	LPF			0,60 %	1		
23	LPF					0,03 %	1

24	LPF					0,05 %	1
25	LPF					0,10 %	1
26	LPF					0,03 %	2
27	LPF					0,05 %	2
28	LPF					0,10 %	2
29	LPF					0,03 %	3
30	LPF					0,05 %	3
31	LPF					0,10 %	3
32	LPF	0,20 %	1	0,03 %	1		
33	LPF	0,20 %	1			0,03 %	1
34	LPF	0,20 %	1			0,03 %	2
35	LPF	0,20 %	1			0,03 %	3
36	LPF	0,20 %	1	0,05 %	1		
37	LPF	0,20 %	1			0,05 %	1
38	LPF	0,20 %	1			0,05 %	2
39	LPF	0,20 %	1			0,05 %	3
40	LPF	0,10 %	2	0,03 %	1		
41	LPF	0,10 %	2			0,03 %	1
42	LPF	0,10 %	2			0,03 %	2
43	LPF	0,10 %	2			0,03 %	3
44	LPF	0,10 %	2	0,05 %	1		
45	LPF	0,10 %	2			0,05 %	1
46	LPF	0,10 %	2			0,05 %	2
47	LPF	0,10 %	2			0,05 %	3
48	LPF	0,60 %	3	0,03 %	1		
49	LPF	0,60 %	3			0,03 %	1
50	LPF	0,60 %	3			0,03 %	2
51	LPF	0,60 %	3			0,03 %	3
52	LPF	0,60 %	3	0,05 %	1		
53	LPF	0,60 %	3			0,05 %	1
54	LPF	0,60 %	3			0,05 %	2
55	LPF	0,60 %	3			0,05 %	3
56	LPF	0,20 %	4	0,03 %	1		
57	LPF	0,20 %	4			0,03 %	1
58	LPF	0,20 %	4			0,03 %	2
59	LPF	0,20 %	4			0,03 %	3
60	LPF	0,20 %	4	0,05 %	1		
61	LPF	0,20 %	4			0,05 %	1
62	LPF	0,20 %	4			0,05 %	2
63	LPF	0,20 %	4			0,05 %	3

Based on the results obtained from extensional rheology, the following experiments (Table II) were added for further measurements with extensional rheometer.

Table II Additional experiments of the work. LPF resin is a lignin-phenol-formaldehyde resin developed by UPM. Surf = surfactants 2-3, dosage 0,60 % of the weight of resin. Surf/Df = surfactant/defoamer 1, dosage varying 0,03-0,05 % of the weight of resin. Df = defoamers 1-3, dosage varying 0,03-0,10 % of the weight of resin.

EXP	**Resin**	**Surf dosage**	**Surf**	**Surf/Df dosage**	**Surf/ Df**	**Df dosage**	**Df**
64	LPF	0,40 %	2	0,03 %	1		
65	LPF	0,40 %	2			0,03 %	1
66	LPF	0,40 %	2			0,03 %	2
67	LPF	0,40 %	2			0,03 %	3
68	LPF	0,40 %	2	0,05 %	1		
69	LPF	0,40 %	2			0,05 %	1
70	LPF	0,40 %	2			0,05 %	2
71	LPF	0,40 %	2			0,05 %	3
72	LPF	0,40 %	3	0,03 %	1		
73	LPF	0,40 %	3			0,03 %	1
74	LPF	0,40 %	3			0,03 %	2
75	LPF	0,40 %	3			0,03 %	3
76	LPF	0,40 %	3	0,05 %	1		
77	LPF	0,40 %	3			0,05 %	1
78	LPF	0,40 %	3			0,05 %	2
79	LPF	0,40 %	3			0,05 %	3

APPENDIX III: SURFACE CHEMICAL ANALYSES

Surface tension

Surface tension and expanded uncertainty on level of confidence of 95 % of experiments are presented in Table I.

Table I Surface tension of experiments determined by pendant drop shape analysis method with Attension Theta optical tensiometer, in temperature of 23 ± 2 ºC. Drop (volume 4 µl, except for experiment 10, 3,5 µl) formed with 200 µl micropipette, and resin density used 1,2073 g/cm^3. Values obtained after 3,0 s from the beginning of the measurement. Expanded uncertainty on level of confidence of 95 %.

EXP	Description	Surface tension, mN/m	Expanded uncertainty
1	PF resin	71,28	0,91
2	PF curtain resin	36,09	0,11
3	LPF resin	46,52	1,16
4	LPF resin + 0,2 % Surfactant 1	35,58	0,24
5	LPF resin + 0,4 % Surfactant 1	33,75	0,38
6	LPF resin + 0,6 % Surfactant 1	31,57	0,10
7	LPF resin + 0,1 % Surfactant 2	37,01	0,11
8	LPF resin + 0,2 % Surfactant 2	33,81	0,10
9	LPF resin + 0,4 % Surfactant 2	30,27	0,13
10	LPF resin + 0,6 % Surfactant 2	29,67	0,11
11	LPF resin + 0,2 % Surfactant 3	42,45	0,55
12	LPF resin + 0,4 % Surfactant 3	39,81	0,16
13	LPF resin + 0,6 % Surfactant 3	37,95	0,12
14	LPF resin + 0,2 % Surfactant 4	37,07	0,07
15	LPF resin + 0,4 % Surfactant 4	35,05	0,15
16	LPF resin + 0,6 % Surfactant 4	32,01	0,05
17	LPF resin + 0,03 % Surfactant/Defoamer 1	42,42	0,12
18	LPF resin + 0,05 % Surfactant/Defoamer 1	39,07	0,25
19	LPF resin + 0,10 % Surfactant/Defoamer 1	36,53	0,34
20	LPF resin + 0,20 % Surfactant/Defoamer 1	31,64	0,83
21	LPF resin + 0,40 % Surfactant/Defoamer 1	29,86	0,56
22	LPF resin + 0,60 % Surfactant/Defoamer 1	29,86	0,51
23	LPF resin + 0,03 % Defoamer 1	45,77	0,65
24	LPF resin + 0,05 % Defoamer 1	44,99	0,49
25	LPF resin + 0,10 % Defoamer 1	45,81	0,97
26	LPF resin + 0,03 % Defoamer 2	46,89	0,15
27	LPF resin + 0,05 % Defoamer 2	46,23	0,16

28	LPF resin + 0,10 % Defoamer 2	46,23	0,26
29	LPF resin + 0,03 % Defoamer 3	46,32	0,42
30	LPF resin + 0,05 % Defoamer 3	44,78	0,96
31	LPF resin + 0,10 % Defoamer 3	41,54	0,38

Surface free energy

Surface free energy determination was tested for LPF resin and PF curtain resin. Determination could not be made for PF resin due to operational issues in the laboratory. Calculated, total surface free energy and its components are presented in Table II. Lewis acid-base calculation method was performed, since the determination was performed with three liquids and it is the most accurate calculation method.

Table II Surface free energy and its components for Lewis acid-base calculation method determined from contact angle measurements with Attension Theta optical tensiometer, in temperature of 23 ± 1 ºC and relative humidity of 50 ± 2 %. Contact angles were determined for water (drop volume 3 µl), ethylene glycol (drop volume 3 µl) and diiodomethane (drop volume 1 µl) and values obtained after 1,0 s from the beginning of the measurement. Calculation performed with Steven Abbott calculator (Abbott, 2018).

Resin	**Total, mN/m**	**Dispersive component**	**Polar/ acid-base component**	**Acid parameter σ^+**	**Base parameter σ^-**
PF curtain resin	42,1	39,1	3,0	0	70,2
LPF resin	35,2	21,8	13,4	0,5	86,5

The obtained results are in line with surface tension results, since PF curtain resin has higher surface free energy than LPF resin. The higher surface free energy of a solid, the easier wetting, and the lower surface tension of a liquid, the easier wetting. However, the standard deviation between the replicate contact angle determinations was remarkable (even over 7 º). Especially with water, the drops absorbed into the solid resin very fast and contact angles were very small. This affects the validity of Lewis acid-base polar component results. Deviation may be due to non-uniform surface of the resins. After drying of resins, it was noticed that especially the surface of LPF resin was wrinkled. However, the deviation was also remarkable for PF curtain resin even though visually the surface seemed smooth.

Water evaporates from resin during drying and may thus cause crosslinking in the resin structure. This may vary also the surface chemical properties of the resin. In practice resin

is not used in a solid form. Thus, surface free energy of resin was not considered applicable or relevant way of describing the properties of resin, when considering the scope of this work.

However, Matsushita et al. (2006) determined the surface characteristics of LPF resin with kraft lignin (7 % and 15 %) and lignosulfonates (15 % and 30 %) by contact angle measurement and inverse gas chromatography (IGC). For contact angle measurements, resins were dried to obtain a resin film and for IGC, resins were converted into powders. Total surface free energies of samples and Lewis acid-base components of work of adhesion are presented in Table III. Lewis acid-base component of work of adhesion (W_a^{AB}) was calculated from equation (Matsushita et al., 2006):

$$W_a^{AB} = 2\,[(\sigma_S^+\sigma_L^-)^{1/2} + (\sigma_S^-\sigma_L^+)^{1/2}], \qquad (1)$$

where σ^+ acid (electron acceptor) parameter of surface free energy of solid (*S*) or surface tension of liquid (*L*)

σ^- base (electron donor) parameter of surface free energy of solid (*S*) or surface tension of liquid (*L*).

Lewis acid-base parameters for liquids are known.

Table III Total surface free energy of PF and LPF resins, determined by contact angle measurement with three liquids (water, diiodomethane and formamide), and Lewis acid-base components of work of adhesion for water and ethylene glycol (collected from Matsushita et al. (2006)).

Sample	**Total surface free energy, mN/m**	**Lewis acid-base component of work of adhesion, water/ethylene glycol, mN/m**
PF resin	42,8	56,8/29,7
Kraft lignin-PF resin (7 % phenol substitution)	41,8	50,0/18,0
Kraft lignin-PF resin (15 % phenol substitution)	41,9	46,6/12,8
Lignosulfonate-PF resin (15 % phenol substitution)	38,4	58,7/24,6

Lignosulfonate-PF resin (30 % phenol substitution)	37,6	59,0/16,2

Differences in the surface free energy between the samples may be due to chemical component changes, e.g. lignin and sulfonic acid group side chains in the resin composition. From the work of adhesion results it can be concluded, that the kraft lignin PF resin has the best resistance to water (lowest values), PF resin has the second best resistance and lignosulfonate-PF resin the lowest resistance to water. Resistance to water was further improved by the higher substitution of phenol with kraft lignin. Results from IGC were partly different, which may be due to different measuring principles. (Matsushita et al., 2006)

Surface free energies determined for PF curtain resin and LPF resin in this work are in principle in good agreement with surface free energies determined by Matsushita et al. (2006). However, as mentioned, the surface free energy results of this work are not completely reliable. Apparently, Matsushita et al. (2006) did not have issues with drying of the resins and contact angle determinations. Lewis acid-base component of work of adhesion for water calculated based on equation (46) for PF curtain resin and LPF resin are 84,6 mN/m and 101,1 mN/m, respectively. These values are not in line with the results of Matsushita et al. (2006). This is probably due to invalid results of contact angle determination with water in this work. Water contact angles determined by Matsushita et al. (2006) were 56-63 º, whereas water contact angles obtained in this work were 8-10 º.

APPENDIX IV: RHEOLOGICAL ANALYSES

Shear rheology

In Figure 1, amplitude sweeps of the reference resins are presented.

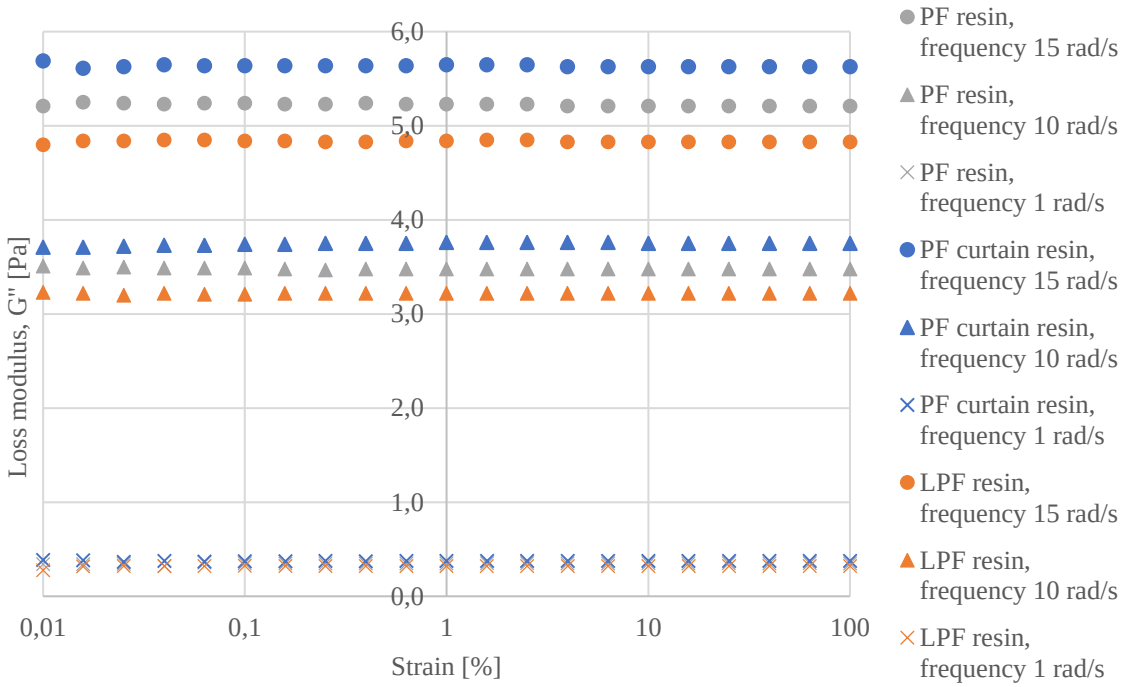

Figure 1 Amplitude sweeps of the reference resins, loss modulus as function of strain on logarithmic scale, determined by MCR302 shear rheometer and CC27 cylinder, in temperature of 25 ºC. Storage modulus not obtained. Strain varied from 0,01-100 % and frequencies of 15 rad/s, 10 rad/s and 1 rad/s were used.

Amplitude sweep was done to determine linear viscoelastic region of the resins. However, storage/elastic moduli were not plotted for any of the resins. Storage moduli were measured 0 throughout the measurements at all frequencies tested. In addition, loss/viscous moduli remained constant throughout the measurements at all frequencies for all resins. This implies that the resins are ideal Newtonian liquids with no elastic behavior. Linear viscoelastic region cannot thus be determined. The loss moduli of all of the resins are at same level at the same frequency. This is probably due to same type of the composition of all the resins, water, phenol and formaldehyde as the main components. Lignin as a structural component does not have any remarkable effect on this property of the resins.

However, frequency sweeps of the reference resins were determined, and are presented in Figure 2.

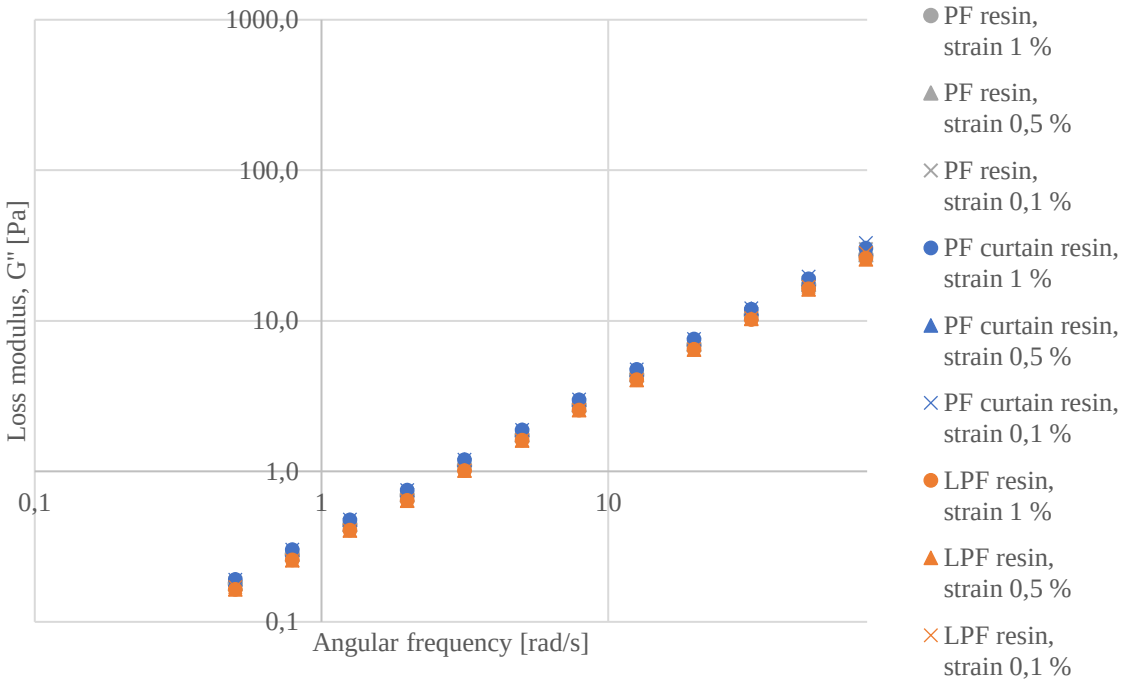

Figure 2 Frequency sweeps of the reference resins, loss modulus as function of frequency on logarithmic scale, determined by MCR302 shear rheometer and CC27 cylinder, in temperature of 25 ºC. Storage modulus not obtained. Frequency varied from 500-0,5 rad/s and strains of 1 %, 0,5 % and 0,1 % were used.

Frequency sweep is supposed to be measured at a strain level determined by amplitude sweep. Since linear viscoelastic region could not be determined, different strains were tested. Again, storage moduli were not plotted for any of the resins, since it was measured 0 throughout the measurements at all strains tested. This confirms ideal Newtonian liquid type of behavior. The loss modulus curves of the resins are the same for all the resins at all strains. This is again probably due to same type of the composition of all the resins.

Based on these results, it could be concluded that the resins used in this work are ideal Newtonian liquids, with no elastic behavior and thus no viscoelastic behavior. However, this conclusion is unexpected due to visual evaluation of the resins and results based on literature (Domínguez et al. 2013; Moubarik, 2014; Yang and Frazier, 2016a). Resins used in this work are syrupy, but however flowing, and for example remarkably thicker than water or

oil. This would imply that the resins have also elastic behavior. It was considered, that maybe cylinder is not an appropriate measuring head for the resins, and also a paddle spindle stirrer head was tested. This removed the possible doubt that the resin would not move in the small gap between the cylinders. However, storage moduli were still not plotted for amplitude or frequency sweeps.

Domínguez et al. (2013) compared the rheological behavior of commercial phenolic resin and resin with partial substitution (30 %) of phenol with modified ammonium lignosulfonates. PF resin exhibited close to Newtonian flow behavior and LPF resin pseudoplastic flow behavior. Viscoelastic behavior of LPF resin can be considered as an advantage in coating applications and composite production, but as a drawback for some other applications. Characterization was performed with frequency sweep (0,5-80 Hz, constant strain 2 %) within the linear viscoelastic region of both resins. The profiles of the storage and loss moduli of both resins were typical for polymer solution. High water content of both resins (more than 50 wt-%) can be a cause for this. Storage and loss moduli were lower for PF resin than for LPF resin. Lignosulfonates may cause interferences with the polymer which can cause different behavior of LPF resin. Storage modulus is more sensitive for structural analysis of the fluid than loss modulus. Lower storage modulus of PF resin can thus also imply that it has lower molecular weight and lower degree of branching (Domínquez et al., 2013). This was also supported by the relaxation spectra calculations (frequency as a function of relaxation time), where the time peak was lower for PF resin than to LPF resin. Lower peak implies to easier mobility of the polymer chains and thus lower branching. The researchers also studied the structural and thermal behavior of the resins by Fourier transform infrared spectroscopy (FTIR), differential scanning calorimeter (DSC) and thermogravimetric analysis (TGA), resulting that PF resin has higher reactivity and LPF resin has higher thermal stability (Domínguez et al., 2013).

Rheological properties of LPF resin containing 30 % of sugar cane bagasse lignin were studied by rotational rheometer by Moubarik (2014). Linear domain of the resin was determined by amplitude sweep (strain 0,01-10 %, constant frequency 1 rad/s) and it was between strain range 0,01 % and 1 % (similar to reference PF resin). Time sweep resulted constant moduli (both G' and G'') after 50 min (constant strain 1 % and frequency 1 rad/s), which indicated excellent structural stability of the resin (similar to reference PF resin). In

frequency sweep, both moduli of the LPF resin increased as the frequency increased (0,1-100 rad/s, constant strain 1 %). *G*' and *G*'' curves were approximately parallel, and *G*' was larger than *G*'', which is typical for weak gels (Moubarik, 2014). This indicates LPF resin containing crosslinked structure which can be broken and reformed. Time sweep performed in industrial polymerization temperature (125 °C) for LPF resin resulted constant moduli after 7,5 min, which indicated the optimal cure time of the resin. Temperature sweep (20-180 °C, constant strain 1 % and frequency 1 rad/s) resulted three stages of variation of the viscoelastic properties. First, slight increase of both moduli as the temperature increases (maybe due to evaporation of water). Second (between 110-125 °C), sharp increase of moduli due to activation of polymerization. Third, (between 125-160 °C), sharp decrease of moduli (maybe due to foam formation).

Rheology of PF adhesives is considered to affect bulk flow, prepress tack, precure moisture retention, gap-filling properties, and cured glue joint strength and durability (Yang and Frazier, 2016a). The influence of organic fillers (flours of walnut shell, red alder bark and corn cob residue) on flow properties of PF adhesives were determined by analyzing viscosity curves, creep/recovery measurements and frequency sweeps. Viscosity curves were performed for resin and adhesives by first increasing the shear rate 0,05-4000 1/s and then decreasing the shear rate 4000-0,05 1/s. PF resin showed principally Newtonian flow behavior, shear thinning occurred in shear rates above 1250 1/s. PF adhesive with wheat flour extender showed gradually shear thinning behavior. PF adhesives with extender and different organic fillers showed rather similar behavior, first shear thinning at low shear rates, plateau at intermediate shear rates, and again shear thinning at high shear rates. In the second step, when decreasing the shear rates, viscosity was regained gradually or first gradually and then more rapidly at lower shear rates. There was no significant reorganization in hysteresis curves (plots of increasing and decreasing shear rates in the same figure) of adhesives with corn cob and walnut shell fillers, but adhesive with alder bark filler showed a crossover at low shear region, which implies structural reorganization (Yang and Frazier, 2016a). In creep/recovery measurement (constant shear stress of 0,05 Pa), adhesive containing alder bark filler showed first mostly viscous behavior and after shearing viscoelastic behavior, implying to development of some type of network structure (Yang and Frazier, 2016a). This was also recognized in frequency sweep, where loss modulus was greater than storage modulus prior to shearing and almost equal after shearing. In contrast,

adhesive containing corn cob filler showed first viscoelastic behavior and shearing causing dramatic development of elastic behavior. In frequency sweep (0,01-0,05 Hz, constant shear stress 0,05 Pa), crossover point for storage modulus to exceed loss modulus was observed after the second shearing at low frequencies. Both moduli also tend to toward plateau value, which implies greater network development. The cause for development of viscoelastic network structures was unknown, but it was suggested that fillers aggregate colloidal effects within the liquid, alkaline PF resin. Here, compounds of the extender and fillers would interact with PF chains and form colloidal structures.

Both Domínguez et al. (2013) and Yang and Frazier (2016a) concluded PF resin indicating close to Newtonian flow behavior, but still exhibiting elastic behavior as the storage modulus plot was obtained in frequency sweep measurements to determine structural properties of the resin. LPF resin exhibited pseudoplastic behavior (Domínguez et al., 2013) and adhesives shear thinning behavior (Yang and Frazier, 2016a). Domínguez et al. (2013) reported some similarities in PF and LPR resin behavior (explained by similar composition) but differences in structure (PF resin having lower molecular weight and lower degree of branching). Moubarik (2014) reported initially similar properties of PF and LPF resin (linear viscoelastic region and structural stability), but not all determinations were performed to PF resin. Yang and Frazier (2016a) reported structural reorganization and development of some type of network structure for some adhesives, possibly due to filler compounds and PF resin interaction to form colloidal structures, but structural analyses for PF resin without extender or fillers were not performed. Domínguez et al. (2013) and Moubarik (2014) used plate-plate and Yang and Frazier (2016a) concentric cylinder geometry for analyses.

So, the literature results and results from this work vary when considering the shear rheological properties of the resins. The results obtained from this work imply that the resins are ideally Newtonian liquids and do not differ from each other, except for the viscosity level. Overall it was considered, that elastic behavior should exist. Since the storage modulus was not found also the calculation of other results may not be reliable. Relaxation time (λ), complex shear modulus (G^*) and further complex viscosity (η^*) and zero-shear viscosity (η_0) could be determined from shear rheology of the resins. Without storage modulus, complex shear modulus is equal to loss modulus values, and complex viscosity curves correspond to viscosity curves.

Extensional rheology

In Figure 3, Figure 4, Figure 5, Figure 6, Figure 7 and Figure 8 the effect of surfactant and defoamer combinations on LPF resin elongational properties are presented.

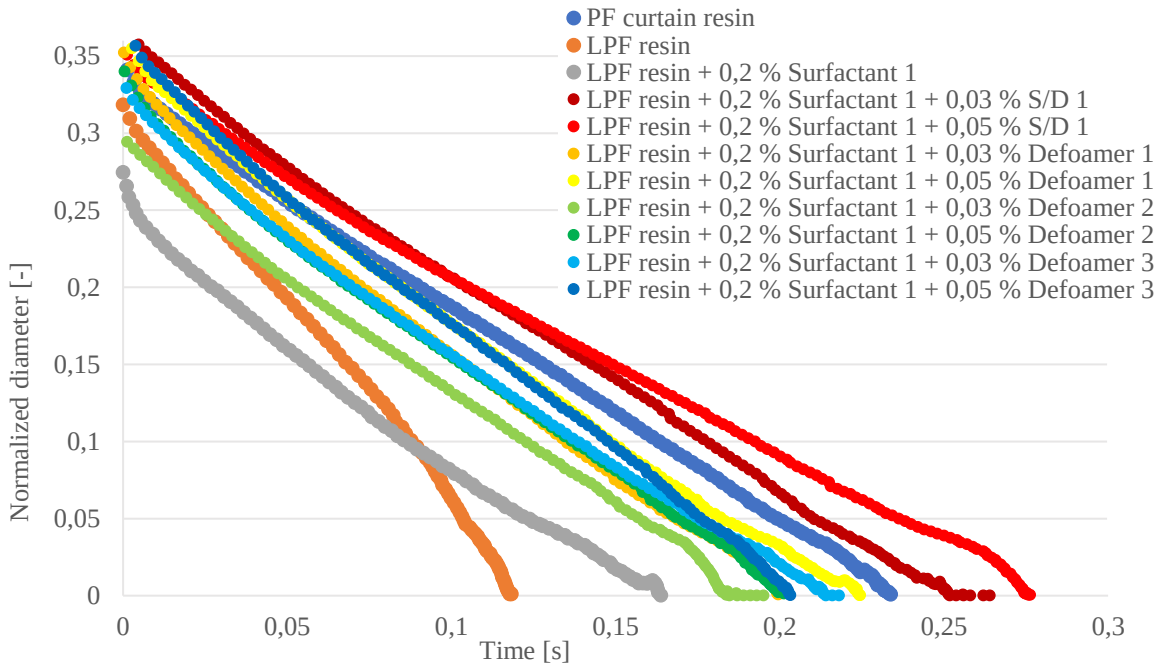

Figure 3 Effect of surfactant 1 (dosage 0,2 % of the weight of resin) and defoamer combinations on LPF resin elongational properties. Normalized diameter of filament elongation and break-up as a function of time determined by HAAKE™ CaBER™ 1. Measurement was performed with 6 mm plates with initial and final aspect ratio of 1,00 and 2,75, respectively, and in temperature of 25 ± 2 ºC.

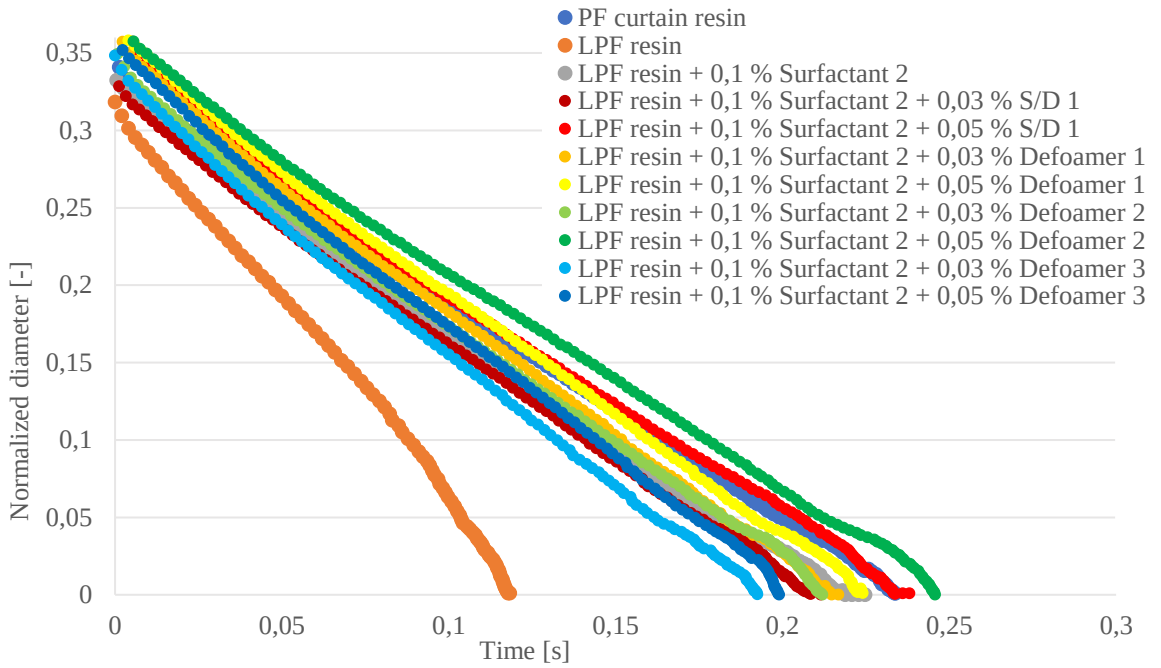

Figure 4 Effect of surfactant 2 (dosage 0,1 % of the weight of resin) and defoamer combinations on LPF resin elongational properties. Normalized diameter of filament elongation and break-up as a function of time determined by HAAKE™ CaBER™ 1. Measurement was performed with 6 mm plates with initial and final aspect ratio of 1,00 and 2,75, respectively, and in temperature of 25 ± 2 ºC.

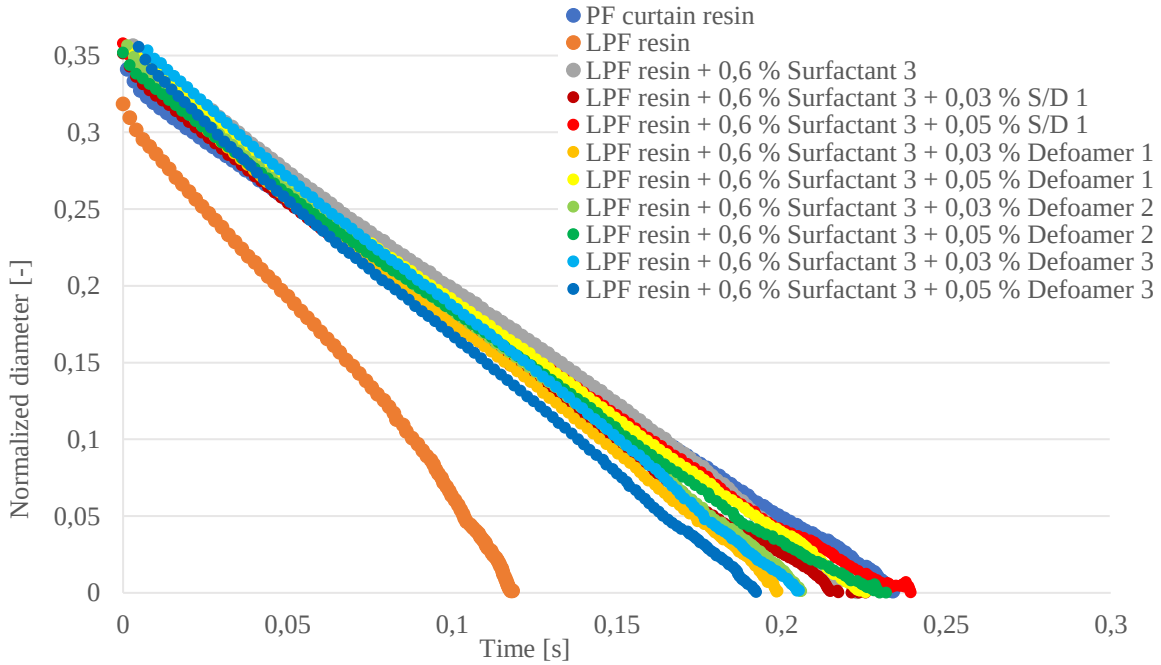

Figure 5 Effect of surfactant 3 (dosage 0,6 % of the weight of resin) and defoamer combinations on LPF resin elongational properties. Normalized diameter of filament elongation and break-up as a function of time determined by HAAKE™ CaBER™ 1. Measurement was performed with 6 mm plates with

initial and final aspect ratio of 1,00 and 2,75, respectively, and in temperature of 25 ± 2 ºC.

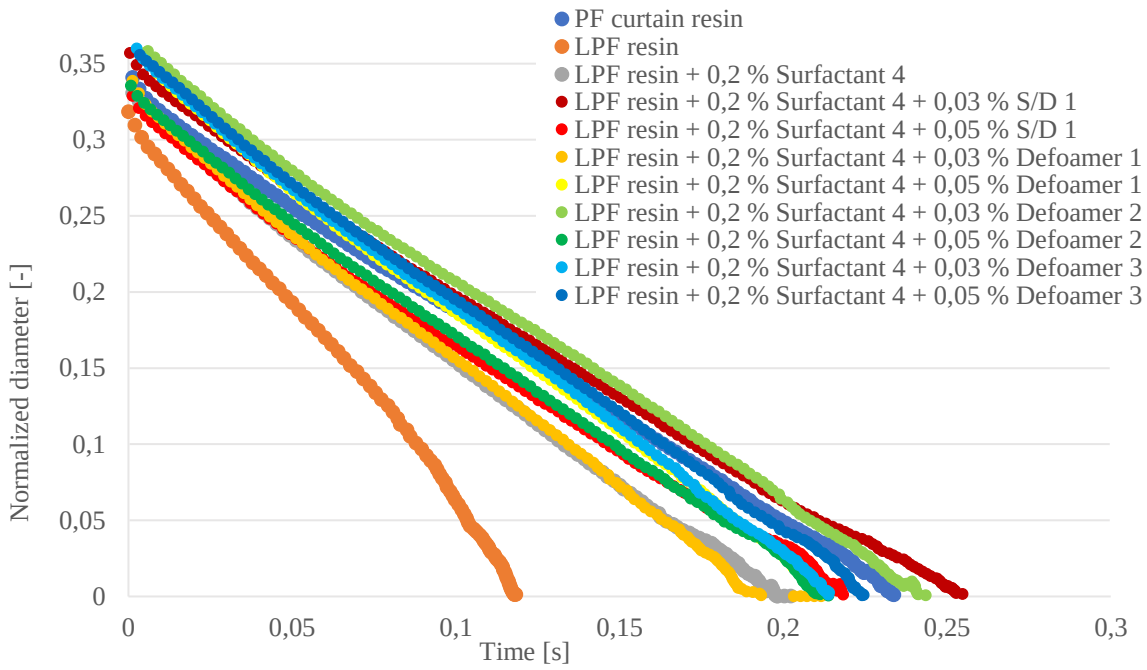

Figure 6 Effect of surfactant 4 (dosage 0,2 % of the weight of resin) and defoamer combinations on LPF resin elongational properties. Normalized diameter of filament elongation and break-up as a function of time determined by HAAKE™ CaBER™ 1. Measurement was performed with 6 mm plates with initial and final aspect ratio of 1,00 and 2,75, respectively, and in temperature of 25 ± 2 ºC.

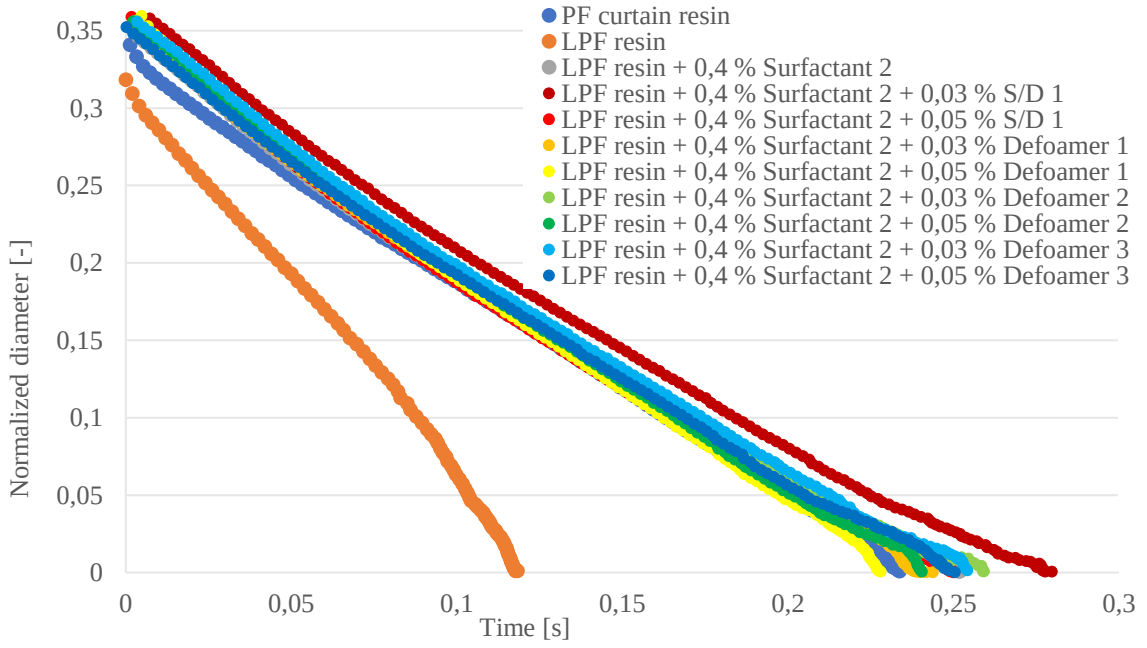

Figure 7 Effect of surfactant 2 (dosage 0,4 % of the weight of resin) and defoamer combinations on LPF resin elongational properties. Normalized diameter of

filament elongation and break-up as a function of time determined by HAAKE™ CaBER™ 1. Measurement was performed with 6 mm plates with initial and final aspect ratio of 1,00 and 2,75, respectively, and in temperature of 25 ± 2 ºC.

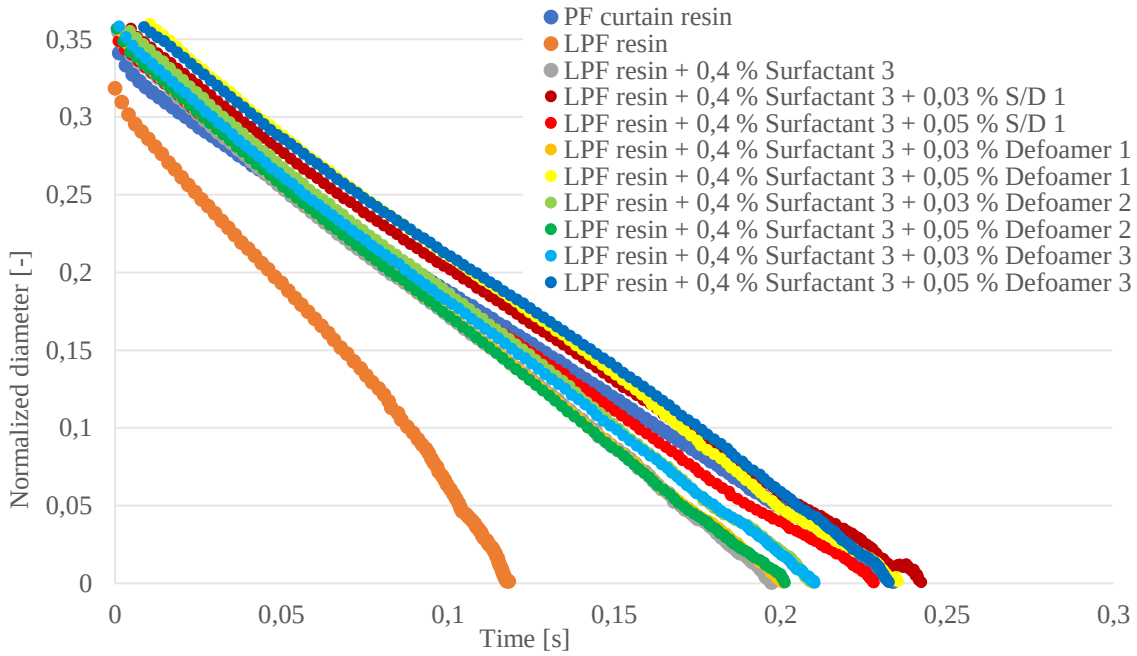

Figure 8 Effect of surfactant 3 (dosage 0,4 % of the weight of resin) and defoamer combinations on LPF resin elongational properties. Normalized diameter of filament elongation and break-up as a function of time determined by HAAKE™ CaBER™ 1. Measurement was performed with 6 mm plates with initial and final aspect ratio of 1,00 and 2,75, respectively, and in temperature of 25 ± 2 ºC.

In Table I, the break-up time and capillary velocity of the experiments, determined by HAAKE™ CaBER™ 1 extensional rheometer, are presented. In Table II, the results of additional experiments are presented.

Table I Break-up time and capillary velocity of the experiments determined by HAAKE™ CaBER™ 1 extensional rheometer. Measurement was performed with 6 mm plates with initial and final aspect ratio of 1,00 and 2,75, respectively, and in temperature of 25 ± 2 ºC.

EXP	Description	Break-up time, ms	Capillary velocity, mm/s
1	PF resin	91	3,429
2	PF curtain resin	234	1,390

3	LPF resin	118	2,598
4	LPF resin + 0,2 % Surfactant 1	164	1,501
7	LPF resin + 0,1 % Surfactant 2	218	1,475
13	LPF resin + 0,6 % Surfactant 3	223	1,587
14	LPF resin + 0,2 % Surfactant 4	202	1,622
17	LPF resin + 0,03 % Surfactant/Defoamer 1	176	1,890
18	LPF resin + 0,05 % Surfactant/Defoamer 1	193	1,751
19	LPF resin + 0,10 % Surfactant/Defoamer 1	255	1,491
23	LPF resin + 0,03 % Defoamer 1	141	2,358
24	LPF resin + 0,05 % Defoamer 1	204	1,710
25	LPF resin + 0,10 % Defoamer 1	178	1,875
26	LPF resin + 0,03 % Defoamer 2	147	2,246
27	LPF resin + 0,05 % Defoamer 2	150	2,169
28	LPF resin + 0,10 % Defoamer 2	152	2,210
29	LPF resin + 0,03 % Defoamer 3	155	2,204
30	LPF resin + 0,05 % Defoamer 3	146	2,322
31	LPF resin + 0,10 % Defoamer 3	168	2,002
32	LPF resin + 0,2 % Surfactant 1 + 0,03 % S/D 1	252	1,400
33	LPF resin + 0,2 % Surfactant 1 + 0,03 % Defoamer 1	200	1,627
34	LPF resin + 0,2 % Surfactant 1 + 0,03 % Defoamer 2	195	1,506
35	LPF resin + 0,2 % Surfactant 1 + 0,03 % Defoamer 3	214	1,451
36	LPF resin + 0,2 % Surfactant 1 + 0,05 % S/D 1	276	1,195
37	LPF resin + 0,2 % Surfactant 1 + 0,05 % Defoamer 1	225	1,537
38	LPF resin + 0,2 % Surfactant 1 + 0,05 % Defoamer 2	201	1,555
39	LPF resin + 0,2 % Surfactant 1 + 0,05 % Defoamer 3	203	1,691
40	LPF resin + 0,1 % Surfactant 2 + 0,03 % S/D 1	209	1,519
41	LPF resin + 0,1 % Surfactant 2 + 0,03 % Defoamer 1	217	1,617
42	LPF resin + 0,1 % Surfactant 2 + 0,03 % Defoamer 2	212	1,543
43	LPF resin + 0,1 % Surfactant 2 + 0,03 % Defoamer 3	193	1,708
44	LPF resin + 0,1 % Surfactant 2 + 0,05 % S/D 1	234	1,460
45	LPF resin + 0,1 % Surfactant 2 + 0,05 % Defoamer 1	224	1,580
46	LPF resin + 0,1 % Surfactant 2 + 0,05 % Defoamer 2	246	1,426
47	LPF resin + 0,1 % Surfactant 2 + 0,05 % Defoamer 3	199	1,703
48	LPF resin + 0,6 % Surfactant 3 + 0,03 % S/D 1	217	1,546
49	LPF resin + 0,6 % Surfactant 3 + 0,03 % Defoamer 1	199	1,711
50	LPF resin + 0,6 % Surfactant 3 + 0,03 % Defoamer 2	206	1,667
51	LPF resin + 0,6 % Surfactant 3 + 0,03 % Defoamer 3	205	1,763
52	LPF resin + 0,6 % Surfactant 3 + 0,05 % S/D 1	239	1,442
53	LPF resin + 0,6 % Surfactant 3 + 0,05 % Defoamer 1	226	1,554
54	LPF resin + 0,6 % Surfactant 3 + 0,05 % Defoamer 2	229	1,503
55	LPF resin + 0,6 % Surfactant 3 + 0,05 % Defoamer 3	192	1,827
56	LPF resin + 0,2 % Surfactant 4 + 0,03 % S/D 1	255	1,342
57	LPF resin + 0,2 % Surfactant 4 + 0,03 % Defoamer 1	193	1,654

58	LPF resin + 0,2 % Surfactant 4 + 0,03 % Defoamer 2	241	1,471
59	LPF resin + 0,2 % Surfactant 4 + 0,03 % Defoamer 3	214	1,629
60	LPF resin + 0,2 % Surfactant 4 + 0,05 % S/D 1	218	1,419
61	LPF resin + 0,2 % Surfactant 4 + 0,05 % Defoamer 1	212	1,639
62	LPF resin + 0,2 % Surfactant 4 + 0,05 % Defoamer 2	211	1,515
63	LPF resin + 0,2 % Surfactant 4 + 0,05 % Defoamer 3	225	1,548

Table II Break-up time and capillary velocity of the additional experiments determined by HAAKE™ CaBER™ 1 extensional rheometer. Measurement was performed with 6 mm plates with initial and final aspect ratio of 1,00 and 2,75, respectively, and in temperature of 25 ± 2 ºC.

EXP	**Description**	**Break-up time, ms**	**Capillary velocity, mm/s**
9	LPF resin + 0,4 % Surfactant 2	252	1,357
12	LPF resin + 0,4 % Surfactant 3	197	1,730
64	LPF resin + 0,4 % Surfactant 2 + 0,03 % S/D 1	280	1,299
65	LPF resin + 0,4 % Surfactant 2 + 0,03 % Defoamer 1	239	1,415
66	LPF resin + 0,4 % Surfactant 2 + 0,03 % Defoamer 2	259	1,363
67	LPF resin + 0,4 % Surfactant 2 + 0,03 % Defoamer 3	254	1,381
68	LPF resin + 0,4 % Surfactant 2 + 0,05 % S/D 1	250	1,395
69	LPF resin + 0,4 % Surfactant 2 + 0,05 % Defoamer 1	228	1,520
70	LPF resin + 0,4 % Surfactant 2 + 0,05 % Defoamer 2	241	1,446
71	LPF resin + 0,4 % Surfactant 2 + 0,05 % Defoamer 3	251	1,363
72	LPF resin + 0,4 % Surfactant 3 + 0,03 % S/D 1	242	1,464
73	LPF resin + 0,4 % Surfactant 3 + 0,03 % Defoamer 1	201	1,718
74	LPF resin + 0,4 % Surfactant 3 + 0,03 % Defoamer 2	210	1,693
75	LPF resin + 0,4 % Surfactant 3 + 0,03 % Defoamer 3	210	1,652
76	LPF resin + 0,4 % Surfactant 3 + 0,05 % S/D 1	228	1,484
77	LPF resin + 0,4 % Surfactant 3 + 0,05 % Defoamer 1	235	1,587
78	LPF resin + 0,4 % Surfactant 3 + 0,05 % Defoamer 2	201	1,715
79	LPF resin + 0,4 % Surfactant 3 + 0,05 % Defoamer 3	233	1,552

If neglecting the absence of storage modulus in shear rheology results, and determining the zero-shear viscosity based on the available data, zero-shear viscosities are 355 mPas, 379 mPas and 323 mPas, respectively for PF resin, PF curtain resin and LPF resin. Then, Trouton ratio can be calculated and plotted as a function of Hencky strain. In Figure 9, the Trouton ratios of the reference resins are presented.

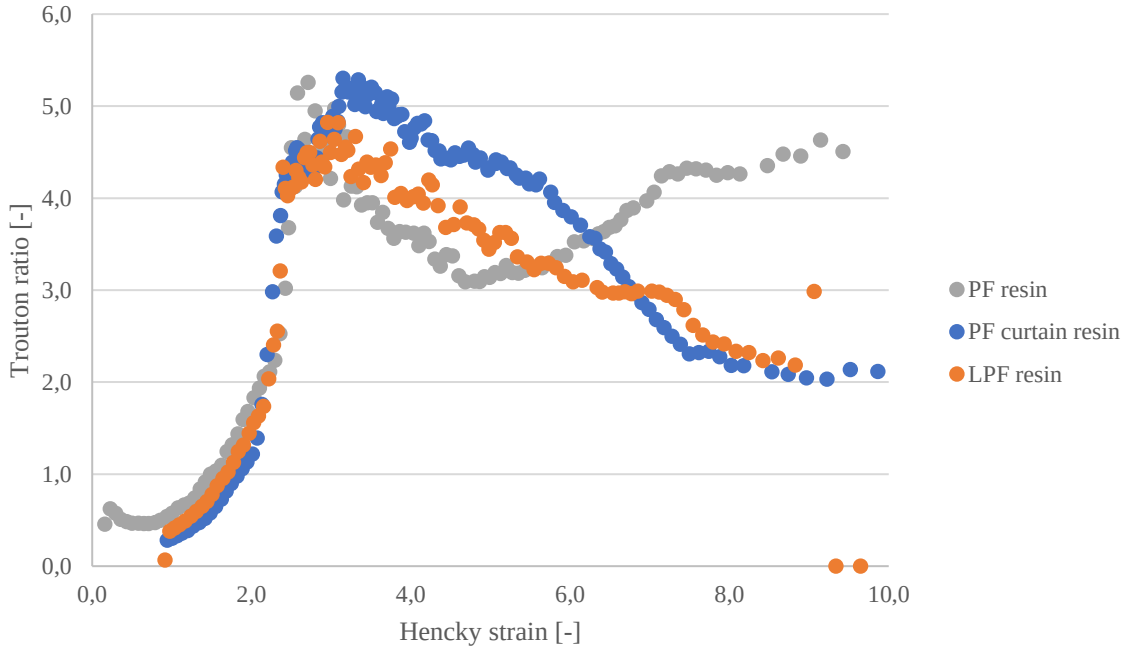

Figure 9 Trouton ratio of the reference resins as a function of Hencky strain. Extensional viscosity determined by HAAKE™ CaBER™ 1. Measurement was performed with 6 mm plates with initial and final aspect ratio of 1,00 and 2,75, respectively, and in temperature of 25 ± 2 ºC. Zero-shear viscosities 355 mPas, 379 mPas and 323 mPas, respectively for PF resin, PF curtain resin and LPF resin obtained from shear rheology measurements.

In Figure 9, differences between the resins can be observed slightly better, but no clear conclusions can be drawn. At small strain range, the resins imply clear extensional thickening, as the Trouton ratio increases as the strain increases. At strain range > 3, the consistency of the curves disappears. The steady-state values are not completely reached at this strain range, but approximately Trouton ratios of 4,5; 2 and 2 could be applicable for PF resin, PF curtain resin and LPF resin, respectively. Trouton ratio for Newtonian liquids is 3.

Interfacial viscoelasticity

Interfacial viscoelasticity curves of reference resins are presented in Figure 10.

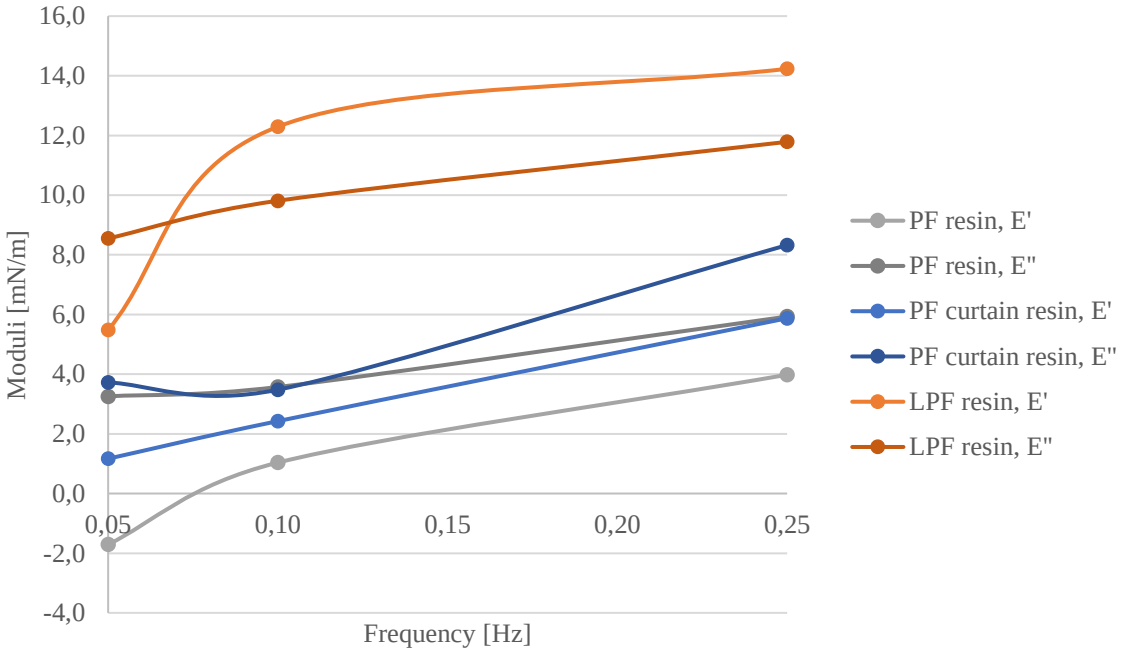

Figure 10 Interfacial viscoelasticity of the reference resins, storage (*E*') and loss (*E*'') moduli as a function of frequency, determined by CAM 200 optical tensiometer and PD-100 module, in temperature of 23 ± 1 ºC and relative humidity of 50 ± 2 %. Drop volumes of 27 µl, 11 µl and 15 µl for PF resin, PF curtain resin and LPF resin, respectively, and resin density 1,2073 g/cm^3 used.

For PF resins, loss/viscous modulus (*E*'') is higher than storage/elastic modulus throughout the measurement. This implies, that the resins are more liquid-like fluids than solid-like. For LPF resin, a crossover point is observed at 0,07 Hz. The level of the LPF curves is also higher. This is probably due to lignin in resin structure, since it is the most remarkable difference between the resins. However, PF curtain resin is assumed to contain additives due to its curtain formation ability.

Standard deviation between the replicates at each frequency was variable and sometimes remarkable. Frequency range used in this work was relatively narrow, which was due to practical issues. Lower frequencies were not applicable due to drying of the resin drop during a long measurement. Camera of the device was not able to record frames faster, and thus higher frequencies could not be applied. Overall, higher frequencies would be interesting to measure. Here, the results could be possibly compared to shear rheology results.

Interfacial rheology studies mostly focus on foam and emulsion stability characterization. Thus, the availability of reasonable reference results from literature is limited. Beneventi & Guerin (2005) have mentioned the study of surface viscoelastic modulus above the critical micelle concentration of the surfactant as a part of their paper curtain coating study. They conclude that low surface elasticity, below 16 mN/m, is desired for successful curtain formation. The interfacial viscoelasticity of LPF resin obtained in this work, is below 16 mN/m.

However, pulsating/oscillating drop measurement was further tested for surfactant including resins. The measurement should give insight about the surfactant performance in the solution, and thus, the effect of two surfactants (1 and 4) with different chemical composition and defoamer 3, which is described as nonionic surfactant and defoamer, on LPF resin interfacial viscoelasticity was tested. In Figure 11, Figure 12 and Figure 13 the effect of surfactants (dosages of 0,2 %, 0,4 % and 0,6 %, respectively) and in Figure 14 the effect of defoamer 3 (dosage 0,1 %) is presented.

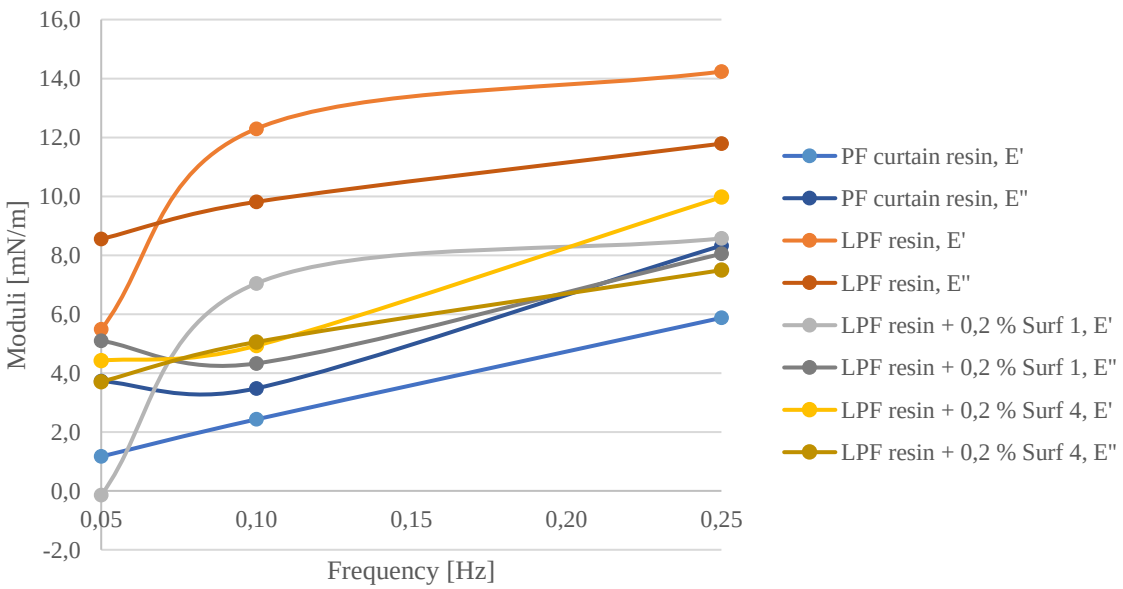

Figure 11 Effect of surfactants 1 and 4 (dosage 0,2 %) on interfacial viscoelasticity of LPF resin, storage (*E*') and loss (*E*'') moduli as a function of frequency, determined by CAM 200 optical tensiometer and PD-100 module, in temperature of 23 ± 1 ºC and relative humidity of 50 ± 2 %. Drop volumes of 13 µl and 14 µl for LPF resin with surfactant 1 and 4, respectively, and resin density 1,2073 g/cm^3 used.

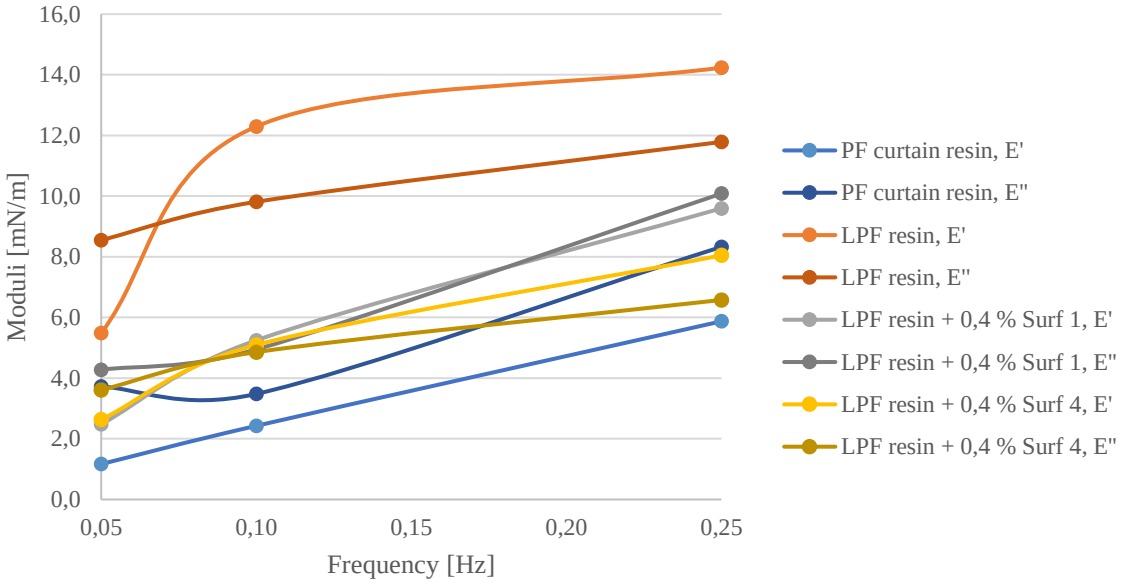

Figure 12 Effect of surfactants 1 and 4 (dosage 0,4 %) on interfacial viscoelasticity of LPF resin, storage (*E*') and loss (*E*'') moduli as a function of frequency, determined by CAM 200 optical tensiometer and PD-100 module, in temperature of 23 ± 1 ºC and relative humidity of 50 ± 2 %. Drop volumes of 12 µl and 13 µl for LPF resin with surfactant 1 and 4, respectively, and resin density 1,2073 g/cm^3 used.

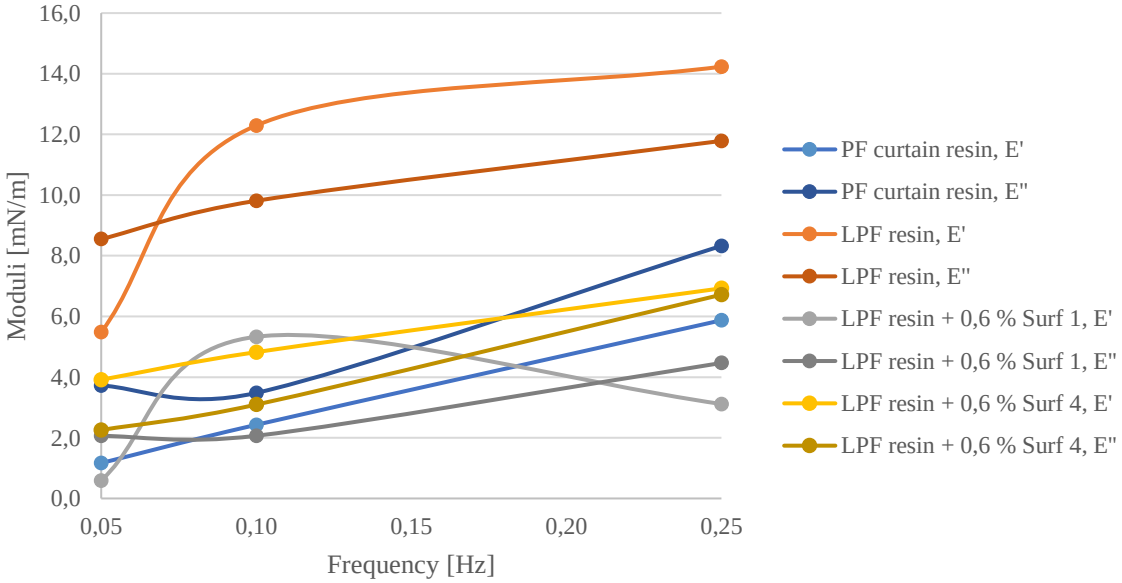

Figure 13 Effect of surfactants 1 and 4 (dosage 0,6 %) on interfacial viscoelasticity of LPF resin, storage (*E*') and loss (*E*'') moduli as a function of frequency, determined by CAM 200 optical tensiometer and PD-100 module, in temperature of 23 ± 1 ºC and relative humidity of 50 ± 2 %. Drop volumes of 10 µl and 12 µl for LPF resin with surfactant 1 and 4, respectively, and resin density 1,2073 g/cm^3 used.

As seen from Figure 11, Figure 12 and Figure 13, surfactants affect the LPF resin interfacial viscoelasticity. With dosage of 0,2 % of surfactant 1, the shape of the *E*' and *E*'' curves is similar to LPF resin without additives, but at lower level. With dosage of 0,4 %, the curves are close to each other and with dosage of 0,6 % there is again a remarkable difference between the curves and actually two crossover points. There is no consistency in the results with surfactant 1. With surfactant 4, however, the loss and storage moduli curves of LPF resin gradually change positions as the surfactant dosage level increases. With 0,2 % dosage of surfactant 4, storage modulus is higher or equal to loss modulus at all frequencies, but with dosage of 0,6 %, loss modulus is higher or equal to storage modulus at all frequencies.

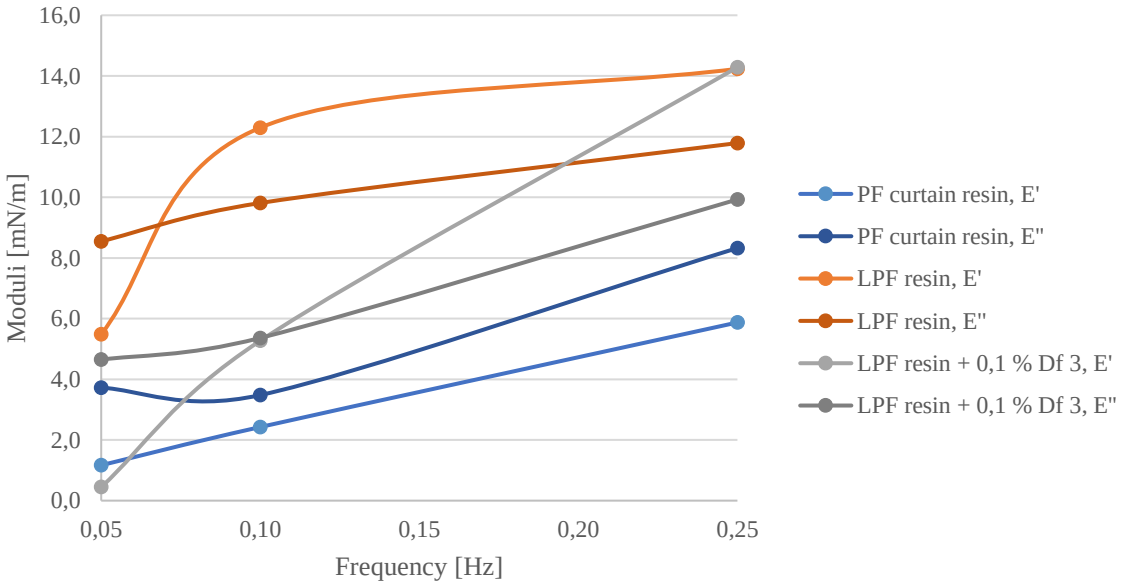

Figure 14 Effect of defoamer 3 (dosage 0,1 %) on interfacial viscoelasticity of LPF resin, storage (*E*') and loss (*E*'') moduli as a function of frequency, determined by CAM 200 optical tensiometer and PD-100 module, in temperature of 23 ± 1 ºC and relative humidity of 50 ± 2 %. Drop volume of 15 µl, and resin density 1,2073 g/cm^3 used.

As seen from Figure 14, also with defoamer 3 the level of *E*' and *E*'' curves is lowered. There is a remarkable effect on storage modulus of LPF resin with defoamer 3 as the difference between the lowest and highest frequency has increased.

Difference between the surfactant 1 and 4 and defoamer 3 performance can be recognized. However, evaluation of the performance, whether the other additive is better than the other, is challenging due to lack of reference results. In the scope of this work, this analytical

method was not considered as valuable as the analytical methods determining surface tension and rheological properties of the resins.

APPENDIX V: MULTIPLE LINEAR REGRESSION ANALYSIS

From multiple linear regression (MLR) analysis, the following values are obtained (Montgomery et al., 2012):

- Multiple R: correlation coefficient
- R Square: squared correlation coefficient
- Adjusted R Square: for system with more than one *x* variable
- Significance F: significance of the model
- P-value: probability value
- t Stat: student's test parameter.

Surfactant 2 and defoamers

In Table I, Table II, Table III and Table IV, the MLR analysis output is presented for surfactant 2 in combination with surfactant/defoamer 1, defoamer 1, defoamer 2 and defoamer 3, respectively. MLR analyses computed with Microsoft Excel Data Analysis Add-Inn.

Table I MLR analysis for surfactant 2 and surfactant/defoamer 1 additive combination. Variable coefficients computed for the working curve model.

Regression Statistics	
Multiple R	0,960601
R Square	0,922755
Adjusted R Square	0,860959
Standard Error	0,017607
Observations	10

ANOVA

	df	*SS*	*MS*	*F*	*Significance F*
Regression	4	0,018515	0,004629	14,932270	0,0054840
Residual	5	0,001550	0,000310		
Total	9	0,020065			

Variables	*Coefficients*	*Standard Error*	*t Stat*	*P-value*	*Lower 95%*	*Upper 95%*
Intercept	0,130829	0,013514	9,680810	0,000200	0,096089	0,165568
x_1	0,767338	0,191015	4,017167	0,010149	0,276319	1,258357

x_2	1,215585	0,227858	5,334826	0,003102	0,629856	1,801314
$x_1 \cdot x_2$	-3,33719	1,374304	-2,42827	0,059507	-6,86995	0,195575
x_1^2	-1,08723	0,425828	-2,55321	0,051066	-2,18185	0,007399

Table II MLR analysis for surfactant 2 and defoamer 1 additive combination. Variable coefficients computed for the working curve model.

Regression Statistics	
Multiple R	0,928515
R Square	0,862140
Adjusted R Square	0,751853
Standard Error	0,021534
Observations	10

ANOVA

	df	*SS*	*MS*	*F*	*Significance F*
Regression	4	0,014499	0,003625	7,817197	0,022266
Residual	5	0,002319	0,000464		
Total	9	0,016818			

Variables	*Coefficients*	*Standard Error*	*t Stat*	*P-value*	*Lower 95%*	*Upper 95%*
Intercept	0,133501	0,016529	8,076969	0,000471	0,091013	0,175990
x_1	0,938075	0,233622	4,015360	0,010167	0,337531	1,538618
x_2	0,593692	0,278683	2,130346	0,086366	-0,12269	1,310071
$x_1 \cdot x_2$	-2,81001	1,680849	-1,67178	0,155430	-7,13077	1,510753
x_1^2	-1,59406	0,520811	-3,06073	0,028079	-2,93285	-0,25527

Table III MLR analysis for surfactant 2 and defoamer 2 additive combination. Variable coefficients computed for the working curve model.

Regression Statistics	
Multiple R	0,982651
R Square	0,965602
Adjusted R Square	0,938084
Standard Error	0,013049
Observations	10

ANOVA

	df	*SS*	*MS*	*F*	*Significance F*
Regression	4	0,02390	0,005975	35,089430	0,000749
Residual	5	0,000851	0,000170		
Total	9	0,024751			

Variables	*Coefficients*	*Standard Error*	*t Stat*	*P-value*	*Lower 95%*	*Upper 95%*
Intercept	0,126181	0,010016	12,59796	5,6E-05	0,100434	0,151929
x_1	1,134920	0,141570	8,016671	0,000488	0,771002	1,498837
x_2	0,346578	0,168876	2,052257	0,095368	-0,08753	0,780689
$x_1 \cdot x_2$	-1,18459	1,018561	-1,16301	0,297309	-3,80289	1,433699
x_1^2	-2,03833	0,315601	-6,45856	0,001325	-2,84961	-1,22705

Table IV MLR analysis for surfactant 2 and defoamer 3 additive combination. Variable coefficients computed for the working curve model.

Regression Statistics	
Multiple R	0,972832
R Square	0,946401
Adjusted R Square	0,919602
Standard Error	0,013731
Observations	10

ANOVA

	df	*SS*	*MS*	*F*	*Significance F*
Regression	3	0,019975	0,006658	35,314440	0,000330
Residual	6	0,001131	0,000189		
Total	9	0,021106			

Variables	*Coefficients*	*Standard Error*	*t Stat*	*P-value*	*Lower 95%*	*Upper 95%*
Intercept	0,137107	0,008831	15,52555	4,52E-06	0,115498	0,158716
x_1	0,746260	0,143848	5,187837	0,002039	0,394277	1,098243
$x_1 \cdot x_2$	-1,16581	0,334810	-3,48200	0,013111	-1,98506	-0,34656
x_2^2	2,830638	1,658047	1,707212	0,138652	-1,22646	6,887734

Surfactant 3 and defoamers

In Table V, Table VI, Table VII and Table VII, the MLR analysis output is presented for surfactant 3 in combination with surfactant/defoamer 1, defoamer 1, defoamer 2 and defoamer 3, respectively. MLR analyses computed with Microsoft Excel Data Analysis Add-Inn.

Table V MLR analysis for surfactant 3 and surfactant/defoamer 1 additive combination. Variable coefficients computed for the working curve model.

Regression Statistics

Multiple R	0,950041
R Square	0,902578
Adjusted R Square	0,853867
Standard Error	0,015341
Observations	10

ANOVA

	df	*SS*	*MS*	*F*	*Significance F*
Regression	3	0,013083	0,004361	18,529200	0,001947
Residual	6	0,001412	0,000235		
Total	9	0,014495			

Variables	*Coefficients*	*Standard Error*	*t Stat*	*P-value*	*Lower 95%*	*Upper 95%*
Intercept	0,130334	0,011786	11,05819	3,26E-05	0,101494	0,159173
x_1	0,158877	0,030310	5,241749	0,001935	0,084711	0,233042
x_2	1,290619	0,207411	6,222507	0,000796	0,783101	1,798136
$x_1 \cdot x_2$	-1,62097	0,718615	-2,25568	0,064932	-3,37936	0,137421

Table VI MLR analysis for surfactant 3 and defoamer 1 additive combination. Variable coefficients computed for the working curve model.

Regression Statistics

Multiple R	0,826521
R Square	0,683137
Adjusted R Square	0,592605
Standard Error	0,023774
Observations	10

ANOVA

	df	*SS*	*MS*	*F*	*Significance F*
Regression	2	0,008530	0,004265	7,545784	0,017908
Residual	7	0,003956	0,000565		
Total	9	0,012486			

Variables	*Coefficients*	*Standard Error*	*t Stat*	*P-value*	*Lower 95%*	*Upper 95%*
Intercept	0,139886	0,016492	8,482045	6,26E-05	0,100888	0,178883
x_1	0,115926	0,030591	3,789574	0,006807	0,043590	0,188261
x_2	0,513813	0,267365	1,921768	0,096079	-0,1184	1,146030

Table VII MLR analysis for surfactant 3 and defoamer 2 additive combination. Variable coefficients computed for the working curve model.

Regression Statistics	
Multiple R	0,964116
R Square	0,929519
Adjusted R Square	0,909381
Standard Error	0,011467
Observations	10

ANOVA

	df	*SS*	*MS*	*F*	*Significance F*
Regression	2	0,012139	0,006070	46,158610	9,3E-05
Residual	7	0,000920	0,000131		
Total	9	0,013060			

Variables	*Coefficients*	*Standard Error*	*t Stat*	*P-value*	*Lower 95%*	*Upper 95%*
Intercept	0,133793	0,007955	16,81919	6,43E-07	0,114983	0,152603
x_1	0,140743	0,014755	9,538606	2,92E-05	0,105853	0,175634
x_2	0,215983	0,128961	1,674795	0,137885	-0,08896	0,520927

Table VIII MLR analysis for surfactant 3 and defoamer 3 additive combination. Variable coefficients computed for the working curve model.

Regression Statistics	
Multiple R	0,928505
R Square	0,862122
Adjusted R Square	0,793183
Standard Error	0,016715
Observations	10

ANOVA

	df	*SS*	*MS*	*F*	*Significance F*
Regression	3	0,010482	0,003494	12,505600	0,005429
Residual	6	0,001676	0,000279		
Total	9	0,012158			

Variables	*Coefficients*	*Standard Error*	*t Stat*	*P-value*	*Lower 95%*	*Upper 95%*
Intercept	0,132731	0,011919	11,13561	3,13E-05	0,103565	0,161896
x_1	0,323721	0,087716	3,690548	0,010202	0,109087	0,538355
x_2	0,307987	0,188857	1,630793	0,154055	-0,15413	0,770104
x_1^2	-0,35664	0,149799	-2,38077	0,054711	-0,72318	0,009908